Structural and functional characterisation of Photosystem II from two His-tagged transplastomic strains of *Nicotiana tabacum*

Dissertation
zur Erlangung des Doktorgrades
der Naturwissenschaften

vorgelegt beim Fachbereich Biowissenschaften
der Johann Wolfgang Goethe – Universität
in Frankfurt am Main

von
Dario Piano
aus Sardara

Frankfurt am Main 2007
(D30)

Vom Fachbereich ----------der

Johann Wolfgang Goethe-Universität als Dissertation angenommen.

Dekan:----------

Gutacher:----------

Datum der Disputation:----------

Table of contents

Zusammenfassung

Photosystem II (PSII) ist ein Polypeptid-Kofaktor-Komplex, dessen Untereinheiten als Homodimer organisiert vorliegen und in höheren Pflanzen in den Granabereichen der Thylakoidmembran eingebettet sind. PSII Monomere wiederum bestehen aus Hetero-Oligomeren, die pseudo-symmetrisch um eine Achse positioniert sind, welche rechtwinklig zur Membranebene steht (Loll *et al.* 2005). PS II agiert als photochemisch aktives Enzym, das mit Hilfe der gebundenen Chlorophylle Photonen einfängt und unter Beteiligung weiterer Kofaktoren einen Elektronenfluss von Wasser zu Plastochinon betreibt. Dabei wird gleichzeitig molekularer Sauerstoff frei gesetzt. Die primäre Ladungstrennung findet nach Absorption eines Photons im PSII Kern statt, welcher sich aus den Untereinheiten D1, D2, den α- und β-Untereinheiten von Cytochrom b_{559} (PsbE und PsbF) sowie den Chlorophyll a-bindenden Kernantennen CP47 und CP43 zusammensetzt (Loll *et al.* 2005). Bei den übrigen Polypeptiden des Photosystems II handelt es sich um niedermolekulare Proteine, deren Funktion in vielen Fällen noch nicht geklärt ist. Einige dieser Untereinheiten werden im Chloroplasten kodiert (PsbE, F, H, I, J, K, L, M, N, T und Z) während andere im Nukleus kodiert werden (PsbR, S, W und X). Im Allgemeinen bilden sie eine bis vier transmembrane Helices (Barber et al. 1997). Der Teil des Photosystems II, der für die Spaltung von Wasser zuständig ist, besteht aus einem Mn_4-Ca Übergangskomplex. Dieser ist im Thylakoidlumen lokalisiert und wird Wasser spaltender oder Sauerstoff bildender Komplex genannt. In höheren Pflanzen wird er durch die extrinsischen Untereinheiten PsbO (33 kDa), PsbP (23 kDa) und PsbQ (17 kDa) stabilisiert (Soursa *et al.* 2006; Ifuku *et al.* 2005). Weder die Struktur dieses Komplexes noch der Reaktionsmechanismus der Wasserspaltung konnten bisher vollständig aufgeklärt werden.

Zurzeit existieren zwei Strukturen mit hoher Auflösung von Photosystem II, welches aus dem Cyanobakterium *Synechococcus elongatus* isoliert wurde (Loll *et al.* 2005; Ferreira et al. 2004). Nichtsdestotrotz bleibt eine Reihe von Fragen unbeantwortet, vor allem in Bezug auf die Funktion und Position der kleineren Untereinheiten des PS II, die in den Strukturdaten nicht ausreichend bestimmt werden konnten, sowie in Bezug auf den definitiven Wasserspaltungsmechanismus (Loll *et al.* 2005; Ferreira et al.

2004). Da für Grünalgen und höhere Pflanzen bisher keine Strukturen mit hoher Auflösung verfügbar sind (Rhee et al. 1997), bleiben einige der wichtigsten Fragen weiterhin offen. Ist die Struktur des Photosystems II höherer Pflanzen tatsächlich äquivalent zur Struktur des Photosystems II der Cyanobakterien? Ist die für höhere Pflanzen typische PsbS Untereinheit stabil an Photosystem II gebunden oder interagiert sie mit den Lichtsammelkomplexen? Die Beantwortung dieser Fragen bildete den Schwerpunkt der vorliegenden Arbeit.

Aufreinigungsprotokolle für Photosystem II aus höheren Pflanzen sind mit einigen Nachteilen verbunden, vor allem in Bezug auf Verunreinigungen durch Photosystem I und LHCII (Light harvesting complex II), die Verwendung starker Detergenzien und die im Vergleich zu thermophilen Organismen geringe Stabilität des Photosystems II. Die bestehenden Protokolle für die Aufreinigung von Photosystem II mittels differentieller Zentrifugation oder Saccharosedichtezentrifugation resultieren entweder in Proben geringer Reinheit oder haben zumindest den Nachteil, auf spezielle, später schwer zu entfernende Detergenzien angewiesen zu sein.

Für diese Arbeit wurde deshalb ein Protokoll zur schnellen Isolierung von Sauerstoff bildenden PSII Kernkomplexen aus *Nicotiana tabacum* entwickelt. Mit Hilfe von sechsfachem oder zehnfachem Histidin-tag am N-Terminus der PsbE Untereinheit war es möglich Photosystem II, nach Solubilisierung der Thylakoidmembranen durch milde Detergenzien, durch Ni-NTA Chromatographie in einem Schritt zu präparieren. Die Bestimmung der Sauerstoffbildungsraten und die Zusammensetzung der Proteinuntereinheiten belegten hierbei, dass die funktionelle Integrität der PSII Reaktionszentren erhalten blieb. Im Endeffekt konnten so signifikante Mengen von hoch reinen PSII Kernkomplexen mit nur einem Aufreinigungsschritt aus solubilisierten Thylakoidmembranen innerhalb von höchstens vierzehn Stunden isoliert werden. Mit Hilfe von Blue Native PAGE, analytischer Gelfiltration, Massenspektroskopie, immonologischem Nachweis und Single Particle Analyse konnte demonstriert werden, dass die isolierten Komplexe mit einer Größe von circa 500 kDa in dimerer Form vorlagen und sich aus den Untereinheiten D1, D2, CP47, PsbO (33 kDa Protein) und einer Reihe niedermolekularer Proteine zusammensetzten. Das auf diese Art und Weise präparierte Photosystem II zeichnete sich durch eine hohe maximale Sauerstoffbildungsaktivität aus, mit Raten bis zu 1800 µmol O_2 / (mg Chl • h). Diese

PSII Komplexe zeigten ein sehr konstantes Mengenverhältnis von PsbO (33 kDa Protein), während die beiden anderen Untereinheiten des Sauerstoffbildenden Komplexes (PsbP & PsbQ) in schwankenden Mengen auftraten. Nichtsdestotrotz zeigte sich, dass die maximalen Sauerstoffbildungsraten nicht von den Mengen an PsbP und PsbQ in der Probe abhängig waren, sondern dass vielmehr das Vorhandensein bestimmter Reagenzien während der Isolation einen maßgeblichen Einfluss hatten. Tatsächlich zeigten die PSII Komplexe eine hohe Sauerstoffbildungsrate von 1390 µmol O_2 / (mg Chl • h) in der Anwesenheit von Betain, während die Aktivität ohne Betain nur 440 bis 680 µmol O_2 / (mg Chl • h) betrug, auch wenn in beiden Fällen die künstlichen Elektronenakzeptoren Kaliumhexacyanoferrat und 2,6-Dichloro-p-benzochinon in der Reaktionslösung vorhanden waren. Die deutlichste Erhöhung der Sauerstoffbildungsraten wurde durch die Verwendung von 1,0 mol/l Glycinbetain während der Aufreinigung von Photosystem II erreicht. Zusammengenommen konnte also festgestellt werden, dass trotz der Einführung des His-tags Photosystem II strukturell intakt bleibt und dass sich daher diese His-PSII Komplexe sehr gut für biochemische, physikochemische und strukturelle Untersuchungen am Photosystem II höherer Pflanzen eignen.

Photosystem II ist direkt an zwei essentiellen Vorgängen der Lichtreaktionen beteiligt. Zum einen sammelt Photosystem II Lichtenergie und leitet diese gezielt zum Reaktionszentrum weiter und zum anderen sorgt es dafür, dass überschüssige Anregungsenergie sicher abgeleitet werden kann. Die Vorraussetzungen für eine hohe Effizienz dieser Funktionen sind funktionelle und strukturelle Flexibilität. Des Weiteren bestehen Kontrollmechanismen darin, dass die Lichtsammelkomplexe (LHCII) auf äußere Signale, wie zum Beispiel den pH-Wert des Thylakoidlumens reagieren können. Das heißt, es existiert eine effiziente Feedbackkontrolle zur Steuerung der Menge an Anregungsenergie, die tatsächlich dem Reaktionszentrum zugeführt wird. Wichtige Funktionen im Abbau überschüssiger Lichtenergie (nicht-photochemisches Quenching, NPQ) werden hierbei durch den so genannten Xanthophyllzyklus und das PsbS Protein übernommen (Szabo *et al.* 2005).

In dieser Arbeit wurden einige neue Informationen in Bezug auf diese beiden Prozesse erarbeitet. Es ist zwar bekannt, dass die viel diskutierte PsbS Untereinheit eine Rolle im NPQ Mechanismus spielt, allerdings sind weder die genaue Position noch die

tatsächlichen Funktionen dieses Proteins bisher geklärt worden. Darüber hinaus ist es weiterhin unklar, ob es sich bei PsbS um ein pigmentbindendes Protein handelt. Zurzeit existieren mehrere Belege, dass die PsbS Untereinheit in der Lage ist zwei Moleküle Zeaxanthin, welches ein Pigment des Xanthophyllcyclus darstellt, zu binden (Szabo *et al.* 2005). Die vorliegende Arbeit konnte zeigen, dass PsbS stabil an PSII Kerndimere, PSII Kernmonomere und unvollständige PSII Partikel, wie die RC47 Komplexe (CP47 + Reaktionszentrum), gebunden ist. Darüber hinaus konnte in qualitativen Pigmentbestimmungen mittels HPLC kein Zeaxanthin, aber stattdessen Violaxanthin, ein weiteres Pigment des Xanthophyllzyklus, in den genannten PSII Komplexen nachgewiesen werden. Die Abwesenheit von Zeaxanthin entspricht insofern den Erwartungen, dass die Pflanzen am Ende der Dunkelperiode geerntet und die PSII Komplexe in völliger Dunkelheit oder unter grünem Licht präpariert wurden. Die Anwesenheit von Violaxanthin war allerdings unerwartet, da es bis zum jetzigen Zeitpunkt noch keinen Hinweis darauf gab, dass Violaxanthin an PS II bindet. Somit ist dies der erste Hinweis für ein Vorkommen von Violaxanthin in PSII Kernkomplexen. Des Weiteren war die Menge an Chlorophyll *b* in den Proben so gering, dass man davon ausgehen kann, dass PsbS - wenn es denn überhaupt Chlorophylle bindet - ausschließlich Chlorophyll *a* bindet. Zusammengenommen lässt dies den Schluss zu, dass PsbS sowohl Violaxanthin als auch Zeaxanthin binden kann, das heißt der gesamte Xanthophyllcyclus kann mit Hilfe der PsbS Untereinheit abgewickelt werden.

Es gilt außerdem zu beachten, dass in den durchgeführten PSII Präparationen auch die extrinsische Psb27 Untereinheit gefunden und mittels Massenspektrometrie eine erste Charakterisierung vorgenommen wurde. Allerdings waren das Vorhandensein und die Mengen an Psb27, welches vermutlich eine Rolle im Reparaturzyklus von beschädigten PSII Komplexen *in vivo* spielt, in den PSII Proben nicht konstant wie das auch für die ebenfalls extrinsischen Untereinheiten PsbP (27 kDa Protein) und PsbQ (17 kDa Protein) der Fall war.

PSII Partikel, die mittels differentieller Solubilisierung und Dichtegradientenzentrifugation aus Spinat isoliert wurden, konnten für 2D Kristallisationsexperimente verwendet und elektronenmikroskopisch untersucht werden. Es zeigten sich röhrenartige Kristalle, die sich durch vollkommen neuartige Einheitszellenkonstanten auszeichneten. Die Analyse der Kristalle wurde für das

Erstellen einer Dichtekarte mit einer Auflösung von 15 Å und einer Raumgruppe von $P22_12_1$ herangezogen. Die ermittelte Dichtekarte zeigt eine interne Symmetrieachse, allerdings ist es bei dieser Auflösung nicht möglich eine Aussage darüber zu treffen, ob es sich hierbei um die Symmetrieachse des PSII Dimers oder die pseudo-symmetrische Achse des Monomers handelt.

Abschließend lässt sich feststellen, dass die bestehenden Protokolle für die Kristallisation von PSII aus Spinat durchaus verbessert werden können und sich damit Dichtekarten mit höherer Auflösung erreichen lassen. Diese verbesserten Protokolle können nun für Kristallisationsversuche mit His-tag PSII aus Tabak herangezogen werden, um mit diesen hochreinen Präparationen die Auflösung nochmals zu verbessern.

Summary

Photosystem II (PSII) is a polypeptide-cofactor complex organised as a homodimeric multisubunit protein embedded in the thylakoid membrane. PSII monomers are hetero-oligomers related to each other by a pseudo-twofold axis perpendicular to the membrane plane (Loll *et al.* 2005). PSII acts as a photochemical enzyme that through the chlorophylls and the other cofactors catalyses photon capture and electron transfer from water to the plastoquinone pool with concomitant evolution of oxygen. Photon capture and charge separation take place in the PSII core which consists of the D1 and D2 proteins, the cytochrome b559 α- and β- chains (PsbE and F subunits) and the chlorophyll a-binding antenna proteins CP43 and CP47 (Loll *et al.* 2005). The remaining polypeptides are low molecular mass proteins with not clearly understood fuctions; they include chloroplast-encoded (PsbH, I, J, K, L, M, N, T and Z) and nucleus-encoded (PsbR, S, W and X) proteins consisting of one to four transmembrane helices (Barber et al. 1997). The oxygen-evolving part of PSII consists of a Mn-Ca transition complex called Mn cluster or oxygen evolving complex that is situated on the luminal side of PSII. In higher plants it is stabilised by the PsbO (33 kDa), PsbP (23 kDa) and PsbQ (17 kDa) extrinsic subunits (Soursa *et al.* 2006; Ifuku *et al.* 2005). The structure and mechanisms related to the oxygen evolving complex of PSII are not completely clarified.

Currently two high resolution structures from the cyanobacteria *S. elongatus* are available (Loll *et al.* 2005; Ferreira et al. 2004) Nevertheless structural information is not as well defined in green algae and higher plants as in cyanobacteria. In fact the 8Å structure available from spinach has too low resolution for addressing questions such as the structural and functional differences in respect to PSII from cyanobateria (Rhee et al. 1997).. Therefore it is obvious that for PSII from higher plants the main general questions are still open: is the structure of PSII from higher plants equivalent to the structures observed in cyanobacteria? Is the typical higher plants subunit PsbS stably or transiently bound to PSII? Finding an answer to these questions was the main focus of this work.

In this work a simple and rapid protocol to isolate the oxygen-evolving photosystem II (PSII) core complex from *Nicotiana tabacum* was developed. A PSII having a His-tag extension made of six or ten consecutive histidine residues at the N- terminus of the PsbE subunit was purified by a single-step Ni^{2+} NTA-affinity column chromatography after solubilisation of the thylakoid membranes using different mild detergents. Characterization of the oxygen evolution and the subunit composition by immunoblotting and mass spectroscopy revealed that the His-tagging did not affect the functional integrity of the PSII reaction center. The final PSII core complex was purified in a single step from solubilised thylakoids in less than 14 hours getting a very pure sample in high amount. The isolated core complex was in a dimeric form as demonstrated by Blue Native PAGE, analytical gel filtration and single particles analysis; with a molecular mass of about 500 kDa, consisting of D1, D2, CP43, CP47, 33 kDa and low molecular weight proteins. The preparation retains a high rate of oxygen-evolving activity but showed different stabilities of the binding of the three extrinsic proteins. The subunit of 33 kDa was always present in the preparations with a constant amount, whereas the 23 and 17 kDa subunits were always in less and unconstant amounts. Nevertheless the oxygen evolution was not depending on the amount of the 23 and 17 kDa subunits. Furthermore the preparation showed a high oxygen-evolving activity of 1390 μmol/mg $Chl \cdot h^{-1}$ in presence of betaine, while its activity was 440-680 μmol/mg $Chl \cdot h^{-1}$ in its absence. The presence of 1.0 mol/L betaine during the isolation of PSII increased the preservation of the photochemical activity hence the oxygen evolution. It was inferred from these results that His-tagging does not affect the functional and structural integrity of the PSII core complex and that the "His-tag strategy" is highly useful for biochemical, physicochemical and structural studies of higher plant PSII.

PSII is directly involved in two essential processes, the efficient capture and funnelling of light energy to the reaction centre and the controlled dissipation of excess excitation energy. Those functions require structural and functional flexibility in order to be performed with high efficiency. Moreover light-harvesting proteins respond to an external signal, the thylakoid pH, to induce feedback control regulating those activities in every moment. This process called non-photochemical quenching (NPQ) is mainly depending on the xanthophyll cycle and the PsbS protein (Szabo *et al.* 2005).

In this work several new evidences related with those two processes were found. The subunit PsbS is a polypeptide whose involvement in the NPQ processes is debated. Nevertheless, its position in the PSII complex and the mechanisms by which this subunit contributes to carry out the NPQ functions are not definitely known. In addition it is not sure if it is a pigment binding protein or not. Currently several lines of evidence indicate that this subunit is able to bind two molecules of zeaxanthin, one of the pigments involved in the xanthophyll cycle. In this work immunolabelling indicated that PsbS is tightly bound to the PSII core dimer, monomer and incomplete PSII particles as Reaction Centre-CP47 (RC-CP47). Furthermore qualitative HPLC indicates a complete absence of zeaxanthin in the sample and the presence of violaxanthin, another pigment involved in the xanthophyll cycle. The absence of zeaxanthin was expected considering that the plants were harvested after the dark period and that the particles were purified in complete dark (or in green light), whereas the presence of violaxanthin was unexpected considering that so far no evidence of violaxanthin bound to PSII cores devoid of LHC proteins was reported. Furthermore the amount of chlorophyll b was not relevant for suspecting this pigment bound to PsbS. Therefore we conclude that if PsbS is able to bind chlorophyll it has to be a chlorophyll a. The results indicate that PsbS could be able to bind not only zeaxanthin but also violaxanthin.

The extrinsic subunit Psb27 was also found in this preparation. The presence and the amount of this subunit, reported to be involved in the repair of damaged PSII, was not constant and therefore behaving as the other two extrinsic proteins 23kDa (PsbP) and 17kDa (PsbQ).

Electron crystallography studies on spinach PSII particles purified by differential solubilisation resulted in crystalline tubes with new unit cell constants. From data analysis a density map at 15Å resolution was obtained with a $P22_12_1$ symmetry. However, at this resolution it cannot be said if the internal symmetry axis is related with the two-fold axis of the dimer or the pseudo two-fold axis of the monomer.

In conclusion a method to isolate functional, pure PSII core complexes was developped. These samples, together with the improved 2d crystallisation protocol could lead to crystals with higher quality hence better resolution density maps in the future.

Abbreviations:

2D: two-dimensional
3D: three-dimensional
AA: Acrylamide
ACA: aminocaproic acid
ATP: Adenosine triphosphate
BisAA: Bis Acrylamide
BN-PAGE: Blue Native Polyacrylamide Gel Electrophoresis
CEB : Crude Extract Buffer
Chl: chlorophyll
CMC: Critical Micelle Concentration
CP24: minor light-harvesting complex (Lhcb6)
CP26: minor light-harvesting complex (Lhcb5)
CP29: minor light-harvesting complex (Lhcb4)
DCBQ: 2,6-dichloro-p-benzochinone
DGDG: digalactosyldiacylglycerol
FRB : First Resuspension Buffer
HPLC: High Performance Liquid Chromatography
LHCII: Light Harvesting Complex II
MALDI-Tof: Matrix Assisted Desorption Ionisation time of flight
MGDG: monogalactosyldiacylglycerol
NADPH: Nicotinamide adenine dinucleotide phosphate-hydrogenated
NPQ: Non Photochemical Quenching
OEC: Oxygen Evolving Centre
PC: Phosphatidylcholine
PEG: Polyethylenglycole
PQ: Photochemical Quenching
PSI: photosystem I
PSII: photosystem II
PVDV : Polyvinylidene fluoride
qI: photoinhibition
qT: state transition
MALDI-Q-Tof: Matrix Assisted Desorption Ionisation Quadrupole time of flight
RCI: Reaction Centre Type I
RCII: Reaction Centre Type II
RCs: Reaction Centres
SRB: Second Resuspension Buffer
TLC: thin layer chromatography
TM: transmembrane (helices)
β-DDM: β-dodecylmaltoside
β-HTG: β-heptylthioglucoside
β-OG: β-octylglucoside
ΔpH: pH gradient across the thylakoid membrane

Introduction

Photosynthesis is the biological process by which plants, some group of bacteria and protists convert the visible sunlight energy in primary molecular bound energy that can be used directly for the basic metabolism or be converted to produce sugar. The sugar is in turn converted by cellular respiration into Adenosine triphosphate (ATP), the "fuel" used by all living organisms. In this way photosynthesis is responsible for the energy production in all earth's ecosystems.

The conversion of unusable sunlight energy into usable chemical energy occurs by an intermediate step where the energy is absorbed by "molecular photon traps", the photosynthetic pigments. These molecules are able to absorb light energy at specific wavelengths and are able to transfer it as excitation energy via other pigments to a final

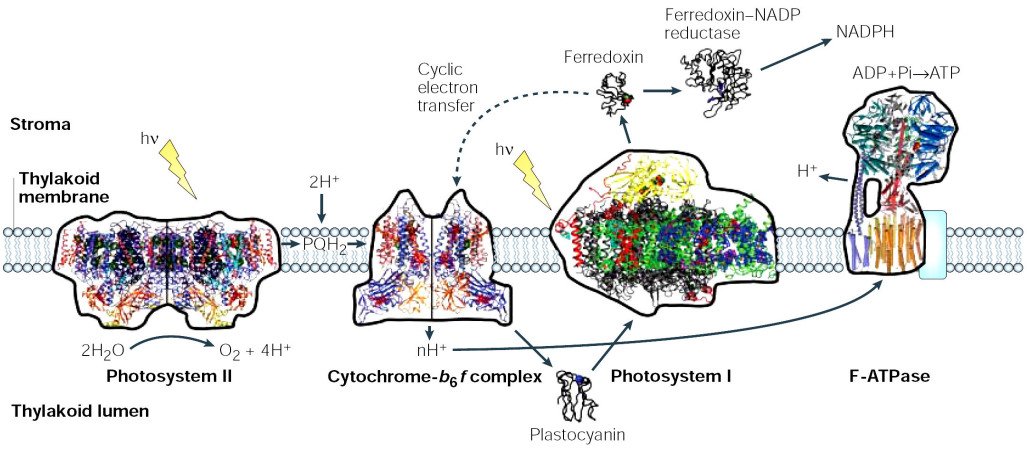

Figure 1. Overview of the main protein complexes involved in oxygenic photosynthesis.
Photosystem II, Cytochrome-b_6f complex, Plastocyanin and Photosystem I are involved in the photoreactions and electron transfer; F-ATPase and Ferredoxin-NADP reductase are involved in the NADP reduction and ATP production respectively. The Light Harvesting Complex (LHCII) trimer, a protein complex typical for higher plants, is not shown.

pigment acceptor. The last pigment acceptor uses this excitation energy for charge separation and to start a redox chain that will release free energy in every redox step. One part of the free energy is used for pumping protons across the photosynthetic membrane and thereby creating a proton gradient which is used to produce ATP by the enzyme ATPase. Simultaneously the electrons are used to produce Nicotinamide adenine dinucleotide phosphate-hydrogenated (NADPH) by the Ferredoxin- NADP reductase. Both ATP and NADPH are crucial molecules in the metabolic processes and particularly in the energetic metabolism.

The different kinds of photosynthetic processes can be classified according to the first electron donor. When water is used as a first reductant in the redox chain it is called oxygenic photosynthesis that is currently the main kind of photosynthesis on earth. Oxygenic photosynthesis is the main producer of O_2 and together with the other kinds of photosynthesis is the main user of CO_2 in the earth. For these reasons this process is the most prominent factor responsible for the dynamics of the O_2 and CO_2 biogeochemical cycles.

In oxygenic photosynthesis the conversion of sunlight into chemical energy is mainly driven by three multisubunit membrane protein complexes named photosystem II (PSII), cytochrome b_6f complex and photosystem I (PSI) (Fig.1).

1.0. Origin and evolution of photosynthesis

Paleontologic data have shown that since the Archaean eon, in the Precambrian Era, it is possible to find first traces of carbon fixation from photosynthetic organisms. The most ancient fossil that testifies the existence of oxygenic photosynthesis was found in rocks that are 3.5 billion years old. In these rocks special formations, called stromatolites, were found. These formations were interpreted as deposits of bacterial and cyanobacterial ancestors, indicating that oxygenic photosynthesis might have evolved by this time (Schopf 1993; Abigail *et al.* 2006). These results lead to the conclusion that photosynthesis has evolved very early in the history of the Biosphere.

1.1. Origin of the photosynthetic machinery: phylogeny and structural origin

As mentioned above, the conversion of light energy into chemical energy is followed by a redox chain that is responsible for the reduction of the last electron acceptor and therefore the production of NADPH as well as for the production of ATP through a proton gradient across the thylakoid membrane. Three groups of prokaryotes and all the chloroplast containing eukaryotes are able to catalyse photosynthetic electron transfer. The three groups of prokaryotes are the purple bacteria divided into two families: Rhodospirillaceae (or non sulphur bacteria) and Chromatiaceae (or sulphur bacteria), the green bacteria and the cyanobacteria (or blue-green algae). The prokaryotic group of Cyanobacteria and the photosynthetic eukaryotes use water as electron donor to perform oxygenic photosynthesis.

It is a common opinion that photosynthetic organisms have evolved from bacteria, where a metabolic pathway with some kind of electron transport was already existent. A primitive cytochrome *b*/Fe-S complex involved in anaerobic respiration could have been a possible predecessor of the reaction centre proteins. This metabolic pathway was widely spread amongst the common ancestor of bacteria and archaea (Xiong et al. 2002; Meyer et al. 1994) before the evolution of photosynthetic bacteria started. The primitive cytochrome *b*/Fe-S complex could have provided the necessary transmembrane apparatus for pigment binding sites and the electron transport cofactors organisation (Xiong *et al.* 2002; Meyer *et al.* 1994).

Phylogenetic studies on genes directly involved in photosynthesis suggest that non-oxygenic photosynthesis is older than oxygenic photosynthesis. Thus purple bacteria could be the earliest photosynthetic bacterial group followed by green-sulphur bacteria and green non-sulphur bacteria, heliobacteria, cyanobacteria and the photosynthetic eukaryotes (Xiong *et al*. 2000; Xiong *et al*. 2002).

Photosynthetic organisms can be classified in two phylogenetic groups depending on the type of photochemical reaction centres. In the Reaction Centre Type I (RCI) the last electron acceptor is a Fe-S cluster as in PSI and RCs of green sulphur bacteria or heliobacteria; in the Reaction Centre Type II (RCII) a mobile quinone is the last acceptor as in PSII and in the RCs of purple or green filamentous bacteria. Phylogenetic

analyses of PSI and PSII core reaction centre proteins show several strong structural similarities which are also found in RCI of green sulphur bacteria and RCII of purple bacteria (Nitsche *et al.* 1991; Barber *et al.* 1999). These similarities support the hypothesis of a common evolutionary origin of all reaction centre complexes (Blankenship *et al.* 1998; Mulkidjanian *et al.* 1997; Schubert *et al.* 1998; Vermaas *et al.* 1994).

The major difference in the two groups of RCs is the relationship between polypeptides and photocofactors. In fact, the core protein in the existing RCI contains both electron transfer components and intrinsic antenna chlorophylls within its 11 transmembrane (TM) helices. In the existing RCII, for example PSII, these functions are separated between different proteins with a smaller number of TM helices. Studies of homology on the PSII intrinsic antenna proteins CP43 and CP47 have shown primary sequence resemblance to the antenna domain in the core protein of the heliobacterial RCI. This supports the hypothesis that the primordial RCII was similar to existing RCIs because it was constructed of large 11 TM helix proteins that contained both the electron transfer components and the intrinsic antenna as opposed to the current PSII and purple bacteria reaction centre. In conclusion the RCII ancestor probably had some RCI characteristics (Nelson *et al.* 2005).

From studies on the RCs phylogeny it seems to be evident that the ancestor of the RCI, similar to the one present in the actual green sulphur bacteria (Chlorobiaceae), could have been the common ancestor of all photosynthetic reaction centres (Büttner *et al.* 1992). In this ancestor a primary gene duplication was responsible for a homodimeric reaction centre as in green sulphur and heliobacteria (Liebl *et al.* 1993) followed by a secondary heterodimerisation leading to the reaction centres currently operating in most photosynthetic organisms (Blankenship *et al.* 1992; Heathcote *et al.* 2003). This theory, in order to be validated, needs a gene encoding for a large protein that operated as a homodimer like the protein PscA from current green sulphur bacteria. In this homodimer each monomer was capable of binding 20–40 bacterial-chlorophylls with two of them in close proximity and in an appropriate environment to form the excitation trap capable of charge separation Heathcote *et al.* 2003). Moreover, the RCs in green sulphur bacteria harbour both an iron-sulphur cluster and loosely bound quinones. This RC is similar to PSI and the involvement of loosely bound quinones suggests that the

origin of both PSI and perhaps PSII reaction centres was a similar homodimeric PSI-like reaction centre (Nelson *et al.* 2005).

1.2 Photosystem II composition in cyanobacteria, algae and higher plants

PSII is a polypeptide-cofactor complex organised as a heterodimeric multisubunit protein embedded in the thylakoid membrane. PSII monomers are related to each other by a twofold axis perpendicular to the membrane plane and each is characterized by a pseudo-twofold symmetry. Constitutive PSII polypeptides are divided in intrinsic and extrinsic subunits. The intrinsic subunits are membrane polypeptides whereas the extrinsic subunits are water-soluble proteins positioned at the luminal side of the thylakoid or plasma membrane (Fig.2) (Ferreira *et al.* 2004; Loll *et al.* 2005).

1.2.1. Intrinsic subunits

The polypeptides D1 and D2 that are located in the centre of each monomer are involved in the processes of charge separation, electron transfer and photoprotection. They have a high homology and consist of 5 transmembrane helices and several large loop regions on the luminal and the stromal side (Ferreira *et al.* 2004; Loll *et al.* 2005).

D1 (PsbA) binds the majority of the cofactors involved in charge separation, electron transport and it is very sensitive to the photoinduced damage. Therefore this polypeptide is involved in a high rate cycle where photodamaged D1 is replaced with functional D1 in order to keep a save and functional PSII. In higher plants but not in red algae and cyanobacteria the N-terminal threonine can be reversibly phosphorylated with a function of regulation activity (Barber 1997; Ohira *et al.* 2005; Ohnishi 2006).

D2 (PsbD) has a slightly higher molecular weight than D1 and also in D2 the N-terminal threonine can be reversibly phosphorylated. The D2 protein is involved in the binding of active cofactors to a lesser extent than D1 but nevertheless it contains active cofactors mainly involved in photoprotection (Barber *et al.* 1997; Kitajima *et al* 2006; Ishikita *et al.* 2007).

CP47 (PsbB) is an highly conserved protein consisting of 6 transmembrane helices with the N and C termini exposed to the stromal surface and a large luminal loop between helices V and VI. Structural data indicate that it binds 16 chlorophylls a and is involved in the binding of 4 β-carotene molecules. CP47 with its pigments creates a core light harvesting system for the reaction centre. In addition a structural function seems to be related with this subunit. In fact several experiments have shown its influence on PSII assembly and stability (Bricker *et al.* 2002).

CP43 (PsbC) is in many ways homologous to CP47 with a motif of 6 transmembrane helices and a large luminal loop in the same position as in CP47. Structural studies show that 13 chlorophyll a and 3 β-carotene molecules are bound to CP43. Therefore the main function of CP43 is just like CP47 the harvest of light. Moreover CP43 is together with D1 involved in the positioning and stabilisation of the manganese cluster. This protein is more weakly bound to PSII than CP47. This can be related to some movement during the D1 cycle in vivo. Furthermore the N-terminal threonine of CP43 in higher plants can also be phosphorylated (Bricker *et al.* 2002).

PsbE and PsbF are two plastid-encoded subunits of one and two transmembrane helices respectively. They are the α and β subunits of the cytochrome b_{559} and create a heterodimer where a haem, the cytochrome b_{559}, is coordinated as a cofactor to the only histidine residue contained in their sequences. This heterodimer that is closely associated with D1 is suspected to have a photoprotective role by acting as an electron acceptor or electron donor under conditions were electron flow is not optimised (Loll *et al.* 2005; Barber 1997; Kitajima *et al* 2006).

The subunits PsbH, I, J, K, L, M, N, T, X, are little single transmembrane helix polypeptides that are found in all types of oxygenic organisms but their role in PSII is not always clear.

From structural data it seems to be evident that the subunits PsbT, L, M have a structural function since they are involved in the dimerisation. They are located in the centre of the dimer around the two-fold symmetry axis (Loll *et al.* 2005). Furthermore the PsbL subunit is also involved in the assembly of CP43 (Suorsa *et al* 2004) and PsbT has also been shown to be required for an efficient repair of photodamaged PSII (Ohnishi *et al.* 2001).

Studies on mutants with deleted PsbJ have shown that this protein is essential for providing the PSII core dimer with a conformation that allows a correct association with the LHCII complex, responsible for a efficient capture of light energy. Besides PsbJ and L of higher plants are involved in the correct association of the extrinsic proteins PsbO, P and Q and hence indirectly related with the oxygen evolution activity of PSII (Suorsa *et al* 2004).

Several functions are related with the subunit PsbH. It seems to be involved in the correct bicarbonate binding on the PSII acceptor side and in the fast PSII repair cycle as response to irradiance damage (Komenda *et al.* 2002; Bergantino *et al.* 2003). Furthermore PsbH increases the affinity of CP47 for the rest of PSII, contributes to a prompt incorporation of new D1 into PSII complexes and enhances the D1 maturation (Komenda *et al.* 2005; Bergantino *et al.* 2003; Rokka *et al.* 2005).

PsbI is involved in the stabilisation of PSII, in the phosphorylation of the main subunits and it has a structural role in the full functionality of the Q_A binding site (Schwenkert *et al.* 2006).

The subunit PsbK has evident effects on the assembly and the stability of PSII complexes and several studies report a strong interaction with CP43 in green algae (Sugimoto *et al* 2003) and in higher plants (Rokka *et al.* 2005). Furthermore several studies on mutants of *Synechocystis* where the PsbX gene was deleted have shown that the function of this subunit is positively related with the amount of active PSII (Funk 2000; Katoh *et al.* 2001).

PsbW and PsbS are two nuclear-encoded photosystem II (PSII) subunits that belong to the group of transmembrane polypeptides exclusively found in higher plants. PsbW is a single helix membrane protein involved in the stabilisation of the higher complexes and the core dimer (Shi *et al.* 2000).

The 22kDa subunit called PsbS has a high homology with the Light Harvesting Complex II (LHCII) proteins and is predicted to have a motif of four transmembrane helices. Function and localisation of this subunit are still not clear although mutational analyses have shown that PsbS is involved in the non photochemical quenching process (Xiao-Ping Li *et al.* 2000). It is still not clear if PsbS is an integral part of the PSII core complex or a dynamic protein that can be attached to the core only at certain light conditions (Funk *et al.* 1995; Szabo *et al.* 2005).

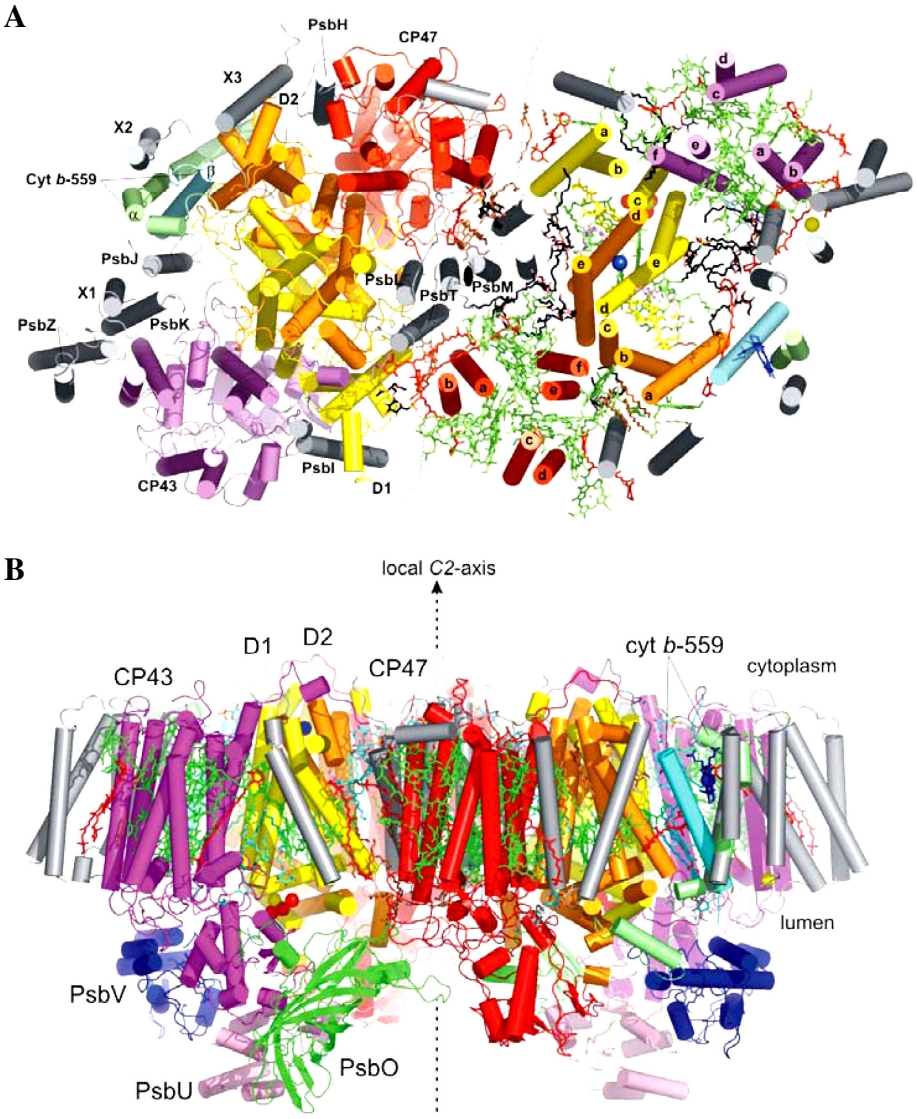

Figure 2: PSII core complex structure.

PSII core complex top view (A) and lateral view (B) from *S. elongatus* (Loll B. *et al.* 2005). The extrinsic subunits PsbV and PsbU are substituted in higher plants with the three subunits: PsbP, PsbQ and PsbR.

1.2.2. Extrinsic subunits

PsbO (33 kDa) is the only extrinsic protein equally conserved in cyanobacteria, green algae and higher plants. The soluble proteins PsbP (23kDa), PsbQ (17kDa) and PsbR (10kDa) are the other extrinsic subunits only found in higher plant Photosystem II.

These polypeptides are exposed to the luminal side of the core and their activity is in general related with the functionality of the Oxygen Evolving Centre (OEC) (Soursa *et al.* 2006; Ifuku *et al.* 2005).

PsbO and PsbQ subunits are required for assembling and stabilising the OEC. It was also shown that they are indispensable for maintaining the photoautotrophy (De Las Rivas *et al.* 2005).

PsbP is involved in retaining Ca^{2+} and Cl^{-}, two inorganic cofactors involved in the water-splitting reaction. PsbR positively influences the light-saturation rate and the oxygen evolution. Furthermore this polypeptide is related with the stable binding of PsbP and PsbQ proteins to the core (Soursa *et al.* 2006; Ifuku *et al.* 2005).

PsbU and PsbV are the cyanobacteria's extrinsic proteins. In the current opinion these proteins are considered as homologues of PsbP and PsbQ, respectively. Nevertheless especially for PsbV this simplification is not completely exhaustive. In fact in PsbV's structure there is a cofactor, the cytochrome b-550, that is absent in the homologue subunit of higher plants (Thornton *et al.* 2004; Loll *et al.* 2005).

Another extrinsic subunit called Psb27 was originally identified as a ~11 kDa polypeptide in a PSII preparation from *Synechocystis* 6803 (Ikeuchi *et al.* 1995). This polypeptide has one predicted membrane-spanning domain followed by a cleavage site for a signal peptidase II. Thus, the Psb27 protein is expected to be a lumen-localized extrinsic protein of PSII. The Arabidopsis homologues (At1g03600 and At1g05385) of Psb27 were found in a proteomics study of the thylakoid lumen (Peltier *et al.* 2002). Although Psb27 is associated with PSII in many model organisms, this protein was not identified in the cyanobacterial PSII crystal structure (Loll *et al.* 2005). Furthermore, analysis on a mutant of *Arabidopsis* with a loss of Psb27 function has been described. This mutant showed a lower PSII activity and lower amount of D1 protein under high-light-illumination compared to the wild-type. Furthermore the quantity of PSII complexes and electron transfer within PSII was not affected. This demonstrated that Psb27 is not essential for oxygenic photosynthesis and PSII formation. Instead it seems to be related with the recovery process of PSII as shown by the decreased levels of D1 protein in the mutant (Hua chen *et al.* 2006).

1.3 Electron-transfer and charge separation in Photosystem II

The origin of photosynthetic pigments seems to be related to anaerobic heterotrophic bacteria that used the solar energy for assimilating organic substances from the environment. In that process, bacteriochlorophyll was used and it evolved the ability to use CO_2 as substrate. The connection of this pathway with the glucose biosynthetic pathway, evolved before, gave the origin for anoxygenic photoautotrophy. During this phylogenetic phase, energy was harvested only by one photosystem and used for producing glucose. This very efficient process which has used hydrogen or iron (Fe^{2+}) as electron source has been limited by the low concentration of these electron donors in the environment. The solution of that limitation was obtained when two interconnected photosystems evolved with one of them, photosystem II, able to use water as electron source. That new hydrolytic form of photosynthesis was typical for cyanobacteria and lead to emission of oxygen, a toxic gas for the anaerobic competitors (Blankenship *et al.*1998).

How could the transition to a new electron source occur? The answer to that question is not completely clear but a strong cooperation between several factors (biotic and abiotic) seems to be responsible. The main theory about origin of the OEC was put forward by Blankenship and Hartman (1998). Their theory assumes an evolutive multi-step process with a co-evolution of both the electron donor complex and the bacteriochlorophylls involved in the primary charge separation. According to this theory probably the Fe^{2+} that was present in high quantities in the Archean oceans was used as early electron donor as in some current photosynthetic purple bacteria. Furthermore a significant amount of hydrogen peroxide was also present in the Archean waters. Hydrogen peroxide was a toxic substance for the bacterial cell so that probably a Mn-catalase with a di-manganese catalytic site was developed in order to detoxify this substance. Later this enzyme could be recruited to extract electrons for the first electron acceptor creating a primeval OEC. Finally, the dimanganese centre evolved to become the four-manganese centre as in the current OEC so that it could extract electrons from water. Even though the sequence of events described above provides a plausible way in which the early reaction centre might have begun to produce oxygen from hydrogen peroxide it does not address the issue how the highly oxidizing species that are needed

to split water developed. In other terms how in the current systems the first electron acceptor and the charge separation developed? According to this theory the answer stays in the reduction potential and in the structure of the primary donor. In fact in purple photosynthetic bacteria the reduction potential of the primary donor ($P870/P870^+$) is higher than the H_2O_2/O_2 couple and in that condition $P870^+$ can accept electrons from the hydrogen peroxide. In opposition to that in the couple H_2O/O_2 which has a higher reduction potential than $P870/P870^+$, the reduction is thermodynamically not possible. According to the theory by Blankenship and Hartman the reduction potential of the oxidized primary donor was in some manner increased up to 1V i.e. higher than the H_2O/O_2 couple and in this way the water splitting become thermodynamically possible. Indeed, several work on *Rhodobacter sphaeroides* have shown that the redox potential of the primary donor bacteriochlorophyll a in reaction centres could have raised from mutations that increased the number of hydrogen bonds in the bacteriochlorophyll. But an increase in the reduction potential for the oxidized primary donor implies at the same time an increase in the reduction potential of the excited primary donor. In these conditions the excited state potential is increased too much and so the quantum yield of electron transfer falls because now the energy of the reduced acceptor lies above the energy of the excited state of the donor. The only way for getting a functional system was a lower increase of the reduction potential which was possible by increasing the photon energy by shifting the absorption maximum from the near infrared into the visible region. Such transition was possible by using chlorophyll a instead of bacteriochlorophyll a (Fig.3a) (Blankenship *et al.*1998).

In the last two years two PSII high resolution structures from the cyanobacterium *S. elongatus* were solved (Ferreira *et al.* 2004; Loll *et al.* 2005). In these structures it was possible for the first time to check directly some details about the Mn cluster architecture and its amino acid interactions. Furthermore that structure gave a confirmation about the strong stabilisation by D1 and PsbO amino acid residues.

In both structures it was not possible to get information about the Mn cluster at a comparable high resolution as for the rest of the holocomplex because of the high sensitivity of PSII for X-rays and the damage induced by X-ray absorption on the Mn atoms. Nevertheless it is possible to assign from the electron densities a place for four Mn organised as a “hook” resembling a “Y- shaped” organisation. Moreover it is also

possible to assign a position for a Ca^{2+} ion positioned on top of the four Mn-atoms between the Mn group and the tyr-Z, an acceptor positioned between the Mn-Cluster and the first electron acceptor chlorophyll P680 (Fig.3b) (Ferreira *et al.* 2004; Loll *et al.* 2005).

Recent PSII structures from *S. elongatus* have clearly shown the distribution of cofactors in both the main and the side branch of the holocomplex. From these structures it was also possible to understand details about the residues involved in the stabilisation of the cofactors involved in the electron transfer.

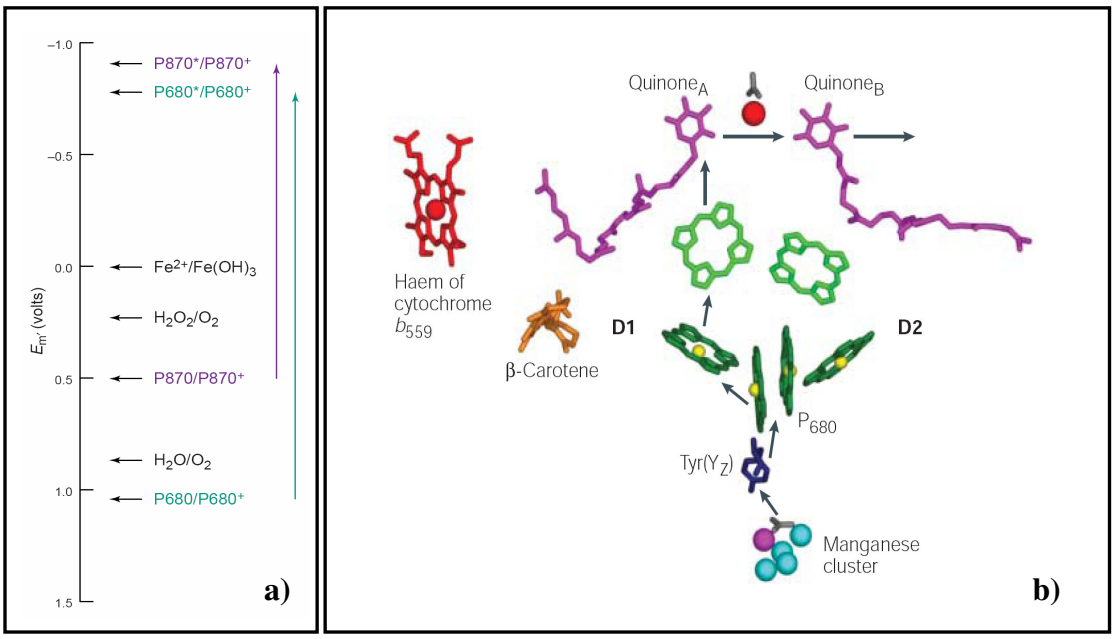

Figure 3:

a) Reduction potentials at pH 7 and 25°C (E_m) of various redox couples involved in the photosynthetic electron transfer.

All potentials shown are relative to the normal hydrogen electrode and are written as reduced/oxidized forms of the redox couple. The vertical arrows on the right indicate the photon excitation in the purple bacterial reaction center ($P870/P870^+$) and the photosystem II reaction center ($P680/P680^+$) (from Blankenship *et al.*1998).

b) Electron transfer in PSII.

In the picture the cofactor composition of PSII is shown. The arrows show the electron pathway involved in the water splitting and charge separation.

Water splitting by OEC and special pair photooxidation ($P680^+$) are the first reactions in the photochemical process. The water splitting reaction releases two protons into the lumen and two electrons that one by one will be transferred reducing Tyrosine Z (Tyr $Z^{\cdot}$).This residue of tyrosine, able to accept only one electron in every redox cycle, is located in the polypeptide D1 of the holocomplex and will reduce $P680^+$.

The driving force of the electron transfer is the photooxidation of P680 to $P680^+$. This step is light dependent and consists in an electron transfer (photooxidation) towards the next acceptor, a Chorophyll a molecule (Chl_{D1}) that will use the electron for reducting a Pheophytin ($Pheo^{\cdot}$)**.** The electron is transferred from $Pheo^{\cdot}$ to Q_A which is a firmly bound plastoquinone positioned in a hydrophobic cavity. All these cofactors are positioned in the D1 region of the PSII core and the redox cycle consists of single electron transfer.

The next electron acceptor, Q_B, is hand by D2 in a lipophilic cavern that in *S. elongatus* opens with two gates, one in the middle of the membrane and the other towards the cytoplasm. Q_B, differently from the previous acceptors, accepts two electrons and two protons for being fully reduced and moves through the membrane from PSII to the Cytochrome b_6f complex. After this step another Q_B in the oxidised state can move by diffusion to the binding pocket so that another redox cycle can start.

1.4 Light harvesting and photoprotection

Photosynthesis works in the visible region of the electromagnetic spectrum at wavelengths between 390 and 760 nm. The photons with wavelength in this range are captured from the pigments and converted to redox energy but how do light and pigments interact in the light reactions of photosynthesis?

These kinds of interactions are well explained from the Stark-Einstein´s law. According to this theory which involves bound electrons of molecular orbitals in the ground state, one photon can excite only one electron each time.

Through excitation, every valence electron of the pigments can move from the ground state to states of higher energy. Thereby the energy between the excited state and ground state is equivalent to the energy of the absorbed photon.

One part of the excited state energy is used for the photosynthesis while the other part is lost as heat and fluorescence in accordance with the thermodynamic's laws. The excited state of the pigments lasts for just a short time in the order of nano or femtoseconds and after this time the energy can decay as heat or/and fluorescence. Alternatively the energy can be transferred from one molecule to the other by inductive resonance. This form of excitonic energy transfer only takes place when pigments are positioned in a specific distance and orientation as in the photosynthetic proteins. This energy transfer funnels energy towards the special pair in the reaction centres where the charge separation and the electron transfer take place.

As mentioned above photosynthetic systems have a variable number of pigments that act as light-harvesting antennas able to absorb and channel photon energy to the photochemical RC.

The efficiency of the energy transfer is not only important within the single light harvesting protein but also in between them. For that reason photosynthetic membranes need a dynamic and harmonic structural organisation that must be able to allow a dynamic and harmonic functionality between the protein complexes. Therefore, the arrangement of light harvesting proteins within the membrane must be in every moment the most efficient adaptation to specific environmental conditions. For this reason the thylakoid membranes of higher plants are not characterised by a static elementary structure. Instead, it is possible to find a repetition of higher complexes constituted of PSII dimers and LHCII trimers organised in higher structures as LHCII-PSII super and megacomplexes (Fig.4) (Dekker & Boekema 2005).

These higher complexes work as functional unities connected to each other by several bridge proteins such as the minor LHCIIs CP24, CP26 and CP29. This enables the plant to a fine tune to specific environmental conditions.

In general the effectiveness of the photosynthetic process is depending on two factors, the efficient collection of sunlight and the funnelling of excitation energy to the RCs.

On one hand this process is selected by nature for driving electron transport at the highest sustainable rate. On the other hand the excited states of chlorophyll and the molecular oxygen provide a potentially harmful environment able to damage proteins, lipids and pigments. For this reason several mechanisms of photoprotection were also developed. In fact the constitutive features in photosystems such as the presence of

carotenoids to scavenge singlet oxygen and trap triplet states of chlorophyll are combined with other photoprotective mechanisms which are induced under high levels of illumination to drive the dissipation of energy excess from excited singlet states of chlorophyll.

In the molecular principles of the light harvesting process chlorophyll a and b are bound to the apoprotein to constitute a protein-pigment complex where pigments are organised

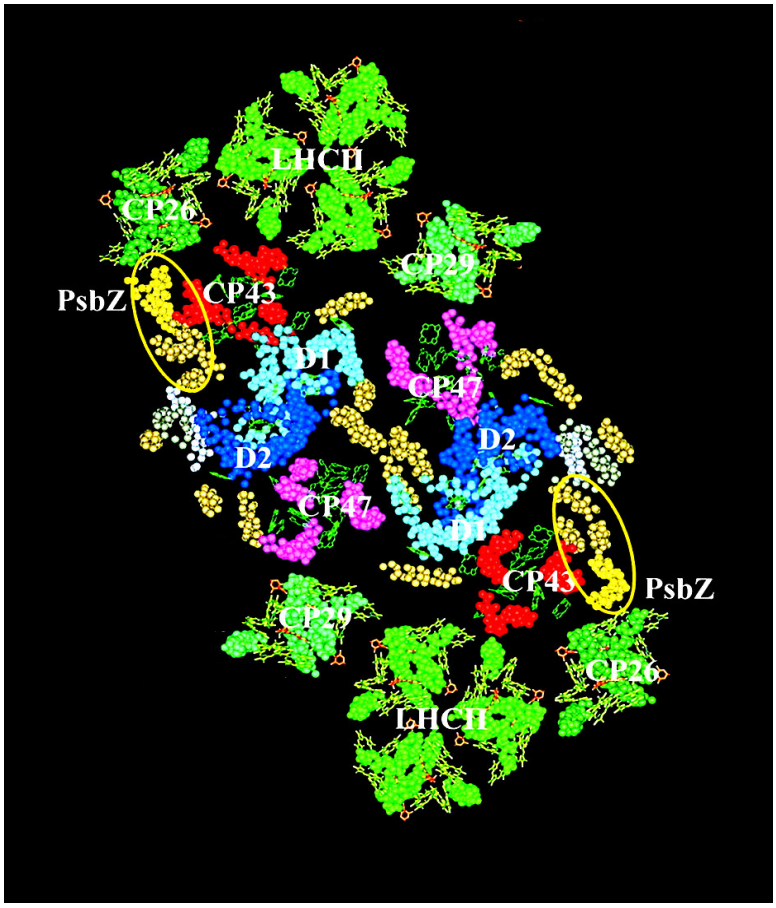

Figure 4. PSII-LHCII supercomplex organisation.

In the central part the PSII dimer with the main subunits D2 (blue), D1 (pale-blue), CP47 (pink) and CP43 (red) is shown. The periphery proteins LHCII trimer, CP26 and CP29 (in green) are also shown. Grey, brown and yellow are the peripheral subunits of PSII. The yellow circle shows the subunit PsbZ together with other three subunits (two of them identified by Loll B. *et al.*-2005- as the subunits PsbJ and PsbK) that seem to be involved in the supercomplex stabilisation (Nancy A. Eckardt 2001).

in different positions and orientations. Energy transfer between and within individual complexes is highly efficient and is exclusively related with the specific structures of the light-harvesting apoproteins. The evolution has worked (and still is working) on these apoproteins in order to have a sufficient amount of pigments to maximize the absorption but also to achieve an optimal pigment orientation which implies a careful tuning of the excited state energy levels to promote energy transfer. Furthermore the pigments must permit protein–protein contacts to allow appropriate routes of energy transfer between the complexes. All these factors are responsible for preventing the excited states tendency to dissipate by non-radiative decay or concentration quenching (Beddard & Porter 1976). In other terms the apoprotein provides a specific 'solvent' in order to create an environment that allows a high chlorophyll concentration without the probability of quenching by close chlorophyll-chlorophyll associations (Horton & Ruban 2005).

These structural and functional observations are valid for the elementar components such as LHCII and PSII as well as for higher organisations like LHCII trimers, PSII dimers, PSII-LHCII super and megacomplex up to the total thylakoid macro-organization. Furthermore PSII core and the light-harvesting system contain a number of other proteins, pigments and lipids that may have an essential role in the structure stability, function and protection of the light-harvesting systems (e.g. a specific phospholipid is required for LHCII trimerization; (Remy et al., 1982).

With this dynamic adaptation the system is able to protect the pigments from the excess of light hence to prevent decrease in efficiency. The photoprotection of the photosynthetic apparatus is related with the processes of Non-Photochemical Quenching (NPQ). This category includes all the processes where fluorescence quenching is not correlated with charge separation (Photochemical Quenching) but with energy dissipation in several ways. In general NPQ is related with three processes: photoinhibition, state transition and ΔpH across the thylakoid membranes.

The phenomenon of state transition (qT) is related to low levels of CO_2 and/or with high light conditions since both factors are responsible for the chloroplast reduction state. State transition consists of a general reorganisation of the protein complexes in the thylakoid membranes by LHCII phosphorylation after kinase activation which is responsible for an increase of LHCII-PSI associations and LHCII-PSII dissociation. The

effect is a reduction of the fluorescence yield of PSII due to the reduction of the antenna size. In these conditions the photosynthetic apparatus is switched from the oxygenic type with two photosystems working in series to an ATP generator type with PSI cyclic electron flow.

Photoinhibition (qI) is a fast response process that doesn't work by modifications in the distribution of absorbed light but through a dissipative de-excitation of absorbed electrons. Under high light conditions the saturation of the photosystems can be responsible for triplet chlorophyll a state (^{*3}Chl a) formation instead of the normal singlet state that is involved in the charge separation. ^{*3}Chl a easily reacts with molecular oxygen inducing the formation of its highly reactive singlet state which can be responsible for oxidative damage of the pigments and other functional components of the membrane. Finally this process is responsible for photooxidation and consequently photoinhibition. Carotenoids associated with the thylakoid photosynthetic complexes are able to prevent qI damage by acting as scavenger and therefore dissipating excess energy as heat (thermalization). Their activity prevents the activation of the oxygen and protects chlorophyll-protein complexes from photooxidation (Szabo *et al.* 2005).

When photosystems are working under light saturation and in general in situations where quinones are reduced in steady state, the charge separation in PSII RC is immediately followed by recombination. This recombination gives energetically the high probability to form triplet and singlet P680 state but in this part of PSII the carotenoids are not close enough to quench the excitation in the special pairs and they are not able to prevent the damage from oxygen activation (Loll *et al.* 2005). In order to prevent damage in PSII RC another mechanism of quenching and photoprotection was developed, the ΔpH dependent NPQ (qE). This is a very rapid feedback process that is regulated by changes in luminal pH, hence changes in ΔpH across the membrane. The pH changes are a function of the water splitting activity and proportional to the amount of electrons transferred in the redox chain. The amount of these electrons is depending on the light intensity. In conclusion the ΔpH across the membrane is a chemical way for sensing the light and the interactions between light and photosynthetic complexes. In other terms the system is able to sense the reduction state level and activates a feedback de-excitation by thermal dissipation if necessary (Szabo *et al.* 2005).

With this very sensitive process the system is capable of fast reactions on environmental changes (e.g. in light intensity) by sensing the reduction state of the membranes. If the reduction state level goes over a threshold, the sensing system reacts by activating the processes responsible for the photoprotection. The qE's molecular mechanisms are only partially understood but several experiments indicate that there are three factors involved in this process: the xanthophyll cycle (fig.5) and its pigments, the PsbS subunit of PSII and some components of the LHCII.

The xanthophyll cycle is a strongly pH dependent metabolic pathway because the enzymes involved, zeaxanthin epoxidase and violaxanthin de-epoxidase, are activated by low and high pH respectively. The metabolites of this cycle are three carotenoids: Violaxanthin (Vio), mainly present in low light conditions, Zeaxanthin (Zea), present in high light conditions and Antheraxanthin (Ant) that is an intermediate product in the interconversion of violaxanthin and zeaxanthin (fig.5). In conclusion, changes in pH

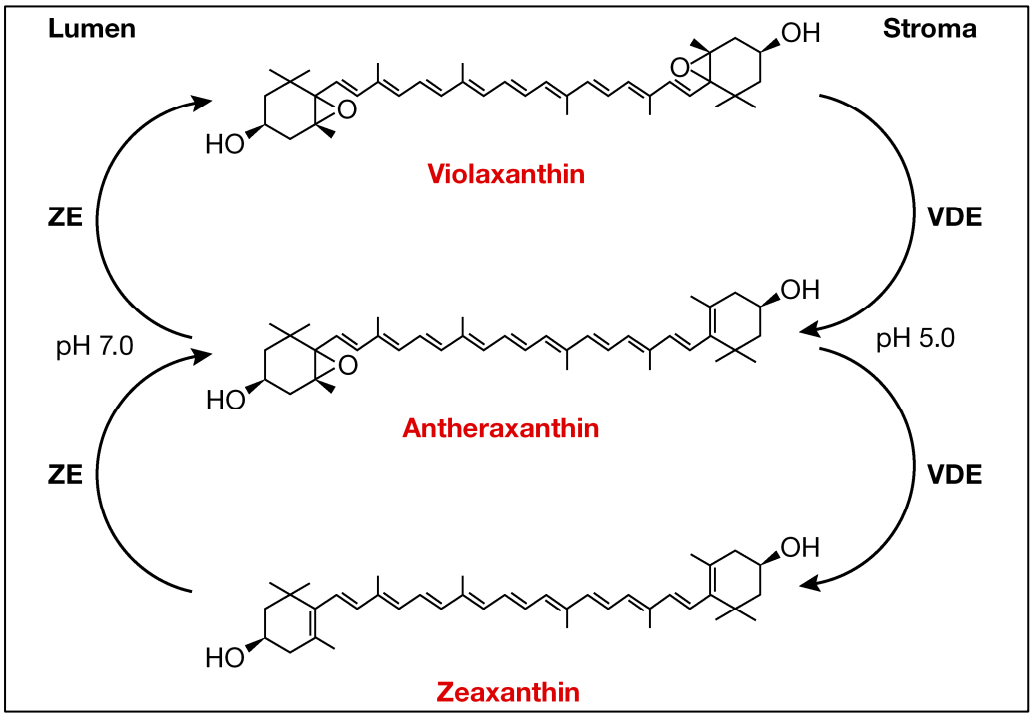

Figure 5. The xanthophyll cycle.

The violaxanthin de-epoxidase and the zeaxanthin epoxidase are indicated by VDE and ZE respectively.

level are responsible for the activation of the enzymes and for increasing the amount of their final products: low light violaxanthin and high light zeaxanthin. These two enzymes have a different localisation, an opposite pH activation and they catalyse the same pathway in opposite directions. Furthermore in both cases the reaction goes through an intermediate step where antheraxanthin is formed (Demmig-Adams & Adams W. W. 1996). All those products are involved in the NPQ process but it is not clear how and where precisely they perform this activity.

Theoretical calculations suggest that all the carotenoids are able to dissipate excitation energy by rapid internal conversion, nevertheless only those with ten or more conjugated carbon–carbon double bonds have an excited singlet state (S1) at an energy level low enough to accept energy from ^{*1}Chl*a* (Szabo *et al.* 2005). However the S1 state energy levels, determined *in vitro* for Zea (11 double bonds) and Vio (9 double bonds), enable not only Zea but also Vio for a direct quenching of ^{*1}Chl through singlet-singlet energy transfer (Polivka *et al*, 1999). In addition, the S1 state of Zea has a very short lifetime (10 ps) which allows rapid thermal dissipation of excitation energy. Furthermore the distinctive feature of Zea with respect to other xanthophylls is its presumed low ionization energy (Dreuw *et al*, 2003; Holt *et al*, 2004). The kinetics of the process have been investigated on pure carotenoids by several techniques (Holt *et al*, 2005) and the same experiments were performed on thylakoids from various *Arabidopsis* mutants with different pigment compositions. The results allowed the authors to conclude that zeaxanthin is responsible for the fluorescence quenching by charge transfer *in vivo* and *in vitro*. Holt *et al* (2005) proposed a model for explaining the process of excess energy dissipation by zeaxanthin cation formation. This model is divided in three steps. The first step is the energy transfer from the singlet Chl to create a Chl*a*–Zea heterodimer within a short time (11 ps), the second step with very fast kinetics (0.1–1 ps) corresponds to an electron transfer with the formation of a charge-separated Chl^{-}/Zea^{+} pair and finally the last step is a charge recombination with slow kinetics (150 ps). This mechanism is proposed to be responsible for excess energy dissipation during qE and indicates a direct quenching from zeaxanthin.

Although the sites of these events are not clear one possible candidate seems to be the PsbS subunit of PSII. Molecular modelling studies (Prafulla *et al.* 2006) and spectroscopical studies, *in vivo* and *in vitro*, have shown that PsbS could be able to bind

zeaxanthin (fig.6) (Aspinall-O'Dea *et al.* 2002) but there are no reports about the binding of violaxanthin. However, some reports claim that psbS is never pigmented (Dominici *et al* 2002). On the other hand, several peculiarities such as formation of Chl-Zea heterodimer and its related spectroscopical properties may be PsbS dependent (Szabo *et al.* 2005), but could also just arise from self-assembled head-to-tail (J-type) aggregates of zeaxanthin (Billstein *et al* 2005)

Furthermore mutants, knockout or defective in PsbS, seem to be also defective in qE but without alterations in PSII, LHCII and the xanthophyll cycle (Li *et al.* 2000; Peterson & Havir 2000). At the moment no molecular structure of PsbS is available hence the possible functional-structural considerations are depending on the sequence (molecular modelling) and on the spectroscopical properties of the protein. The protein sequence shows that PsbS contains several highly conserved acidic amino acid residues positioned on the luminal side. Those residues could be related with the activity of this protein, especially two residues (Glu122 and Glu 226) seem to be important for qE and if mutated affect the normal qE properties (fig. 6). It is generally assumed that

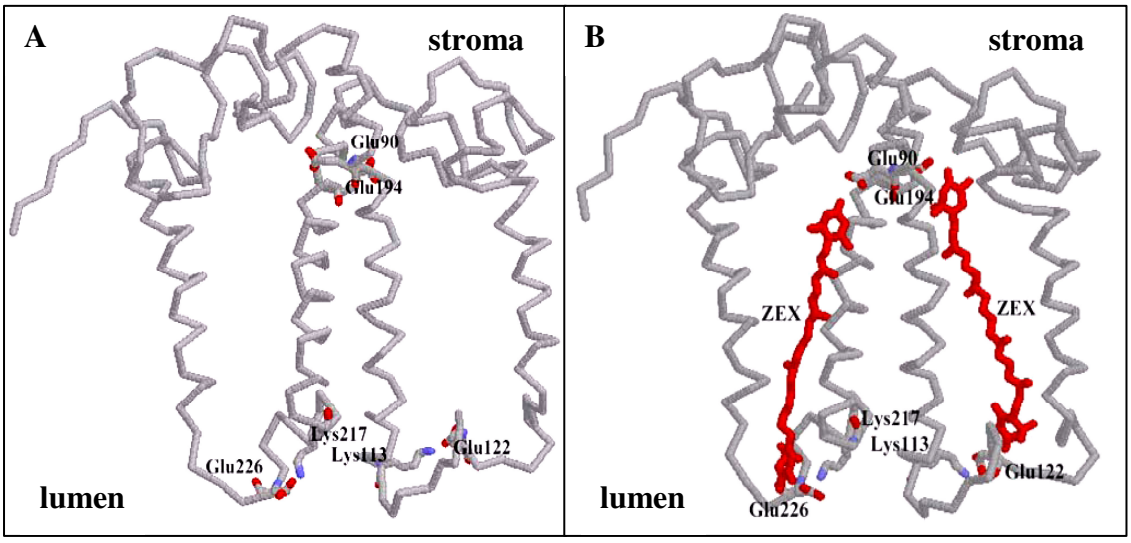

Figure 6. Molecular model for PsbS structure at pH <5.

In A the predicted structure of PsbS with the possible residues involved in the pigment binding is shown. The residues Glu226 and Glu122 could be involved in the binding of pigments and also work as pH sensor. B shows the same model with two zeaxanthin molecules each stabilised by three residues.

those residues are the luminal pH sensor site where they could be protonated inducing some conformational change that affect the possible ability to bind zeaxanthin or enable previously bound zeaxanthin to quench Chl excitation. In summary, PsbS could be the site where the pH sensor is located and also one of the places that play a key role in the xanthophyll cycle and therefore in qE (Niyogi 2005).

1.5 Aim of this work

In spite of the high resolution structure of PSII from cyanobacteria (Ferreira *et al.* 2004; Loll *et al.* 2005) the structural details of PSII from higher plants at present are not equally known. The unequal progresses of the research between these two kinds of PSII are depending on several factors. Current protocols of PSII purifications from higher plants show several disadvantages mainly related with the impurities of LHCII and PSI. This inconvenience can be more pronounced when the protein is purified in high quantity in which especially impurities of LHCII can occur. In crystallisation experiments huge amounts of protein are required and a lot of conditions are tested in order to find the ideal chemical-physical environment for protein crystallisation. In these conditions the high amount of LHCII can be responsible for the low quality of the crystals. Furthermore, protocols for purification of PSII from higher plants relies on the use of strong detergents like Triton that are aggressive to the protein and are difficult to remove after purification. For these reasons residuals impurities of other proteins and detergents can create interferences in the following studies on PSII. Moreover it should be also mentioned that PSII from higher plants is less stable than the PSII from thermophilic organisms. For all these reasons the structural and functional details of PSII from higher plants are not as well known as in the case of PSII from cyanobacteria. The availability of transgenic tobacco strains modified with 6 or 10 His-tags at the plastidic-encoded psbE subunit enables the purification of PSII by NTA affinity chromatography. Through this technique that until now was only used for PSII from algae and cyanobacteria, it was possible to work out the problems reported above. At the beginning of this work no detailed purification procedure was developed so that one aim was the development of a purification protocol for a highly pure and stable PSII

suitable for crystallisation experiments. The functionality of the PSII particles in terms of oxygen evolution and the pigment composition by preliminary HPLC studies were also tested. A second aim was the characterisation of PSII in terms of subunit composition by MALDI-TOF, Q-TOF mass spectrometry, immunoblot analysis and its intactness by gel filtration, Blue Native PAGEs (BN-PAGEs), single particles analysis and spectroscopical studies.

II. Material and methods

2.0. Material

2.0.1 Suppliers

Amersham Bioscience (http://www.amershambiosciences.com)

Anatrace (http://www.anatrace.com)

Biomol (http://www.biomol.de/inhalt.php)

Calbiochem (http://www.emdbiosciences.com/html/CBC/home.html)

Fermentas (http://www.fermentas.com)

Glycon (http://www.glycon.de)

J.T.Baker (http://www.jtbaker.nl/)

Merck KgaA (http://www.merck.de)

Millipore (http://www.millipore.de)

QIAgen (http://www1.qiagen.com)

Roche (http://www.roche.com/home.html)

Roth (http://www.carl-roth.de)

Serva (http://www.serva.de)

Sigma-Aldrich & Fluka (http://www.sigmaaldrich.com)

Vivascience (http://www.vivascience.de)

2.0.2 Chemicals

Acetic acid Merck, Darmstadt (Germany)

Acetone, HPLC grade Merck, Darmstadt (Germany)

Agarose Carl Roth, Karlsruhe (Germany)

$AgNO_3$ Carl Roth, Karlsruhe (Germany)

$AlCl_3$ Merck, Darmstadt (Germany)

6-Aminocaproic Acid Carl Roth, Karlsruhe (Germany)

Ammoniumpersulfat Serva, Heidelberg (Germany)

Ascorbic acid Merck, Darmstadt (Germany)

Betaine Fluka, Buchs (Switzerland)

$BiCl_3$ Merck, Darmstadt (Germany)

$Bi(NO_3)_3$ Merck, Darmstadt (Germany)

Bis-Tris Merck, Darmstadt (Germany)

BSA (Bovine serum albumin) Carl Roth, Karlsruhe (Germany)

Butylated hydroxytoluene (BHT) Carl Roth, Karlsruhe (Germany)

$CaCl_2$ x 2 H_2O Merck, Darmstadt (Germany)

Chloroform Merck, Darmstadt (Germany)

Chlorophyll *a* provided by S. Hobe, Mainz (Germany)

Coomassie Brilliant Blue G-250 Serva, Heidelberg (Germany)

p-Coumaric acid Fluka, Buchs (Switzerland)

DCBQ (2,6-Dichloro-p-benzoquinone) Sigma-Aldrich, St. Louis, MO (USA)

o-Dianisidin Sigma-Aldrich, St. Louis, MO (USA)

Diethyl ether Merck, Darmstadt (Germany)

Dimethylsulfoxid (DMSO) Carl Roth, Karlsruhe (Germany)

β-dodecylmaltoside (DDM) Glycon, Luckenwalde (Germany)

α-dodecylmaltoside (DDM) Antrace, Maumee, Ohio (USA)

Ethylenediaminetetraacetic acid (EDTA) Merck, Darmstadt (Germany)

Ethanol Carl Roth, Karlsruhe (Germany)

NaEDTA (E6760) Sigma-Aldrich, St. Louis, MO (USA)

Formaldehyde Carl Roth, Karlsruhe (Germany)

Glutaraldehyde Carl Roth, Karlsruhe (Germany)

Glycerol Carl Roth, Karlsruhe (Germany)

Glycine Carl Roth, Karlsruhe (Germany)

H_2O_2 Carl Roth, Karlsruhe (Germany)

HCl JTBaker, Deventer (The Netherlands)

HEPES Carl Roth, Karlsruhe (Germany)

n-heptyl-β-D-thioglucoside (HTG) Sigma-Aldrich, St. Louis, MO (USA)

Imidazole Carl Roth, Karlsruhe (Germany)

Iodine Merck, Darmstadt (Germany)

KCl Carl Roth, Karlsruhe (Germany)

KNO_3 Carl Roth, Karlsruh (Germany)

K_3 $[Fe(CN)_6]$ Merck, Darmstadt (Germany)

LiCl Carl Roth, Karlsruhe (Germany)

Luminol Fluka, Buchs (Switzerland)

β-mercaptoethanol Carl Roth, Karlsruhe (Germany)

MES (2-[N-Morpholino]ethanesulfonic acid) Sigma-Aldrich, St. Louis, MO (USA)

Methanol, HPLC grade Carl Roth, Karlsruhe (Germany)

$MgCl_2$ x 6 H_2O Carl Roth, Karlsruhe (Germany)

Milk powder Carl Roth, Karlsruhe (Germany)

Na_2CO_3 Carl Roth, Karlsruhe (Germany)

Na_2 HPO_4 x 7 H_2O Carl Roth, Karlsruhe (Germany)

$Na_2S_2O_3$ x 5 H_2O Merck, Darmstadt (Germany)

NaCl Carl Roth, Karlsruhe (Germany)

$NaHCO_3$ J.T. Baker devent (Holland)

NaOH Carl Roth, Karlsruhe (Germany)

$NiCl_2$ Merck, Darmstadt (Germany)

Ni^{2+}-NTA Agarose Amersham Bioscience

Ni^{2+}-NTA Agarose Qiagen

β-Octylglucoside Glycon, Luckenwalde (Germany)

Phosphatidylcholine Sigma-Aldrich, St. Louis, MO (USA)

Polyethylenglycole (PEG) 2000 Carl Roth, Karlsruhe (Germany)

Polyethylenglycole (PEG) 6000 Carl Roth, Karlsruhe (Germany)

Polyethylenglycole (PEG) 8000 Fluka, Buchs (Switzerland)

Rotiload Carl Roth, Karlsruhe (Germany)

Rotiphorese 40 (40 %) Carl Roth, Karlsruhe (Germany)

Rotiphorese Gel B (2 %) Carl Roth, Karlsruhe (Germany)

Silicic acid (kieselgel 60G) Sigma-Aldrich, St. Louis, MO (USA)

Sodium acetate x 3 H_2O Carl Roth, Karlsruhe (Germany)

Sodium azide Merck, Darmstadt (Germany)

Sodium dodecylsulphate (SDS) Carl Roth, Karlsruh (Germany)

Sodium propionate Sigma-Aldrich, St. Louis, MO (USA)

Sucrose Carl Roth, Karlsruhe (Germany)

TEMED (Tetramethylethylenediamine) Carl Roth, Karlsruhe (Germany)

Tricine Carl Roth, Karlsruhe (Germany)

Trypsine Promega

Tris Carl Roth, Karlsruhe (Germany)

Triton Roche, Mannheim Germany

Uranyl acetate Riedel-de Haën, Hannover (Germany)

Urea Carl Roth, Karlsruhe (Germany)

$ZnCl_2$ Sigma-Aldrich, St. Louis, MO (USA)

Liquid fertiliser Wuxal Top N horticentre (New Zealand)

Substance	Weight proportion (g/kg)	Volume proportion (g/l)
N	120	140
P_2O_5	40	45
K_2O	60	70
B	0.1	0.11
Cu	0.07	0.08
Fe	0.15	0.18
Mn	0.13	0.15
Mo	0.01	0.011
Zn	0.05	0.055

Cu, Fe, Mn and Zn fully chelated by EDTA.

2.1. Equipment

2.1.1. General Equipment

Minispin table top centrifuge, Eppendorf, Hamburg (Germany)

Biofuge fresco table top centrifuge, Heraeus, Hanau (Germany)

Biofuge primo R, Heraeus, Hanau (Germany)

MR 80 Heidolph magnetic stirrer, Labotec, Wiesbaden (Germany)

Reax 1DR Heidolph vortexer, Labotec, Wiesbaden (Germany)

Ultrospec4000 UV/visible spectrophotometer, Pharmacia Biotech Pfizer Pharma (Germany)

pH meter 766 Calimatic, Knick (The Nederlands)

API-ISO2 Balance Denver instruments

2006 MPBalance Sartorius insruments, Goettingen (Germany)

2.1.2. PSII and lipids purification equipment

Blender, Waring, New Hartford, Conn. (USA)

ZK401 centrifuge with ***A8.24*** (8 x 50 ml) and ***AS4.13*** (6 x 250 ml) rotors, Hermle, Wehingen (Germany)

Sorvall Discovery 90 SE ultra centrifuge with Sorvall ***AH-629*** rotor

Column Pharmacia 300ml, Ø 30mm for Ni^{2+}-NTA Agarose Amersham Bioscience Piscataway NJ (U.S.A.)

Ni^{2+}-NTA Agarose Amersham Bioscience Piscataway NJ (U.S.A.)

Ni^{2+}-NTA Agarose Qiagen (U.K.)

LKB pump 1 peristaltic pump, Pharmacia Pfizer Pharma (Germany)

Frac-100 fraction collector, Pharmacia Pfizer Pharma (Germany)

Amicon Centriprep (10 and 30kDa) centrifugal filter devices, Millipore (U.S.A.)
Vivaspin 20 30, 100 and 300 kDa centrifugal filter devices, Vivascience (Germany)
V-550 spectrophotometer Jasco instruments
Ultrospec4000 UV/visible spectrophotometer, Pharmacia Biotech Pfizer Pharma (Germany)
Rotavapor-R solvents evaporator, Büchi, Essen (Germany)

2.1.3. PSII analysis equipment

Analytical gel filtration
Äkta Purifier pH/C-900, UV-900, P-900, Amersham Bioscience Piscataway NJ (U.S.A.) ***Column 10/300GL in Sepharose 6*** Amersham Bioscience Piscataway NJ (U.S.A.)

BN-PAGEs, SDS-PAGEs and immunoblots
Mighty Small SE245 gel system, Hoefer Scientific Instruments, San Francisco, CA (USA)
Desatronic 3x500/100 power supply, Desaga, Heidelberg (Germany)
Trans-Blot SD semi dry transfer cell, Bio-Rad, Hercules, CA (USA)
Voyager STR-DE (Maldi-tof) mass spectrometer, Applied Biosystems

Mass spectrometry
Voyager STR-DE mass spectrometer, Applied Biosystems
Q-tof Ultima ESI (Q-tof) mass spectrometer, Micromass

HPLC
L-2130 HPLC Hitachi High Technologies San Francisco CA (U.S.A.)

Oxygen electrode setup
Perkeo Soft slide projector, Zeiss Ikon, Oberkochen (Germany)

Servogor 310 recorder, BBC Goerz, Nürnberg (Germany)

control unit and ***measuring cell***, Bachofer Reutlingen (Germany)

Electron microscopy setup

Auto 306 Turbo carbon evaporator, Edwards High Vacuum (UK)

EM Copper grids (3.05 mm/400 mesh), Plano, Wetzlar (Germany)

Mica (75 x 25 mm), Plano, Wetzlar (Germany)

CM12 and CM120 transmission electron microscopes, Philips, Eindhoven (The Netherlands)***CCD camera***, Gatan GmbH, München (Germany)

2.2. Methods

2.2.1. Biological material and culture of tobacco plants

Tobacco plants (*Nicotiana tabacum L.* cv. Petit Havana) were grown for 8-10 weeks under a light intensity of 100 to 150 µE/(s·m^2) and with a photoperiod of 8 hours light and 16 hours darkness (for the characteristics of the biological material see table 1). Before sowing, the seeds were incubated for 2 days at 4°C and then soaked for another 2 days in H_2O. The plants were grown at 25°C in 50 % relative air humidity and were fertilised once per week with Wuxal Top N (1:1000).

Table 1: Biological material characteristics:

Tobacco strain	Construct used for transformation*	Construct characteristics
Wild type	-	-
Eh1a/13	pbKS+SacI⁻psbE-His_6NC	His_6-non cleavable
Eh 2a/34	pbKS+SacI⁻psbE-His_{10}NC	His_{10}-non cleavable

*for more informations about the characteristic of the constructs see Fey Holger (2006)

2.2.2. Thylakoid preparation

Thylakoid membranes were prepared as described in Burke et al. (1978) with the following modifications. Spinach or tobacco leaves were washed once in tab water and once in bidistilled water, all the following steps were performed under dark or green

light a 4°C. A mass of 100g of destemmed leaves were mixed with 150ml or 200ml of Crude Extract Buffer (CEB) and the mixture was grounded with a waring blender. The leaf extract was filtered through 8 layers of muslin and one layer of cotton and then centrifuged (10min, 7500rpm, 4°C in a Hermle AS4.13 rotor). The pellets, consisting of chloroplasts and cell debris, were resuspended with about half the initial volume in First Resuspension Buffer (FRB) and washed by a second centrifugation (10min, 7500rpm, 4°C in a Hermle AS4.13 rotor). Depending on the subsequent purification steps, the pellet was either resuspended in Homogenisation Buffer (PSII preparation by differential centrifugation) or resuspended with a Second Resuspension Buffer (SRB) (PSII preparation by affinity chromatography) and washed by a third centrifugation (10min, 11000rpm, 4°C in a Hermle AS4.13 rotor) followed by a third resuspension in SRB. In both cases the samples were resuspended after the last centrifugation at a final chlorophyll concentration of 3-5mg/ml. After homogenisation and a chlorophyll determination in 80% acetone (Porra *et al.* 1989), the thylakoids were either flash frozen in liquid nitrogen and stored at -80°C or submitted directly to the PSII preparation.

Buffers:

Crude Extract Buffer (CEB)

50 mM HEPES, pH 7.5
400 mM NaCl
10 mM $MgCl_2$ 6x H_2O
2 g/l BSA
0.5 g/l Ascorbate

First Resuspension Buffer (FRB)

50 mM Mes-NaOH, pH 6.0
150 mM NaCl
5 mM $MgCl_2$ 6x H_2O
1 g/l BSA
0.5 g/l Ascorbate

Second Resuspension Buffer (SRB)

20 mM Mes-NaOH, pH 6.5
100 mM NaCl
10 mM $NaHCO_3$
12.5 % (v/v) Glycerol
0.5 g/l Ascorbate

Homogenisation Buffer

50 mM Mes-NaOH, pH 6.0
15 mM NaCl
5 mM $MgCl_2$ 6x H_2O

2.2.3. Photosystem II preparation by differential centrifugation

Thylakoid membranes were solubilised by the addition of Triton X-100. With this first solubilisation grana thylakoids which contain mostly PSII and LHCII can be separated from stroma thylakoids which contain mostly PSI. After this first solubilisation grana thylakoids were solubilised by OG or HTG for removing LHCII from the stromal fraction and obtaining the PSII enriched membranes.

After solubilisation of the thylakoid membranes with Triton X-100 at 7% final concentration (Berthold et al., 1981) for 10 minutes, grana particles were sedimented by centrifugation (30 min, 19 000 rpm/ 40 000 g, 4°C in a Beckman JA30.50 rotor), resuspended in Buffer 1, centrifuged again (30 min, 19000 rpm/40000 g, 4°C in a Beckman JA30.50 rotor) and finally homogenised. After homogenisation the grana particles were solubilised with 2.7% HTG (n-heptyl-β-D-thioglucoside) or 2.2% OG (n-octyl-β-D-glucoside) for 20 min at 4°C with a final chlorophyll concentration of 3 mg/ml. The sample was diluted three times by adding two volumes of buffer and the unsolubilised membrane fractions were pelleted by centrifugation (20 min, 17 000 rpm/35 000 g, 4°C in a Beckman JA-20 rotor). The supernatant (PSII enriched membranes) was concentrated to 1-1.5 mg/ml chlorophylls with Amicon centripreps (30kDa cut-off), flash frozen in liquid nitrogen and stored at -80°C.

Buffer 1

40 mM Mes-NaOH, pH 6.5

20 mM NaCl

1 mM $CaCl_2$ 2x H_2O

5 mM $MgCl_2$ 6x H_2O

2.2.4. Photosystem II preparation by Ni^{2+}-NTA affinity chromatography

All the following steps were performed at 4°C under dark or green light conditions. Thylakoid membranes were solubilised with 25 mM DDM (n-dodecyl-β-D-maltoside) for 10 min under gentle stirring at a final chlorophyll concentration of 2 mg/ml. All the

unsolubilised material was removed by two centrifugations (10 and 5min, 17 000 rpm, 4 °C in a Hermle A8.24 rotor) and the supernatant was applied to the Ni-NTA column previously equilibrated with two column volumes of washing Second Resuspension Buffer (wSRB). The whole washing using wSRB was performed for 8-12 hours and was stopped only when the difference in absorbance at 438nm was less than 0.005 compared to the pure buffer. Photosystem II could be eluted by adding 1-2 column volumes of Buffer 1 with 300mM imidazol (eB1). The eluted sample was concentrated by the concentrators Vivaspin 300 (20 or 100kDa cut-off) to a final chlorophyll concentration of 1mg/ml.

Buffers:

washing Second Resuspension Buffer (wSRB)	**elution Buffer 1 (eB1)**
20 mM Mes-NaOH, pH 6.5	40 mM Mes-NaOH, pH 6.5
100 mM NaCl	20 mM NaCl
12.5 % (v/v) Glycerol	1 mM $CaCl_2$ 2x H_2O
0.03 % (or 0.01 %) (w/v) β-DDM	5 mM $MgCl_2$ 6x H_2O
15 mM Imidazole	300mM Imidazole
1M Betaine	0.03 % (or 0.01 %) (w/v) β-DDM
10 mM $NaHCO_3$	1M Betaine
	10 mM $NaHCO_3$

2.2.5. Chlorophyll determination (Chl a + Chl b)

The Concentration of chlorophyll a and chlorophyll b was measured photometrically with a Pharmacia Biotech Ultrospec 4000 UV/visible spectrophotometer (Pfizer Pharma, Germany) in 80 % acetone and calculated with the following formula (Porra *et al.* 1989):

$$[\text{Chl a}] = 12.3 \bullet A_{663.6} - 2.55 \bullet A_{646.6} \; [\mu g/ml]$$

$$[\text{Chl b}] = 20.3 \bullet A_{646.6} - 4.9 \bullet A_{663.6} \; [\mu g/ml]$$

2.2.6. Absorption spectroscopy

Absorption spectra were recorded between 370 and 750nm using a V-550 spectrophotometer (Jasco instruments) with an optical path length of 1cm and a band-pass of 2nm.

2.2.7. SDS Polyacrylamide gel electrophoresis

Based on the protocol of Schägger & v. Jagow (1987), protein samples were loaded on 10 % separating polyacrylamide/urea gels with a 4 % stacking gel using the Biometra gel casting system. The samples, solubilised and denatured in Rotiload (Roth), were run for 30 min at 35 V and then switched to 70 V. After the run, the protein bands in the gel were stained with Coomassie brilliant blue over night or silver stained.

Samples of pure PsbP and PsbS were used as a reference for the same subunits in purified PSII samples. The protein PsbS was over expressed and purified from E.coli in our laboratories, the protein PsbP was provided by A. Krieger-Liszkay (CEA Saclay -France-).

Stock solutions:

3x Gelbuffer
3 M Tris/HCl, pH 8.45
0.3 % (w/v) SDS

Acrylamide/Bisacrylamide
40 % Rotiphorese 40 38.96 % AA 1.0
Rotiphorese Gel B --- 2.0 % BA

Cathodebuffer
0.1 M Tris
0.1 M Tricine
0.1 % (w/v) SDS

Anodebuffer
0.2 M Tris/HCl, pH 8.9

Staining solution (100 ml)
175 mg Coomassie Brilliant Blue G-250
50 ml 100 % Ethanol
7 ml 100 % Acetic acid
43 ml H_2O

Destain solution
10 % Ethanol
7 % Acetic acid

2.2.8. Blue Native Polyacrylamide gel electrophoresis

Based on the protocol of Schägger & v. Jagow (1991), protein samples were loaded on a 6-13.5 % gradient non-denaturating gel with a 4% stacking gel using the biometra gel casting system. Thylakoid membranes isolated as described above were used as markers and mixed with an equal volume of solubilisation buffer at a final chlorophyll concentration of 1mg/ml. The solution was incubated for 30 min on ice and centrifuged at 13000rpm 2min. After incubation the marker was mixed in a ratio 9:1 with BN buffer and loaded in the gel. PSII samples at 1 mg/ml chlorophylls were mixed in a ratio 3:1:1 with ACA buffer and Coomassie Blue Solution. The electrophoresis was carried out at 205 V for 5 hours in ice under slow stirring of the anode buffer.

Stock solutions:

BN-Page Cathode Buffer
50mM Tricine
15mM Bis-Tris pH 7 at 4°C
0,02% (w/v) Serva Blue G 250

BN buffer
5% serva Blue G
750mM aminocaproic acid
35% sucrose

BN-PAGE Anode Buffer
50 mM Bis-Tris pH 7 at 4°C

ACA buffer
750mM aminocaproic acid,
50mM BisTris-HCl pH 7.0
0.5mM EDTA

Coomassie Blue Solution
5% serva Blue G, 750mM aminocaproic acid, 35% sucrose

Solubilisation buffer
25mM Bis-Tris pH 7.0
20% glycerol
2% DDM

2.2.9. Western blot

After the run, BN-PAGE and SDS-PAGE gels were equilibrated in Cathodebuffer and then the proteins were blotted for 45 min at a current of 1.5 mA/cm^2 of the gel onto the membrane. For this transfer the membrane and the gel were surrounded by filter papers soaked in Anodebuffer and Cathodebuffer, respectively.

After blotting the membranes were incubated for one hour with specific antibodies against the PsbA (D1), PsbD (D2), His-PsbE, LHCII or PSI proteins. After binding the membranes were washed for 15' in PBS and finally treated another hour with a peroxidase coupled secondary antibody. After ECL reaction the bands were visualised and recorded on X-ray film.

All the antibodies were suspended in a Western Blocking Solution (see below) at a final dilution of 1:10000 before use.

Rabbit polyclonal antibodies against PSI, LHCII and D1 were kind gift sfrom Prof Feierabend, Frankfurt University. Rabbit polyclonal antibodies against PsbS were provided by Christiane Funk, Umea Univerity. Rabbit antibodies against D2 were gifts from Dr Barbato, University of Alessandria. Rabbit antibodies against His-Tag were purchased from Sigma (http://www.sigmaaldrich.com).

Stock solutions:

Anodebuffer I
0.3 M Tris/HCl, pH 10.4
10 % Methanol

Anodebuffer II
25 mM Tris/HCl, pH 10.4
10 % Methanol

Cathodebuffer
25 mM Tris/HCl, pH 9.4
40 mM Glycine
10 % Methanol

PBS
137 mM NaCl
2.7 mM KCl
4.3 mM $Na_2 HPO_4$ 7x H_2O
1.4 mM $KH_2 PO_4$

Western Blocking Solution
5 % Milk powder
(0.05 % Tween 20) (optional) in PBS

ECL detection solution (Peroxidase coupled antibodies)

200 µl Luminol (250 mM in DMSO) (store in the dark)

89 µl p-Coumaric acid (90 mM in DMSO) (store in the dark)

2 ml Tris/HCl, pH 8.5 (1 M)

fill up to 20 ml with H_2O

2.2.10. Protein identification by MALDI-TOF, MALDI-Q-TOF mass spectrometry and bioinformatics

This work was made in collaboration with W. Schröder and R. Horn (Umea University -Sweden-). Bands of interest from commassie stained gels were subjected to in-gel digestion using sequencing-grade modified trypsin (Promega). Protein identification by peptide mass fingerprint and PSD MS/MS was carried out using a Voyager STR-DE mass spectrometer (Applied Biosystems) (Yao et al. 2007). Protein identification by CapLC/MS/MS analysis was carried out using a Q-tof Ultima ESI mass spectrometer (Micromass) (Rouhier et al. 2005). Fragment ion spectra were submitted to MASCOT (http://www.matrixscience.com/) for database search and identification.

2.2.11. Gel filtration

Gel filtration chromatography was performed using a Sepharose 6 10/300GL Column (Amersham Bioscences) connected to an ÄKTA Purifier (Amersham Bioscience). The column was equilibrated with 40mM Mes (pH 6.5), 20mM NaCl, 1mM $CaCl_2$ $2xH_2O$, 5mM $MgCl_2$ $6xH_2O$, 0.03 % (w/v) β-DDM at a flow rate of $1mL \cdot min^{-1}$. The elutant solution was monitored for its absorbance at 664nm by the ÄKTA Purifier unity UV-900. All the experiments were performed at room temperature in the dark.

2.2.12. Oxygen evolution

Oxygen evolution was measured with a Clark-type electrode (electrode setup: Perkeo Soft slide projector, Zeiss Ikon; Servogor 310 recorder, BBC Goerz; Bachofer control

unit and measuring cell) at 20°C under a light intensity of 5000 $\mu Em^{-1}s^{-2}$ with 1 mM DCBQ and 1mM ferricyanide as electron acceptors in the reaction mix. The measurements were carried out in SRB or eB1 at 0.01 or 0.03% DDM with a total chlorophyll concentration of 5µg/ml.

2.2.13. Two-dimensional crystallisation of photosystem II

Two-dimensional crystals of Photosystem II from spinach were obtained by using the hockey stick technique (Kühlbrandt 1992). PSII was crystallised in presence of either 4mM n-heptyl-β-D-thioglucoside (HTG) or 4mM n-octyl-β-D-glucoside (OG) at a final chlorophyll concentration of 1 mg/ml. The sample solution was dialysed against a crystallisation buffer for 30 min at 35°C, 1 day at 30°C and 6 days at 20°C as described by Büchel land Kühlbrandt 2005. According to the respective experiments the dialysis buffer also contained different salts as additives.

Stock solutions:

Crystallisation buffer

40 mM Mes-NaOH, pH 6.5
1 mM Sodium azide
1 mM Sodium ascorbate
30 % Glycerol

2.2.14. Electron microscopy

Sample preparation and single particle analysis

That work was made in Collaboration with E. Boekema and S. Kereike (University of Groningen -The Netherlands-). Samples of purified Photosystem II core dimers were negatively stained by using the droplet method with 2% uranyl acetate on glow-discharged, carbon coated copper grids. Electron microscopy was performed on a CM120 electron microscope (Philips, Eindhoven, The Netherlands) operated at 120 kV. Images were recorded under low dose conditions (a total dose ~ $25e^-/Å^2$) with a 4000 SP 4K slow-scan camera (Gatan, Pleasanton, CA) at -340 nm defocus and at a

magnification of 80000x. Images were digitized and analysed with GRACE software for semi-automated specimen selection and data acquisition (Penczek et al. 1992). After binning of the images this resulted in a pixel size of 3.75 Å at the specimen level. In total, about 1200 images were recorded and 18.000 single particle projections were selected for image analysis. A major part of projections was selected using Boxer, a graphical program for semiautomatic particle selection from the EMAN software package. Single-particle analysis was performed with the Groningen Image Processing (GRIP) software package on a PC cluster. Selected single-particle projections were aligned by multi-reference and reference-free alignment procedures (Penczek et al. 1992. Particles were then subjected to multivariate statistical analysis followed by hierarchical classification (van Heel et al, 2000). Resolution was measured using Fourier-ring correlation and the 3σ criterion (Van Heel 1987).

Electron crystallography

Electron micrographs of negatively stained crystals were recorded with a CM12 or a CM120 electron microscope (Phillips) at 120 kV acceleration and a magnification of 59.000x. Images were taken with a 2 s exposure time using the low dose mode. The total electron dose was 5-10 $e^{-}Å^{-2}$. Images were recorded on Kodak SO-163 films. The time of development was 12 min using full strength Kodak D-19 developer. The micrographs were screened by optical diffraction. Thereby the best areas with the best symmetrical distribution of sharp spots were determined. These images were then digitized using a Zeiss SCAI scanner with a 7-μm step size over an area of 7,000 X 7,000 pixels. Distortion of the crystal lattices, effects of the contrast transfer function (CTF) and objective-lens astigmatism were corrected using the MRC image-processing programs (Crowther R., Henderson R. 1996). Computer generated diffraction patterns (Fast Fourier Transformation) each giving one averaged lattice with an IQ value (a numerical grade of the signal-to-noise ratio of spots) ≤ 7, from two groups of images, were merged by phase origin refinement. Both groups consisted of four images. Data up to 15 Å resolution were used to calculate a two-dimensional map of the complex projected onto the membrane plane.

2.2.15. Isolation of thylakoid lipids

Tobacco thylakoid lipids were isolated according to the method used previously by Morris et al. (1997).

2.2.16. Thin layer chromatography

Tobacco lipid stocks and lipid composition in PSII samples were analysed by thin layer chromatography. TLC plates (Silica gel 60 t254) were run in a solvent solution consisting of 10:3.3:0.5 chloroform:methanol:water. The lipids were visualized by iodine evaporation.

2.2.17. Pigment determination by HPLC

Pigment composition in PSII samples were determined by a L-2130 HPLC (Hitachi High Technologies) after extraction of the pigments in 90 % methanol and precipitation of the proteins (centrifugation at 4°C for 10 min at 13 000 rpm).

Pigment species were separated on a reversed-phase column (LichoCART 250-4; Lichrosorb RP-18, 5µm) with a flow rate of 1.250 ml·min^{-1} using a multi-step linear gradient (tab.2). Pigments were identified by their absorption spectra in solution (online diode array detector).

Table 2. HPLC elution gradient

Time (min.)	80%Methanol	80%Methanol 40%Acetone
0	100%	0%
5	20%	80%
15	0%	100%
28	0%	100%
30	100%	0%

II. Results

3.0. PSII purification and characterisation from transplastomic tobacco

Several attempts have been made in order to obtain more pure PSII particles with respect to the current protocols where other techniques such as differential centrifugation, sucrose gradient and anionic exchange (Boekema *et al.* 1995, Hankamer *et al.* 1997, Kern *et al.* 2005) were used. In this work it could be shown that the final PSII purity and functionality strongly depends on several critical steps including thylakoid preparation, thylakoid membrane solubilisation, PSII separation and PSII concentration. To judge the quality of the different preparations several parameters were tested: final yield, oxygen evolution, purity and the presence of the relevant subunits of PSII in stoichiometric amounts. In particular PSII stability in terms of composition and proportionality between subunits was valuated empirically by SDS-PAGE.

3.1. Thylakoid purification

Thylakoids were prepared by differential centrifugation using tobacco leaves harvested after the dark period. The leaves were washed, destemmed and blended in a crude extract buffer (CEB). After centrifugation the pellet was resuspended in the first resuspension buffer (FRB), centrifuged again and redissolved in the second resuspension buffer (SRB). SRB was also used as solubilisation and washing buffer during the successive PSII purification. Thus, after the second resuspension the sample always stayed in the same chemical-physical environment. Finally the washing buffer was exchanged during the elution by a final storage buffer.

Several experiments on the second resuspension step using the SRB were performed (tab.1).

After this group of experiments the protocol was modified twice. The speed during the third centrifugation was increased from 7500rpm to 11000rpm. Furthermore the sample

was resuspended a third time in SRB. The modifications led to an increase in stability and column binding of PSII particles.

Table 1. Centrifugation and Resuspension screening.

	First resuspension (FRB)	Second resuspension (SRB)	Third resuspension (SRB)	Observations		
	Centrifugation	Centrifugation	Centrifugation	PSII Ni-NTA binding	PSII Stability	Final Yield (% of chls)*
Starting condition	7500rpm	7500rpm	-	+	+	~0,4
First modification			7500rpm	++	++	~0,6
Second modification			11000rpm	+++	++	~0,9

* chlorophyll ratio calculated between the final amount in the PSII sample and the initial amount in the thylakoids.

To further increase the general quality of the protocol several tests on SRB composition were made. In a first step several thylakoid purifications were performed with several pH conditions. Thylakoids were purified with SRB at pH 5.5, 6.0 and 6.5 respectively. Only at pH 6.5 it was possible to increase the final amount of purified PSII particles. In figure 1 an SDS-PAGE shows the preserved composition in subunits of PSII samples at pH 6 and 6.5 whereas the LHCII impurities could be reduced considerably only at pH 6.5.

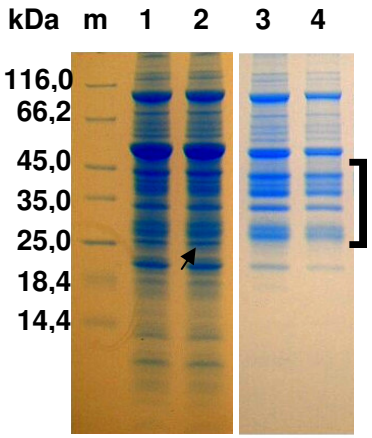

Figure 1. PSII of two different thylakoid preparations purified with a Ni-NTA resin.
Blue Coomassie stained SDS-PAGE gels. Lane 1 and 2: PSII purified at pH 6; lane 3 and 4: PSII purified at pH 6.5. The arrow indicates the LHCII impurity; the parenthesis indicates the main PSII core subunits: PsbB, PsbC, PsbO, PsbD, PsbA.

After optimising the pH other additives such as $NaHCO_3$, ascorbic acid or/and betaine were tested in a second step. With the use of 10mM $NaHCO_3$ and 0.5gr/l ascorbic acid, the oxygen evolution could be increased in the final purified PSII from 350 to about 450 µmol/h·mg·chls. Nevertheless, the use of betaine did not increase the protein quality and also interfered with the next solubilisation step.

In conclusion, the best results were obtained by using a SRB at pH 6.5 with the addition of $NaHCO_3$ (10mM) and ascorbic acid (0.5gr/l). After this step the sample was homogenised, frozen in liquid nitrogen and kept at -80°C at a concentration of 3-5 mg/ml chlorophylls.

Another essential factor for the thylakoid quality was the effect of the initial thylakoid chlorophyll concentration on the solubilisation. When the sample was at initial concentrations higher than 6 mg/ml chlorophylls, the solubilisation was not as good as with initial concentrations between 3-5 mg/ml. In fact, when the chlorophyll content was higher than 6 mg/ml the amount of unsolubilised material increased considerably. This could be seen in the pellet after solubilisation.

In conclusion, the apparent increase in thylakoid quality has a physical and chemical basis. In fact, the washing by centrifugation at higher speed and the resuspension two times in the same SRB is responsible for a physical cleaning leading to a better removal of the residuals of CEB and FRB. In particular, the residual amount of CEB could be problematic considering that the pH of this buffer is not ideal for keeping the stability of PSII. Furthermore chemical factors such as pH and $NaHCO_3$ are important for the protection of the oxygen evolving centre (OEC) and the ascorbic acid has a relevant effect in preventing oxidations. All these tests were performed using both 10x and 6xHis-PSII getting similar results.

3.2. PSII purification

3.2.1. Thylakoid solubilisation

From purification protocols on membrane proteins, it is well known that solubilisation is a key step in keeping a protein functional and integer (Deutscher 1990). In this work, after the development of a protocol to isolate tobacco thylakoids, the conditions to

purify a 6x or 10x His-tagged PSII via Ni-NTA were determined. The homogenised thylakoid membranes were solubilised with several detergents at different concentrations and different solubilisation times. Several buffer compositions were tested as well as the effect of different chlorophyll concentrations. All the tests were performed using both 10x and 6xHis-PSII getting similar results.

The first step during solubilisation was the careful addition of all components which occurred always in the same order. After the thawing of thylakoids in ice-water the buffers were added first, followed by the detergent. All these steps were performed at 4°C under slow stirring in the dark or under green light conditions. Tested detergents were 25mM β-dodecylmaltoside (β-DDM), 75mM β-octylglucoside (β-OG) and 92mM β-heptylthioglucoside (β-HTG) (tab.6). This group of non ionic detergents were chosen according to the main work published on PSII in the last twenty years (Bertold et al. 1981, Santini et al 1994, Rhee et al. 1997). Although these detergents are characterised by different mildness, not any remarkable difference was observed in terms of solubilised thylakoid membranes, final PSII quality and quantity. On the other hand, the time of solubilisation is important for the final PSII quality and the final yield. PSII purifications were tested in conditions where the thylakoids were solubilised for 5, 10, 15 and 20min. The result showed that the final PSII yield increased with duration whereas the PSII quality decreased (tab. 2).

Table 2. Effects of the solubilisation time on the final preparation.

Increase in Stability ↑

Solubilisation time				
PSII stability	**Without stirring**	**With stirring**	**Total time**	**Yield***
++++	0	5	5	0,7%
++++	5	5	10	1,1%
+++	5	10	15	1,1%
++	5	15	20	2,5%
+	10	10	20	3,8%

↓ Increase in Yield

*as a percentage referred to the total chlorophylls amount in the starting material.

In particular, the final yield was directly proportional to the solubilisation time whereas the PSII stability in terms of composition and proportionality between subunits was inversely proportional to it. The optimal compromise for getting the best quality of purified PSII in optimal yield was a solubilisation time between 5 and 10 minutes.

The final chlorophyll concentration in solubilised thylakoids affects the final PSII quality and quantity. To find the optimal ratio between a high PSII yield and the preservation of PSII stability, chlorophyll concentrations between 1-4 mg/ml were tested with a constant solubilisation time. The results showed an increase of both yield and PSII heterogeneity at lower chlorophyll concentrations. With the solubilisation times reported above the optimal concentration estimated was 2mg/ml.

To further stabilise the PSII subunits, ascorbic acid and $NaHCO_3$ were used in the solubilisation buffer (sSRB). The effect was an increased oxygen evolution from 350 to about 450µmol/mg·Chls·h. Besides, sSRB was also tested at several pHs but only pH 6.0 and pH 6.5 were relevant in terms of quality of PSII particles as already shown for the buffers used during thylakoid preparation. However, at pH 6 a relevant amount of impurities related to the Light Harvesting Complex II (LHCII) subunits was present (fig.1). Only at pH 6.5 the amount of LHCII could be depleted significantly (fig.1). Nevertheless, the presence of LHCII in the final sample was not necessarily related with a real impurity but it can also be related with specific interactions between PSII and LHCII (PSII-LHCII supercomplexes) that might be favoured at lower pHs.

After solubilisation the unsolubilised material was removed by centrifugation. Centrifugation experiments were performed with several speeds and times. The best results were achieved with consecutive centrifugations at 17000 rpm (Hermle rotor type A 8.24) for 5 minutes (tab.3). The tests of solubilisation were performed using the tobacco strains with 10x and 6xHis-PSII getting similar results.

Table 3. Changes in centrifugation time after solubilisation.

Centrifugations (17000rpm)				
First Centrifugation		**Second centrifugation**		**Observations**
Time (minutes)	**Pellet**	**Time (minutes)**	**Pellet**	
5	++	0	-	After elution a high amount of residues in the column and an increased amount of impurities in the sample was observed.
10	+++	0	-	The impurities in the sample and residue in the column were removed only in part.
10	+++	10	+	The residues on the column and the impurities in the sample were almost completely removed.
10	+++	5	+	Results as above but in a shorter time.
5	++	5	+	

3.2.2. Ni-NTA binding and washing

After the development of a protocol for thylakoid isolation and solubilisation the ideal conditions for purifying His-PSII by Ni-NTA had to be found. Also in this case several conditions were tested. The best results were obtained by working with a batch instead of loading the thylakoids on the pre-packed resin. Quality and amount of PSII as well as the ratio between protein and impurities directly depend on the conditions of the batch step (tab.4).

Table 4. Batch and equilibration in sample purity and yield.

Batch (minutes)	Yield	PSII purity	
		Equilibration with SRB in 15 mM imidazol	Equilibration with SRB in 0 mM imidazol
30	+	+++	++
40	++	+++	++
50-70	+++	+++	+

Potential problems during the purification are due to the dimension of PSII and the steric disturbances associated with the position and the dimension of the His-tag. The batch procedure increases the probability to have a correct binding between the His-tag and the NTA. The presence of 5-15mM of imidazol in the washing SRB (wSRB) during the resin equilibration reduced the unspecific binding and thereby decreased impurities.

As mentioned before, after the second centrifugation in the thylakoid preparation, the main buffer composition remained unchanged until the final PSII preparation step. In particular, the same SRB was used as solubilisation buffer (sSRB) and washing buffer (wSRB).

After the batch a long washing step had to be included. For that reason it was necessary to protect the proteins by several additives in the wSRB. The first chemical tested was betaine at concentrations of 100mM and 1M (tab.5). In general, this substance is able to

Table 5. Effects of Betaine on several purification steps and on the quality parameters.

Betaine (mM)	SRB	Solubilisation	Washing/Elution		
			O_2 evolution (µmol/mg·Chls·h)	Impurities	Stoichiometry*
0	-		350-450	++	+
100	-		-	+	++
1000	Disturbance during solubilisation		1400-1700	+	++

*as qualitative valuation of the preserved composition in PSII core subunits analysed by SDS-Pages.

act on proteins as osmoprotectant and cryo protectant (Sakamoto *et al.* 2000; Coughlan *et al.* 1982; Gorham *et al.* 1995). In particular, several authors reported that betaine, as demonstrated also in this work, is able to protect the luminal part of PSII preserving the stability of the oxygen evolving centre (Suleyman I. *et al.* 2003). In a first group of experiments 1M betaine led to a very high oxygen evolution (tab.10), a good ratio between subunits and a reduction in the amount of the main copurified proteins (fig.14). Few experiments with 100mM betaine were done in order to check if it was possible to protect PSII at concentrations lower than 1M. Preliminary results of these experiments have shown that betaine at concentration of 100mM is still able to protect PSII to the same extent. Probably the ability of betaine to protect PSII also at low concentrations depends on the purification system. Previous work that made use of this chemical were performed using purification methods as differential centrifugation and sucrose gradient on solubilised membranes (Boekema *et al.* 1995, Hankamer *et al.* 1997, Kern *et al.* 2005).

As the interaction between detergent and protein is critical, β-DDM, β-OG and β-HTG were used in order to test their effect during the washing (tab.6). In fact, in membrane proteins purification protocols the constant presence of detergents is important for keeping the protein in the micelles solution. It is well known that on the same protein

Table 6. Detergents screening.

Detergents	CMC	Solubilisation (mM)	Washing/Elution (mM)	Observation
α-DDM	0,15mM (0,0076%)	25mM (~1,28%)	0,01% and 0,03%	PSII quality increase with concentration of 0,01%.
β-DDM	0,17mM (0,0087%)			
β-OG	18-20mM (0,53%)	75,24mM (~2,2%)	0,6 and 0,75%	Precipitation during the washing at every tested concentration.
			1,1%	
			1,6%	
β-HTG	70mM (1,9%)	99,47mM (~2,7%)	-	-

several detergents behave in different manner. The protection is related with the intrinsic detergent mildness but it is also depending on the interaction between specific detergent-protein systems. Positive results were found only in experiments with β-DDM. In the other cases, using concentrations one to three times above the critical

micelle concentration (CMC), the proteins were still not kept in solution but precipitated in the column. DDM was tested at concentration of 0.03% and 0.01%. In general, composition and activity of the final PSII were similar but showing a better oxygen evolution using 0.01% DDM (tab.10).

0.5 gr/l ascorbic acid and 10mM $NaHCO_3$ were used for preventing oxidations and increasing OEC stability. In both cases the use of these components was effective in an increased oxygen evolution (tab.10) and an increased stoichiometric quality as demonstrated by SDS-PAGEs (fig.5). To further increase the washing effect 15mM imidazol was added with the aim to reduce the unspecific binding by creating a competition with unspecific ligands.

The whole washing was performed for 8-12 hours at very low speed and was stopped only when the difference in absorbance at 438nm was around 0.005 compared to the pure buffer. The slow washing had to be used since SDS-PAGEs of PSII samples purified by a faster washing speed demonstrated loose binding of the CP43 and CP47 subunits. The same results were obtained for both 10x and 6xHis-PSII tobacco strains.

3.2.3. Elution and concentration

After washing the bound material was almost pure PSII and was eluted by using the elution buffer (eSRB). Several imidazol gradient elution experiments were performed to determine the minimal imidazol concentration in the eSRB capable of protein elution. Therefore an imidazol gradient was applied with concentrations between 15mM and 400mM. The protein elution started around 150mM with a maximal peak around 300mM. A further increase did not lead to significant changes. Accordingly the eSRB composition was kept at a concentration of 300mM imidazol. During the elution the sample was collected in fractions where protein concentration, subunit composition and absorption spectra were investigated (fig. 2, 3, 4).

After the elution and concentration of the PSII sample, the total amount of chlorophylls was measured to determine the efficiency of the process. The yield calculated between chlorophylls in the sample and in the initial thylakoids was found to be in a range between 0.7 and 1.4%. Nevertheless, this efficiency increased if the amount of unsolubilised material was subtracted from the thylakoid`s chlorophyll concentration. In fact using also this data the final yield stayed between 3.2 and 4% of chlorophylls.

One of the main focuses of this preparation was the use of PSII for crystallisation experiments. For that reason, after a group of preliminary experiments, the elution buffer was exchanged with a crystallisation buffer that previously had been used successfully in PSII 2D crystallisation experiments (Nakazato *et al.* 1996). The

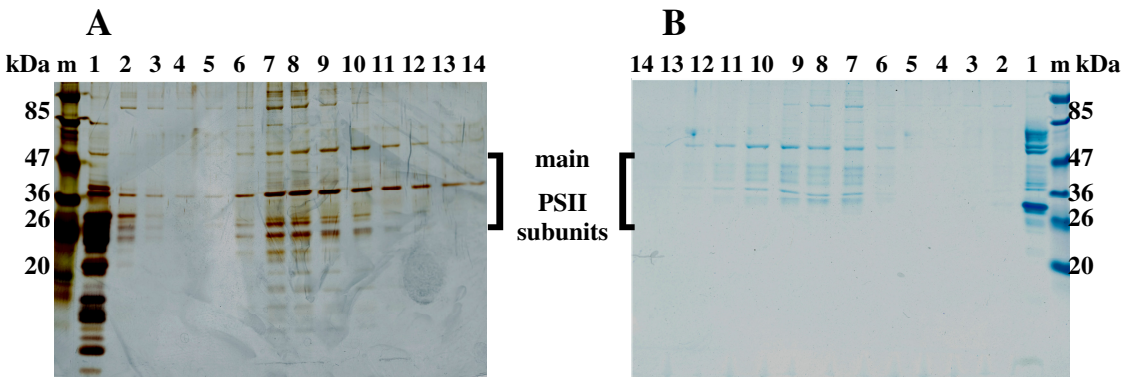

Figure 2. Purification profile analysed by SDS-PAGE.

Gels from the same elution fractions stained in silver (a) and in Coomassie (b). The elution was performed at 300mM imidazol. Lane m: marker; lanes 1-4: final washing fractions; lanes 5-14: elution fractions. Note the different staining intensity of the same subunits of PSII with Coomassie and silver respectively.

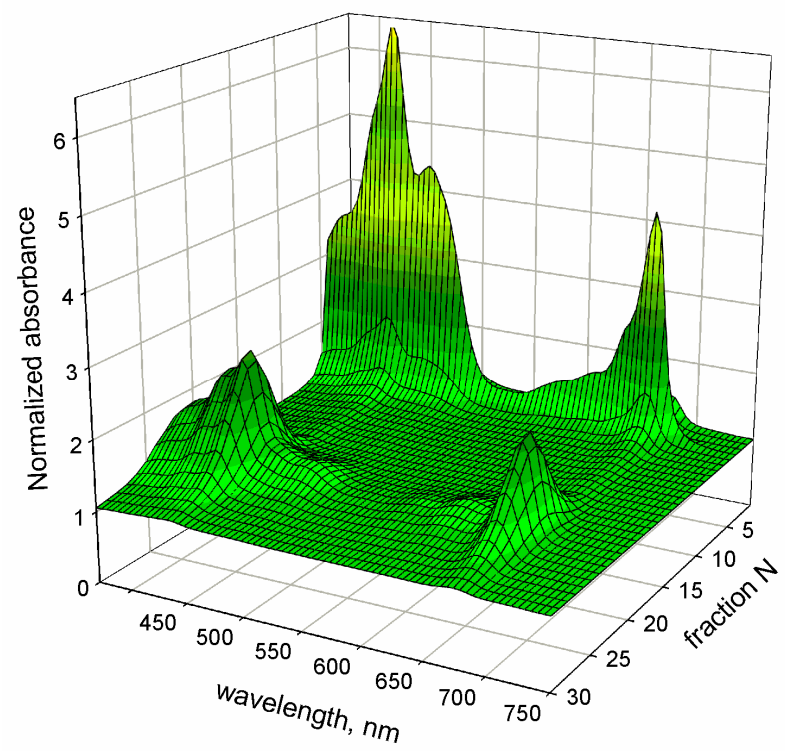

Figure 3. Purification profile expressed as absorption spectra of the fractions.

The washing from the fractions 1 to 15 has several peaks related with all the other pigmented proteins. The fractions 16 to 30 are pure PSII.

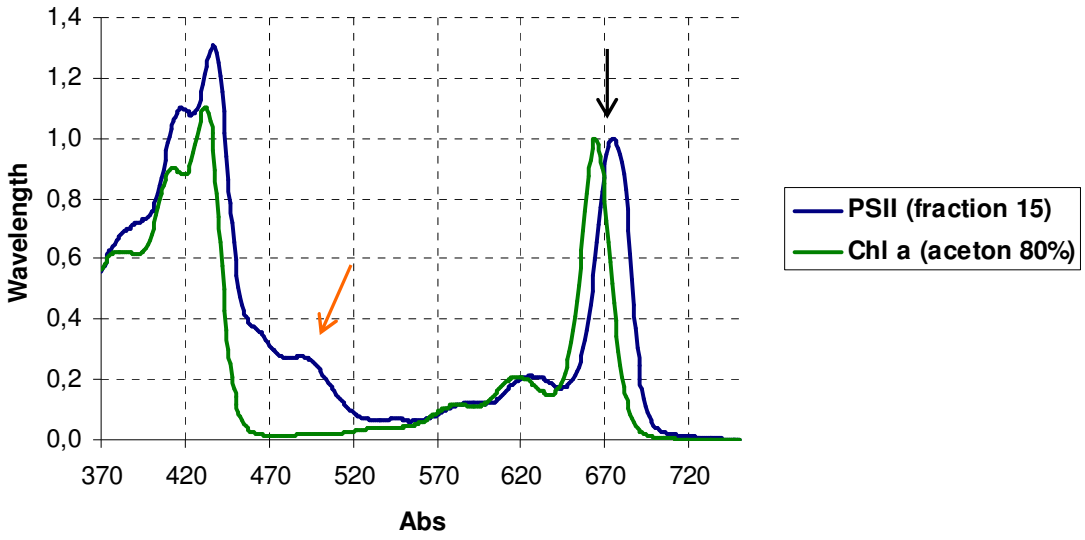

Figure 4. Absorption spectra of the fraction 15 from figure 3 and comparison with pure chlorophyll a in acetone.

The graph shows a red shift of PSII chlorophyll a compared to pure chlorophyll a (black arrow). Between 470-530nm the absorbance is related to PSII carotenoids (orange arrow).

additives betaine, ascorbic acid and $NaHCO_3$, were also added to the new buffer. PSII still could be purified in the same quality and without any changes in its characteristics. Eluted PSII particles were concentrated with two different strategies (tab.7). In the first

Table 7. Summary of the screened conditions used for protein concentration.

Technique		Speed (rpm)	Concentration time (h)	Observations
PEG	2000	28000	3	After resuspension the protein doesn't stay completely in solution and tends to form aggregates.
	6000		2	
	8000		1.5	
Concentrators	300 kDa	6000	4	The protein tends to accumulate on the filter.
	100 kDa			
	30 kDa	3500	3	Small cut-offs concentrate both impurities and free subunits.
	10 kDa			

one PSII particles were pelleted in a single ultracentrifugation step in 10% polyethylenglycole 6000 (PEG) and successively resuspended. The second strategy took use of gravimetric filtration by concentrators (concentration devices). In both cases the samples were concentrated up to a final chlorophyll concentration of 1mg/ml. Although concentration by PEG was faster, the resuspension of the pellet in buffer with 0.03% DDM was ineffective. After the resuspension a major part of the protein stayed aggregated with a consequent loss of material. This was probably due to the low amount

of detergent. Nevertheless, concentration with PEG had the advantage that changes in buffers and detergents were possible during resolubilisation.

Concentration by concentrators enables to choose between several cut-offs. Therefore, it was possible to remove all impurities with less molecular weight with respect to the cut-off. In this work, experiments with concentrators of 10kDa, 30kDa, 100kDa and 300kDa cut-off were performed. In terms of purity and homogeneity the best result was obtained with concentrators of 300kDa cut-off. With these devices not only impurities but also PSII monomers and incomplete PSII particles were removed.

3.3. Sample characterisation

After purification the sample was tested for its purity, functionality and integrity. The general subunit composition was analysed by SDS-PAGEs (fig.5).

3.3.1. PSII subunit characterisation

PSII characterisation required the identification of the different bands in the SDS-PAGEs. Preliminary analyses were performed with immuno-decoration using antibodies against PsbA (D1), PsbB (D2), PsbE and PsbS (fig.5). This lead not only to the identification of the corresponding subunits but also gave information about the remaining bands referring to their apparent molecular weight. Moreover, subunits PsbS and PsbP which were provided in their purified form were used as markers to identify the equivalent bands in the sample (fig.5).

Anti-His antibodies against the His-tagged PsbE subunit proved not only that the transformation of PsbE was successful but also that PsbE in the sample was a subunit component of PSII (fig.5).

After this general characterisation, the techniques of Maldi and Q-tof were used to obtain a fine and precise identification of every peptide in the sample (in coll. with Ruth Horn and Thomas Kieselbach, University of Umeå). With these techniques it was possible to reveal 13 polypeptides equivalent to the subunits PsbA, PsbB, PsbC, PsbD, PsbE, PsbF, PsbH, PsbO, PsbP, PsbQ, PsbS and Psb27 (fig.5). When characterisation

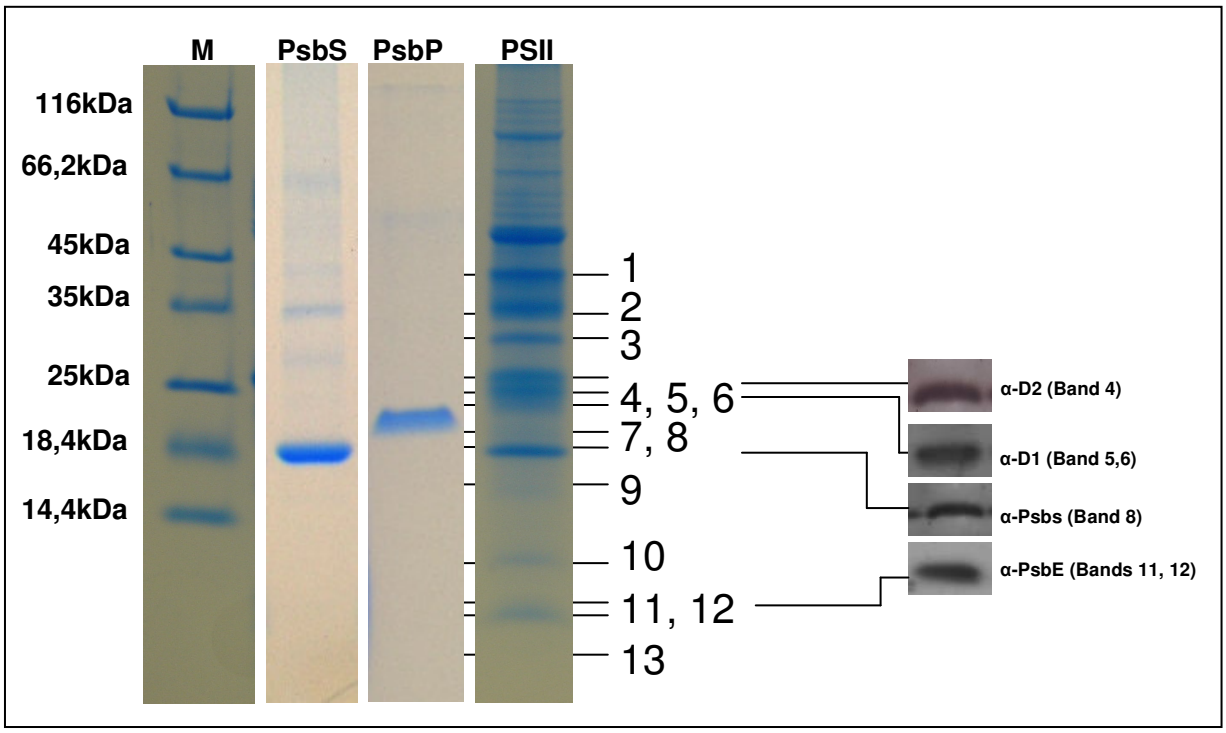

Figure 5. PSII core subunit characterisation.

In the first lane (M) a molecular marker is shown. Lane 2 and 3 show pure subunits PsbS and PsbP respectively. Lane 4 shows the purified PSII sample. Band 1 and 2 represent the core subunits PsbB and PsbC respectively, band 3 is the extrinsic subunit PsbO, band 4 is the core subunit PsbD, bands 5 and 6 represent the core subunit PsbA. Band 7 is the extrinsic subunit PsbP, band 8 is the peripheral subunit PsbS and band 9 is another extrinsic subunit, PsbQ. The last four bands are the small subunits Psb27 (band 10), PsbE and F bands (11 and 12), and PsbH (band 13). The subunits revealed by immunoblots are shown in the right part of the picture.

was completed, the main bands in the gels had been identified by two or three different methods (tab.8). Besides, experiments with gradient SDS-PAGE were made to increase the resolution in the range between 60kDa and 5kDa. First results indicated several bands with a molecular weight less than 10 kDa that were not characterised so far but most probably correspond to the smaller PSII subunits.

At this point the sample was also tested by analytical gel filtration and blue native PAGE (BN-PAGE) to determine the ratio between the PSII dimer and monomer. The elution profile in the analytical gel filtration showed two separated components, one main peak followed by one less pronounced peak during the migration of the sample in

Table 8. Techniques used to identify the bands obtained by SDS-PAGE.

	Maldi-tof	Q-Tof	Immunoblot	Pure subunits as marker
PsbA (D1)	+	+	+	-
PsbB (D2)	+	+	+	-
PsbC (CP43)	+	-	-	-
PsbD (CP47)	+	-	-	-
PsbE-PsbF	+	-	+	-
PsbH	+	-	-	-
PsbO	+	-	-	+
PsbP	-	-	-	-
PsbQ	-	-	-	-
PsbS	+	-	+	+
Psb27	-	+	-	-

the column (fig.6A). The first peak eluted was the component of the sample with the highest molecular weight. The second peak, eluted 5 minutes later with approximately 10 times less absorbance intensity was the component with a lower molecular weight. Therefore we suggest the dominant peak to be the dimer and the second peak eluted at about 22 minutes to be the monomer. Furthermore, two additional peaks were observed. The first eluted before the major peak, was suspected to be a PSII–LHCII supercomplex whereas the latest eluted at 23 minutes should consist of impurities or incomplete PSII complexes like Reaction Centre-CP47 (RC-CP47). The monomer was not more pronounced with respect to the impurities or the PSII-LHCII supercomplex shoulders.

BN-PAGEs were run with similar samples to confirm the results obtained above. The band pattern obtained were equivalent to the number of peaks from the gel filtration. More precisely, a major band between 450kDa and 500kDa together with a second less pronounced band around 200kDa were observed. Two more bands, one at higher and the other one at lower molecular weight were interpreted as the secondary bands also observed in the analytical gel filtration. As molecular marker solubilised thylakoids were used (fig.6B) and identification of the bands was done according to (Suorsa *et al.* 2006; Kügler *et al.* 1997).

In conclusion these two experiments proved that the PSII samples are almost homogeneous with a very high ratio between dimer and monomer. Nevertheless, it should be mentioned that the observed sample purity and homogeneity is not only related with the intrinsic tendency of PSII to stay in dimer form but also with the high cut-off (300kDa) of the concentrators used during the concentration. In fact this step is responsible for removing material such as PSII monomers, incomplete particles and

other impurities. Nevertheless, experiments performed with concentrators having a cut-off lower than 100kDa showed that the PSII composition in terms of subunits and dimer/monomer ratio stayed unchanged and demonstrated therefore that the step of concentration can further increase the purity but that a good sample homogeneity was already achieved in the step of elution. These tests were performed using the strain of tobacco with 6xHis-PSII.

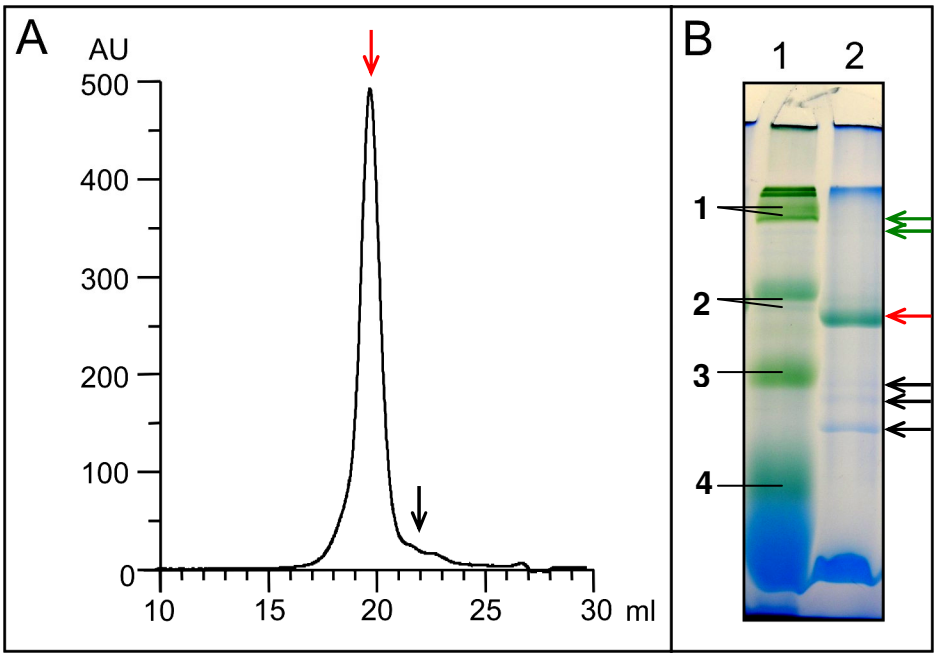

Figure 6. Analytical gel filtration and Blue Native PAGE from PSII.

In A the gel filtration elution profile is shown. The main peak (red arrow) is supposed to be the PSII core dimer eluted at about 19ml (minutes). Further little shoulders can be seen at 16, 22 and 23ml. The shoulder at about 22ml (black arrow) could be the PSII monomer. In B the BN-PAGE from the same sample is shown. Lane 1 is the thylakoid marker with the PSII-LHCII higher complexes in the upper band (1), PSI and PSII dimer in the second band (2), PSII monomer in the third band (3) and LHCII trimer in the fourth band (4); in lane 2 is the main band (red arrow) the PSII core dimer whereas the other three bands are PSII monomers and incomplete PSII complexes like the Reaction Centre-CP47 (RC-CP47) (black arrows); the bands at higher molecular weight related with the PSII-LHCII supercomplex are only faintly visible (green arrows).

3.3.4. The PSII subunits PsbS and Psb27

During the characterisation of PSII two unexpected proteins were found, the subunits PsbS and Psb27. PsbS was identified by Maldi-tof and immunoblotting, Psb27 was

identified by Q-Tof (tab.8). Since PsbS was a constant component in the preparations (e.g. SDS-PAGEs in fig.1, 2, 5) we suppose this subunit to be stablely bound to the PSII core. This suggestion is not in agreement with the current opinion about the position of PsbS in thylakoids (Nield *et al.* 2000). To confirm our data immunodecorations of BN-PAGEs were performed. If PsbS is bound to the core and not just a copurified protein, the immunodecoration signal should be coherent with the signal of the dimer. Since subunits D2 and D1 are the physiological and structural heart of PSII, they are both candidates as a positive control in the immunodecoration experiments. D2 was preferred to D1 considering that D1 is involved in a strong turnover cycle that could have interfered with the experiment. The results showed that both antibodies, α-D2 and α-PsbS, reacted with the protein bands that were previously assigned to the dimer and the monomer of PSII (fig.7). From these results we assumed that PsbS is stablely bound to

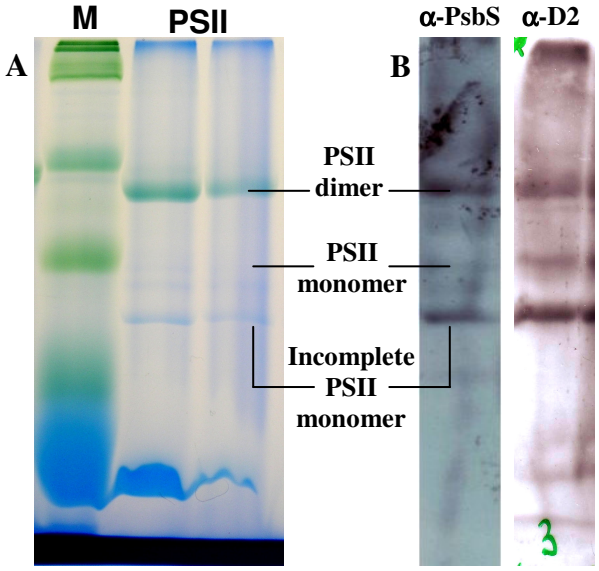

Figure 7. BN-PAGEs of PSII particles and related immunoblots.
In A a BN-PAGE of PSII particles is shown (see fig. 6B). The fist lane, labelled with M, shows tobacco thylakoid used as marker; in the second and third lane are two PSII samples at 0.01 and 0.005mg/ml chls respectively. In B immunoblots using α-PsbS and α-D2 on the PSII lanes from A are shown.

the PSII dimer. Unfortunately, these experiments gave no information about the position and the stoichiometry of PsbS. The only technique that in this research phase could be used for getting some structural evidence about stoichiometry and position of PsbS was single particle analysis. Therefore, single particle analysis experiments were done

whereas others are still in progress (in coll. with Sami Kareïche and Egbert J. Boekema, University of Groningen) (fig. 8). By transmission electron microscopy it is possible to get a range of images of single PSII complexes that are demonstrating the shape of the PSII particles in the sample. With this data, pictures of averaged particles of Arabidopsis PSII which do not contain PsbS and pictures of tobacco PSII were subtracted in order to get a so called different density (fig. 8). Through this method it is possible to get information about dimension, position and number of possible extra densities of the particles. At the moment averaged images of 18000 particles are available. From this preliminary investigation only slight differences were observed (fig. 8). This preliminary result does not show any evidence for the presence of PsbS

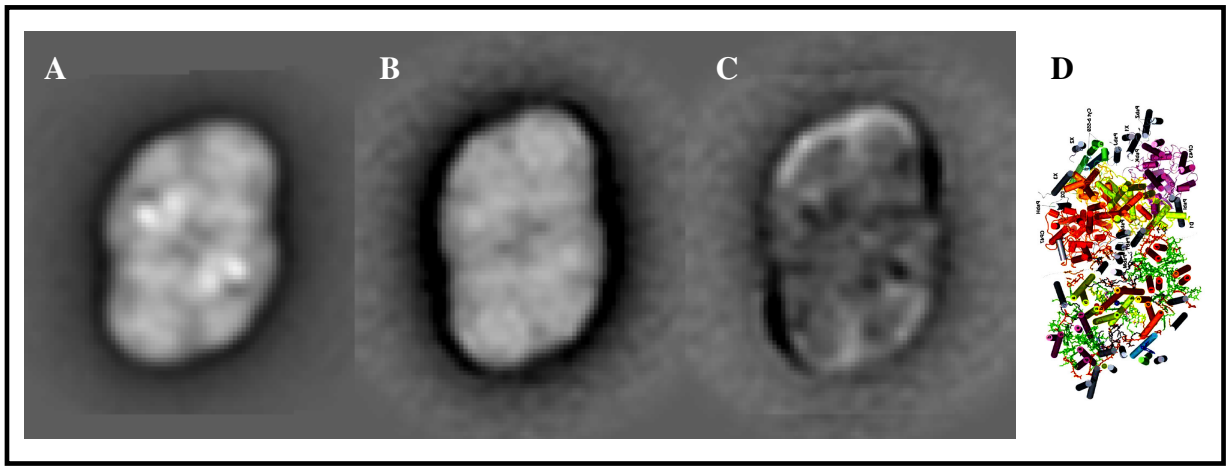

Figure 8. Single particle electron microscopy analysis of 18000 projections of PSII core.
In A and B PSII core dimer density maps from *A. thaliana* (A) and from transplastomic *N. tabacum* (B) are shown; in C the difference density between B and A is given. Four black spots and two black lateral belts are absent areas in B with respect to A. The four black spots in the centre are densities related to the extrinsic subunits that are only loosely bound in B. Two white areas related with B were also found in the higher and lower peripheral parts of C; in D is the map of the PSII structure from *S. elongatus* as comparison.

and also no evidence for the extrinsic subunits, which, according to the high oxygen yields measured, should be attached. Thus, psbS just like the extrinsic proteins, could have been lost during the preparation of the sample for electron microscopy.
Concerning the polypeptide Psb27 it was not possible to study the structural relationship with the PSII core because of its variable concentration (fig.5). Nevertheless the presence of varying levels of Psb27 indicates a similar behaviour with respect to the

extrinsic subunits PsbP and PsbQ that were also not constant. Furthermore the low concentration of Psb27 and the high oxygen evolution (Section 2.4) observed in the sample could be a good indication for a predominant amount of intact PSII as will be discussed in the section III.

3.3.3. PSII lipids and cofactors characterisation

One of the aims of this work was the preparation of PSII particles suitable for crystallisation experiments. It is well known that in membrane protein crystallisation the amount of lipids in the sample is a critical point. Especially in cases of His-tagged membrane protein purifications lipids can be drastically depleted during the step of washing (Kühlbrandt 1992). Lipids are not only related with the crystallisation process but also with the functionality of the protein. The lipid amount of PSII samples purified by differential centrifugation and PSII samples purified by Ni-NTA were determined by thin layer chromatography (TLC) experiments (tab.9). The analyses were performed

Table 9. Lipid determination in lipid stocks and in PSII samples.

			(mg/L)			Residual detergent		
			DGDG	**MGDG**	**PC**	**OG**	**DDM**	**Triton**
Controls	MGDG	Reference values	1,8	-	-	-	-	-
	DGDG		-	1,8	-	-	-	-
	PC		-	-	11,25	-	-	-
Samples	Lipids	Calculated values	1,8	0,3	3,75	-	-	-
	His-PSII		Values under TLC sensitivity			-	+	-
	PSII		0,45	0,225	1,875	+	-	+

running pure lipids (Merck) and lipid extracts from tobacco leafs as positive controls. Through that it was possible to find the amount of lipids that had to be added to the His-PSII sample in order to induce crystallisation. From TLC analyses of His-PSII samples it was evident that the lipids were hardly detectable and therefore occurred in very low amount. This will require an additional amount of pure lipids during crystallisation trials (tab.9) (fig. 9). In conclusion in PSII samples purified by differential centrifugation three different kinds of lipids were found: monogalactosyldiacylglycerol (MGDG),

digalactosyldiacylglycerol (DGDG) and Phosphatidylcholine (PC). Their concentration was also calculated (tab.9).

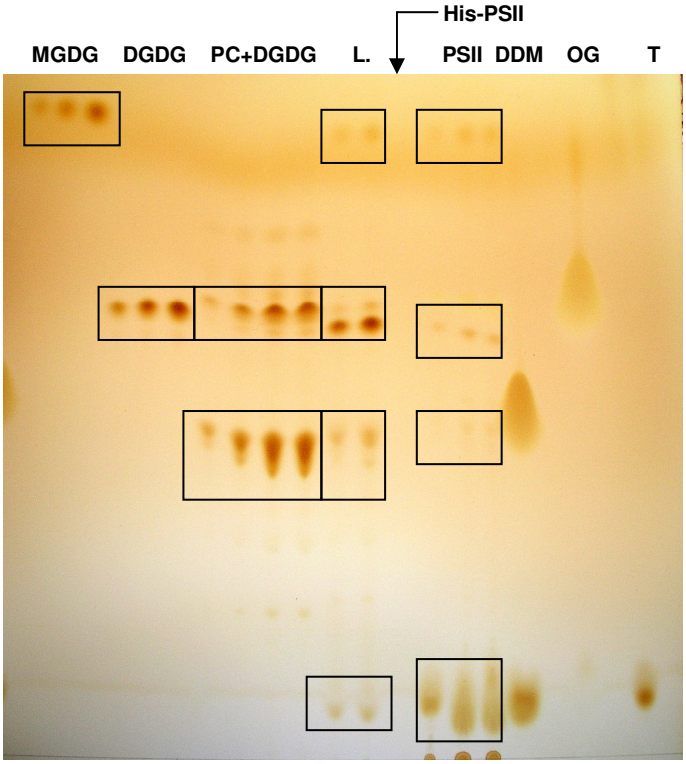

Figure 9. TLC analysis on several samples.

First, second and third group of lanes are MGDG, DGDG and PC+DGDG used as reference. MGDG and DGDG samples are in a final amount of 1.8, 3.6, and 5.4µg; PC+DGDG samples are in a final amount of 11.25, 22.5, 33.75µg. In the third group (PC+DGDG) the last reference amount (33.75µg) was repeated two times. The fourth group of lanes (L.) are whole tobacco lipids; the fifth lane labelled with His-PSII is the sample purified by Ni-NTA; the sixth group labelled with PSII are three lanes of spinach PSII samples capable of crystallisation. The last three lanes represent DDM, OG and triton (T) respectively.

The cofactor composition of His-PSII samples was analysed by high performance liquid chromatography (HPLC) (fig.10). Several HPLC elution profiles recorded at 435nm have shown five main peaks that according to the absorption spectra were assigned to lutein, violaxanthin, chlorophyll a, chlorophyll b, pheophytine and carotenes (fig.10,11). From the HPLC elution profile the absorption spectra associated to the peaks of chlorophyll a (retention time 14.5 min.) and chlorophyll b (retention time 12.8 min.) were resolved. Even though no calibration for all pigments was carried out, the relative absorbance between those chlorophylls, considering their similar structures, can be

reasonably used for qualitative observations. In the figure 11C and D the absorption spectra of chlorophyll b and chlorophyll a obtained from the same sample are shown. Those pictures showed that the ratio between the maximum absorptions in the red, at 665nm for Chl a and 650nm for Chl b, is ~60 times higher for Chl a with respect to Chl b. Considering that the molar extinction coefficients for Chl a and Chl b in acetone 80% is 8.25×10^{-7} cm^2/mol at 660 nm and 4.68×10^{-7} cm^2/mol at 642 nm (Lichtenthaler 1987) the ratio indicated above divided by two can be reasonably used to indicate a predominant amount (about 30 times) of chlorophyll a with respect to chlorophyll b.

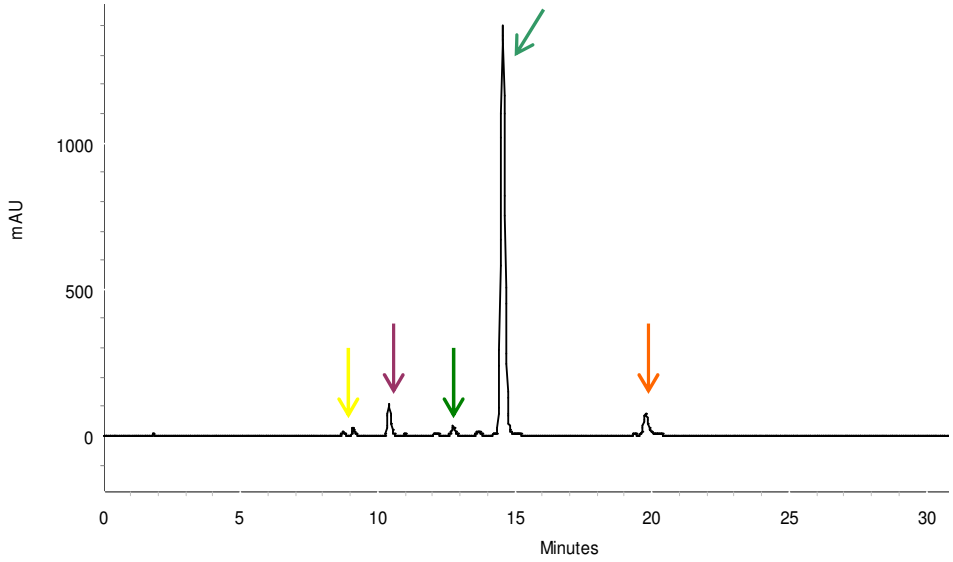

Figure 10. HPLC elution profile for a typical His-PSII sample recorded at 435nm.

Arrows represent the five main peaks with their relative retention times. In yellow are two peaks both related to Lutein; in violet the peak related to violaxanthin; in brilliant green chlorophyll b; in dark green chlorophyll a and finally in orange are three peaks (one main and two secondary) related with pheophytin and β-Carotene.

The result obtained once again gave evidence about the purity of the sample considering that chlorophyll a is the only type of chlorophyll in PSII. At the same time the low amount of chlorophyll b is also a demonstration for low impurities from other pigmented proteins such as LHCII.

The other interesting result was a complete absence of zeaxanthin and the presence of violaxanthin which are involved in the xanthophyll cycle. This result was expected considering that the leaves were harvested during the dark period where zeaxanthin is converted to violaxanthin (Section I fig.5).

In order to find out which polypeptides were related to violaxanthin several hypothesis can be put forward. In the first hypothesis the violaxanthin found comes only from the major LHCII (Liu *et al.* 2004; Stanfuss *et al.* 2005). Nevertheless considering the low amount of chlorophyll b in the sample this pigment was unlikely solely related with LHCII impurities. Considering the similar structures between lutein and violaxanthin, a comparison between their absorption spectra obtained from the same HPLC elution profile is possible. In the figure 11A and B the absorption spectra of lutein and violaxanthin obtained from the same sample are shown. The ratio between violaxanthin and lutein calculated in the maximum of both pigments was ~5 (130mAU violaxanthin / 26mAU lutein). Also in this case considering that the extinction coefficients in ethanol for violaxanthin and lutein is 153 10^3 l mol^{-1} cm^{-1} and 144 10^3 l mol^{-1} cm^{-1} respectively (Jeffrey *et al.* 1997) the ratio obtained can be reasonably used to indicate a predominant amount of violaxanthin. Also this result was in contrast with the structural data of the major LHCII where the ratio between violaxanthin and lutein is 0.5.

The second hypothesis valued a possible correlation of violaxanthin with the minor LHCII components CP24, CP26 and CP29. HPLC studies of these proteins revealed a ratio of 1-2 between lutein and violaxanthin (Moya *et al.* 2001). Also in this case lutein is in higher amount with respect to violaxanthin; furthermore it should be mentioned that the polypeptides related with these pigments were not found during the characterisation of the sample in terms of polypeptide composition.

Molecular modelling studies (Prafulla *et al.* 2006) and spectroscopical studies, *in vivo* and *in vitro*, have shown that PsbS could be able to bind zeaxanthin (Section I fig.6) (Szabo *et al.* 2005), whereas in the case of violaxanthin no evidences of any binding sites are found. However after a valuation of all the possible options especially those reported above the only protein candidate for binding violaxanthin was the protein PsbS. This hypothesis is corroborated from the high purity of the sample and the fact that PsbS is the main difference with respect to PSII from *S. elongatus* where no binding sites for violaxanthin were found (Loll *et al.* 2005).

3.3.4. PSII purity analyses

With the protocol developed in this work it was possible to purify PSII almost free of LHCII and PSI impurities. Immunodecoration tests on those impurities were able to

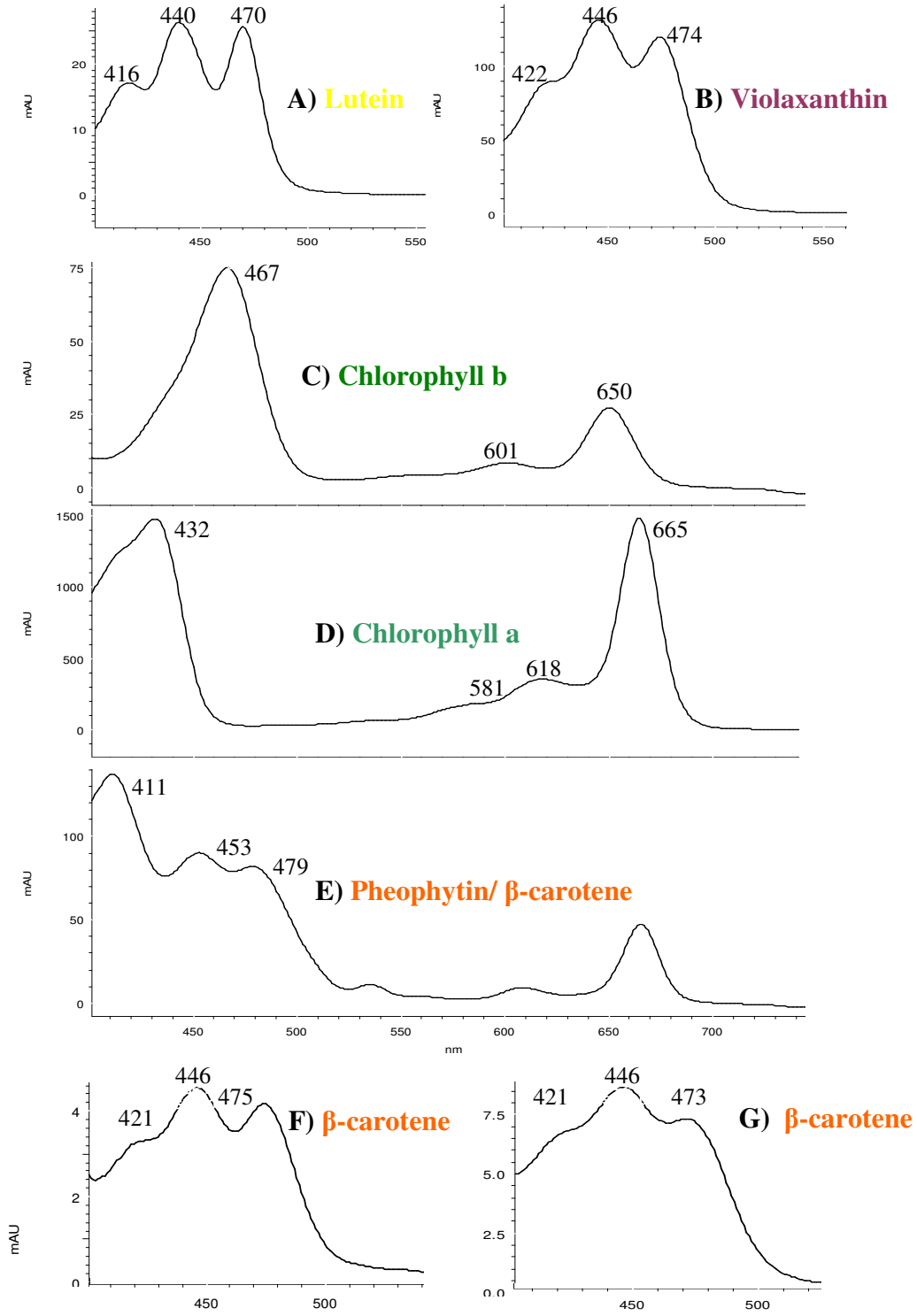

Figure 11. Absorption spectra from PSII pigments separated by HPLC.

A to E show the absorption spectra taken in the maximum from the main peaks of figure 10. In F and G the absorption spectra from the two shoulders before and after the peak at 19.7 min retention time (figure 9) are shown.

show a lower amount of PSI and LHCII in the His-PSII samples with respect to those purified by differential thylakoid centrifugation (fig.12). The amount of these impurities in His-PSII samples were estimated by using pure PSI and LHCII proteins as references. In both cases the final protein amount was too low and therefore it was not possible to estimate any quantity of the impurities (fig.12A).

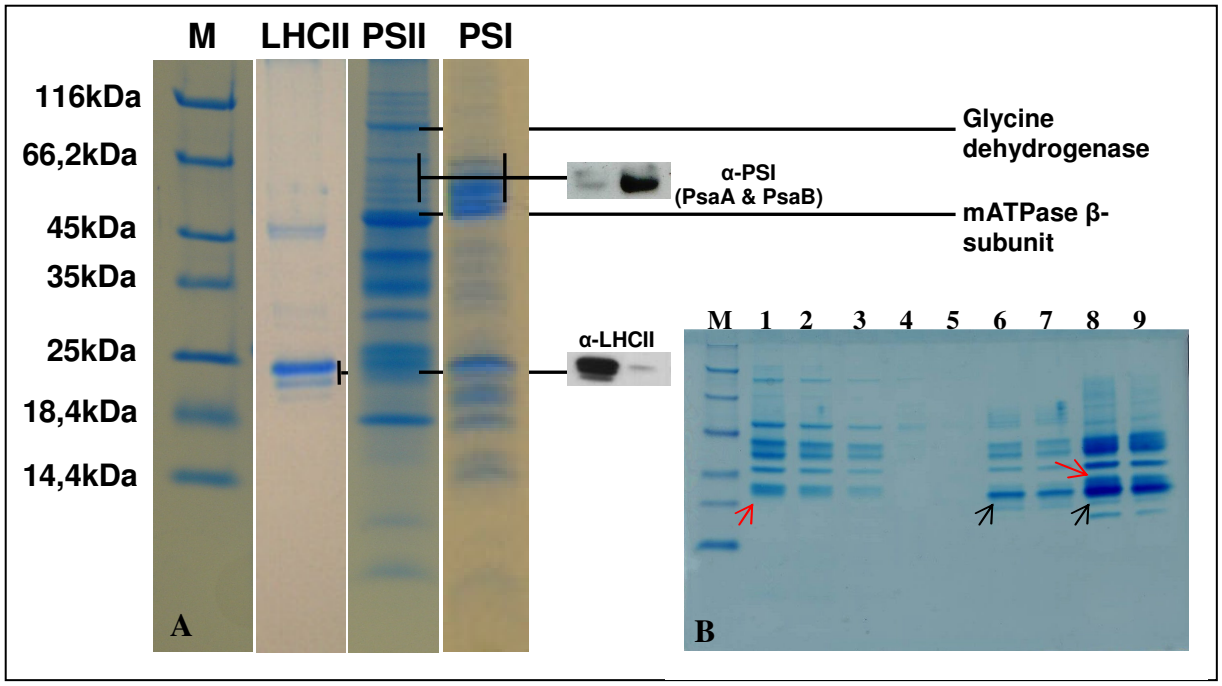

Figure 12. Impurities characterisation in His-PSII samples.

In A the lane M is the marker, the lane LHCII is pure Light Harvesting Complex II, the lane PSII is Photosystem II purified by Ni-NTA and lane PSI is Photosystem I. PSI and LHCII lanes where used as control for impurities in the PSII lane. α-LHCII and α-PSI show the immunoblots for the main subunits of LHCII and PSI, respectively; in α-LHCII the first band is the immunodetection of pure LHCII and the second band is the immunodetection of the PSII sample purified by Ni-NTA; in α-PSI the first band is the amount of PSI impurity in PSII purified by Ni-NTA and the second band is the reaction with pure PSI. In the lane PSII the two bands labelled with Glycine dehydrogenase and mATPase β-subunit were characterised by Maldi-Tof. In B the lane M is the marker, the lanes 1 to 5 are PSII samples purified by Ni-NTA at different concentrations, lanes 6 and 7 are PSII from spinach purified by differential centrifugation and lanes 8 and 9 are PSII samples purified from wild type tobacco by differential centrifugation. The two black arrows show the band of LHCII impurity that is absent in the samples obtained by Ni-NTA. Note that in the lanes 6, 7, 8 and 9 the band immediately above LHCII consists of the polypeptides D1 and D2 (red arrows) which is the only band in this area in the samples purified by Ni-NTA.

Nevertheless it was possible to prove their qualitative presence in the sample by a small signal in the immunoblot. But on the other hand there weren't any of these impurities detected in the bands of the SDS-PAGE analysed by Maldi-tof.

The impurities related with LHCII showed a strong dependence on pH (fig.1) and washing time. Samples purified at pH 6.0 had a higher amount of LHCII which was even more pronounced at shorter washing times. In any case the characterisation of the sample by SDS-PAGE showed two reproducible bands at high molecular weight. Maldi-tof characterisations identified them as the glycine-dehydrogenase and the β-subunit of the mitochondrial ATPase (fig.12A).

The problem of co-purified proteins was the main inconvenience related with the Ni-NTA technique. This problem is depending on the density of histidines at the protein surface that can be responsible for an increased resin affinity for proteins without His-tag. In order to solve this problem several strategies were adopted with the aim of getting a differential affinity of the His-tagged proteins and the co-purified components for the Ni-NTA resin. Where the proton concentration is not a limiting factor for the His-tagged protein functionality, the pH in the washing buffer can be decreased in order to decrease the affinity for all the binding sites. In the case of PSII this possibility cannot be used because the pH range for its stability is preferentially between 6 and 6.5. For that reason the pH is a critical factor for PSII stability and in particular the optimal pH in PSII is different between the luminal part (around 6) and the stromal part (around 7). From these peculiarities it is obvious that the pH must be changed only for getting the optimal compromise between the lumen and stromal parts in order to guarantee the overall optimal functionality in the complex. The use of higher amounts of imidazol in the washing buffer and a simultaneous increase of the washing time was the only possibility for reducing impurities. Furthermore, when the washing was performed in presence of betaine the effectiveness of the final washing was increased (fig.14).

Characterisation of the mATPase β-subunit by maldi-tof was obtained with high scores demonstrating a high probability that the protein is indeed the β-subunit of mATPase. Contrarily, in the case of the glycine-dehydrogenase the related scores were much lower so that the protein in the gel was maybe just a protein homologous to the glycine-dehydrogenase.

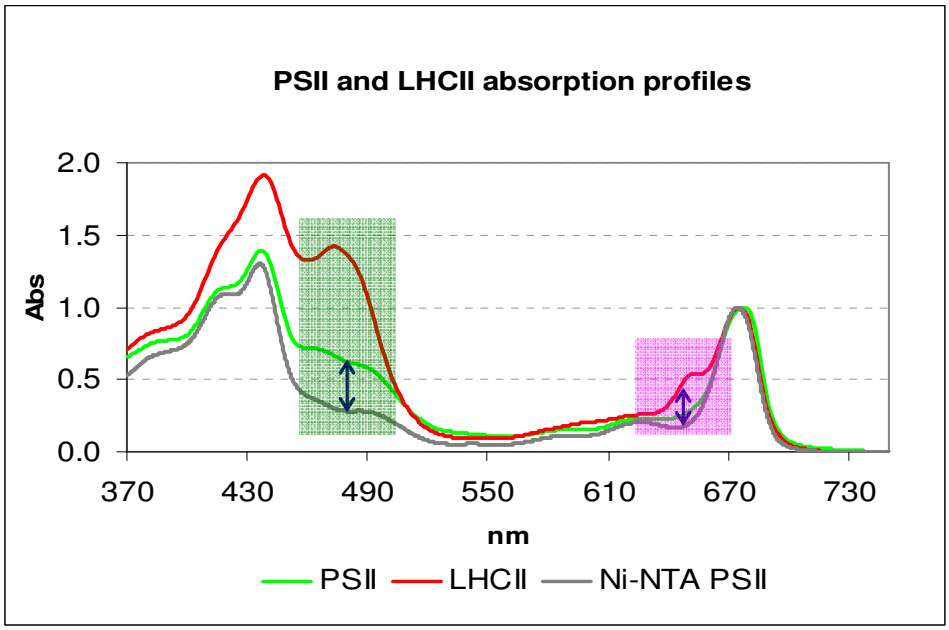

Figure 13. Absorption spectra and LHCII impurities.

In the picture the absorption spectra from pure LHCII in red, from PSII purified by differential centrifugation in green and from His-PSII in grey are shown. The coloured areas show the differences in absorbance between PSII samples purified by differential centrifugation and Ni-NTA at the main wavelengthes where LHCII impurities are absorbing. The lower absorbance of Ni-NTA samples (in grey) shows the lower concentration of LHCII with respect to PSII (left arrow) and pure LHCII (right arrow) both purified by differential centrifugation.

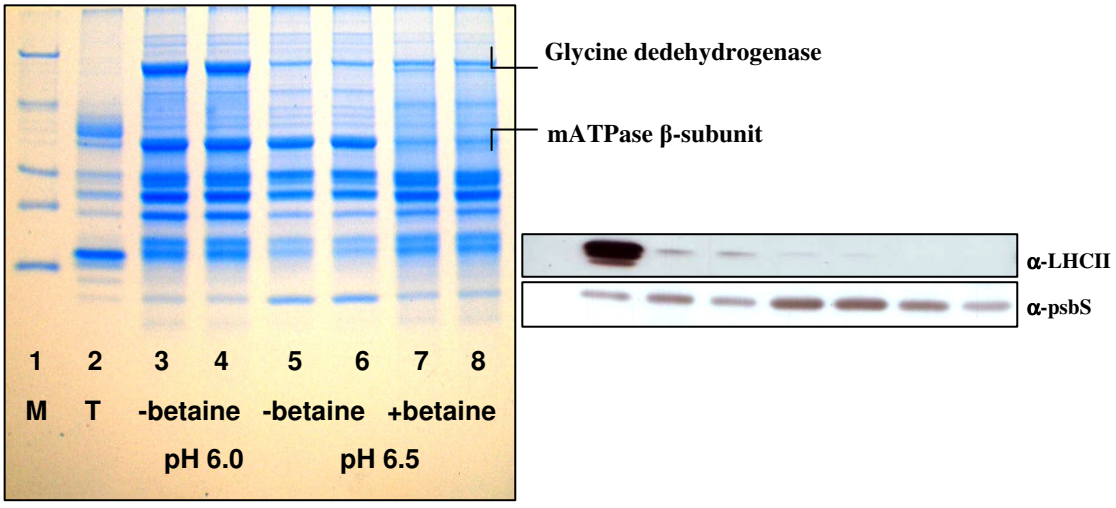

Figure 14. Effects of pH and betaine on PSII impurities.

SDS-PAGE of samples purified at pH 6.0 without betaine (lines 3 and 4), pH 6.5 without betaine (lines 5 and 6) and ph 6.5 with betaine (lines 7 and 8). The amount of LHCII impurities was tested with α-LHCII, α-PsbS was used as internal reference.

3.4. PSII functionality assay

PSII functionality is important for the intactness of the holocomplex. Oxygen evolution measurements by Clark electrode was the main technique applied for testing the intactness of the complex. PSII activity hence oxygen evolution derives from the intact OEC, the charge separation on which the final electron transport process is depending as well as the effectiveness of the electron acceptor. Oxygen evolution tests were performed in order to find out the best conditions able to induce the highest oxygen evolution in these specific PSII particles.

During purification the main changes leading to an increase in the oxygen evolution were the use of 10mM $NaHCO_3$ in presence of 1M betaine and a decreased concentration of DDM (0.01% instead of 0.03%) in the washing and elution buffers. Experiments with only $NaHCO_3$ showed a lower PSII oxygen evolution than purifications where also 1M betaine was used. Moreover purifications with all three conditions together gave the highest oxygen evolution rate. Practically, the addition of those three components was able to change the oxygen evolution rate from 350 µmol to 1400 µmol O_2/h mg chls. Besides, at the same condition some samples showed an oxygen evolution rate around 1800 µmol O_2/h mg chls (tab.10).

Table 10. Tested conditions for oxygen evolution

	Oxygen evolution (µmol O_2/h mg chls)				
	+10mM $NaHCO_3$			-10mM $NaHCO_3$	
	+0,01% β-DDM	+0,03% β-DDM		+0,03% β-DDM	-0,03% β-DDM
PSII particles	+Betaine (1M)	+Betaine (1M)	-Betaine	-Betaine	-Betaine
	1389±314	746±40	427±55	606	440±16.4
Number of measurement	21	9	12	3	9

These results were also depending on the optimisation of the use of the oxygen evolution devices and the buffer used in the test. After several tests, the buffer chosen for diluting the PSII stock was the elution buffer with electron acceptors but without betaine and ascorbic acid. Furthermore, 1mM and 5mM $CaCl_2$ in the buffer were also tested but without any big difference for the final PSII activity. All these tests were performed using both 10x and 6xHis-PSII getting similar results.

3.5. Two dimensional crystallisation of PSII from spinach

As known from basic physics, well ordered crystalline areas are able to diffract waves. The phenomenon of diffraction depends on the structure of matter that interacts with e.g. the light (diffraction pattern). The diffraction pattern can be used as source for structural studies. When crystals are grown in two dimensions (2D crystals), the diffraction pattern can be obtained by the electron beam employed in transmission electron microscopes. 2D crystals can be obtained from biological materials such as DNA, RNA and proteins. 2D crystals of membrane proteins are obtainable from purified protein in detergent solution mixed with other additives like lipids, detergents and specific salts (Kühlbrandt 1992). In this solution the protein forms micelles together with the detergent and lipids. After the removal of the detergent the protein and lipids get organised in proteoliposomes or reconstituted membrane sheets.

In this situation the protein can form 2D lattices under favourable conditions. The analysis of 2D crystals of Photosystem II Reaction Centre-CP47 (RC-CP47) from higher plants led to the current structural model with a resolution of 8Å (Rhee et al. 1997).

In this work PSII core dimers isolated from spinach chloroplasts were used to produce two-dimensional crystals. Spinach PSII was purified by differential centrifugation in presence of HTG or OG (Nakazato *et al.*1996). Preliminarily, crystallisation experiments were made by using a pre-existent protocol (Büchel and Kühlbrandt 2005).

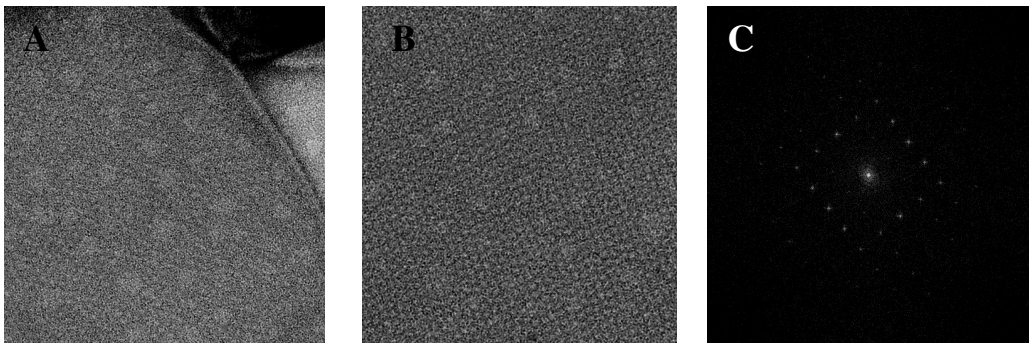

Figure 15. Electron micrographs and diffraction pattern of RC-CP47 2D crystals.
Negative stained 2D crystals at 53kX in A and 60kX in B. In C a Fast Fourier Transformation from the electron micrograph in A is shown.

Accordingly, the protein was purified and crystallised in HTG for RC-CP47 crystals (fig.15). In this protocol (Büchel and Kühlbrandt 2005), PSII cores are used but only a subcomplex of PSII, RC-CP47, is formed in the crystals.

The first part of this work focused on the improvement of the crystal dimension and diffraction (tab.11 and 12). Relevant results by using sodium propionate as additive were obtained. On one hand this salt was able to increase the order of diffraction but on the other hand also the crystal stacking was increased. The stacking can interfere with the steps of crystal data processing. Therefore a group of experiments was done to reduce this tendency. Exchange of HTG with OG in the crystallisation step was able to slightly reduce the stacking.

Table 11. Starting composition of the crystallisation buffer.

PSII (mg chls)	Na propionate	$ZnCl_2$	$CaCl_2$	KCl
0.7-1.0	1mM	1mM	1mM	15mM

To further decrease the staking the protein was purified in OG instead of HTG. In this case the lipids-detergent vesicles that in HTG PSII samples were mainly spherical were now divided in two populations, spherical vesicles and tubular vesicles (tab.13).

Table 12. Tested chemicals using the crystallisation buffer in table 11.

	Concentration (mM)	Crystals	
		[1]Number	[2]Shape
Na Propionate	0	+	S
	0,5	+	S
	1	++	SL
	2	++	SL
	3	++	SL
	4	+	SL
LiCl (instead of KCl)	5	+	S
	10	+	S
	15	+	S
	20	/	-
	25	P	-
	30	P	-
$AlCl_3$	1	+	S
	2	P	-
	4	P	-

[1]**: Number. /:** no crystals; **P:** precipitation; **+:** relative amount

[2]**: Shape. S:** sheet; **SL:** stacked sheets; **T:** tubes

Furthermore, PSII samples that were purified in OG were crystallised by using HTG. The results showed crystals with similar characteristics but less quality. After this step, PSII samples purified and crystallised in OG were also tested with several salts. $BiNO_3$ was able to change the crystalline form from crystalline sheet to tubular crystals (fig.16) (tab.13). These crystals were found to be classifiable in two different groups with respect to the shape of the diffraction pattern. The diffraction gave a typical pattern for these kinds of crystals with four or five orders. This diffraction

Table 13. Tested chemicals using the crystallisation buffer in table 11.

	Concentration (mM)	Crystals	
		[1]Number	[2]Shape
$Bi(NO_3)_3$	1	+	S and T
	5	++	T
	10	+	T
$BiCl_3$	1	+	T
	5	+	T
KNO_3	1	P	-
	5	P	-
	10	P	-

For [1] and [2] see legend in table 12.

pattern, typical for tubular organisations, can be considered as the superimposition of two crystalline areas, the two faces of the tubular crystal. Both faces of the tube are able of diffraction. The relative orientation of one diffraction pattern compared to the other is depending on the relative orientation of the particles in the crystal. More precisely the micrographs were able to show a spiral distribution of the crystalline particles. This means that the diffraction patterns were depending on the spiral distribution (spiral number) in the tube. After that step the electron micrographs of the sample were digitised with an high resolution scanner. Data processing from scanned images was started in order to obtain the electron densities of the particles. The processing was performed for diffraction patterns of several groups. The results of the data processing of different groups of tubes showed that there were the two types of crystals showing two different unit cells. Both maps calculated from the diffraction patterns showed a resolution of 15Å. From those preliminary electron densities it could be concluded that the protein was crystallised with a space group $P22_12_1$ and seemed to have an internal symmetry axis. So far, at this resolution, it cannot be said if it is related with the two-fold axis of a dimer or the pseudo two-fold axis of a monomer (fig.16 C and F).

Furthermore, as can be seen from the different maps it is possible that the differences observed in the units cells could be related with crystals from two different populations of particles, RC-CP47 in figure 16C and PSII in figure 16F.

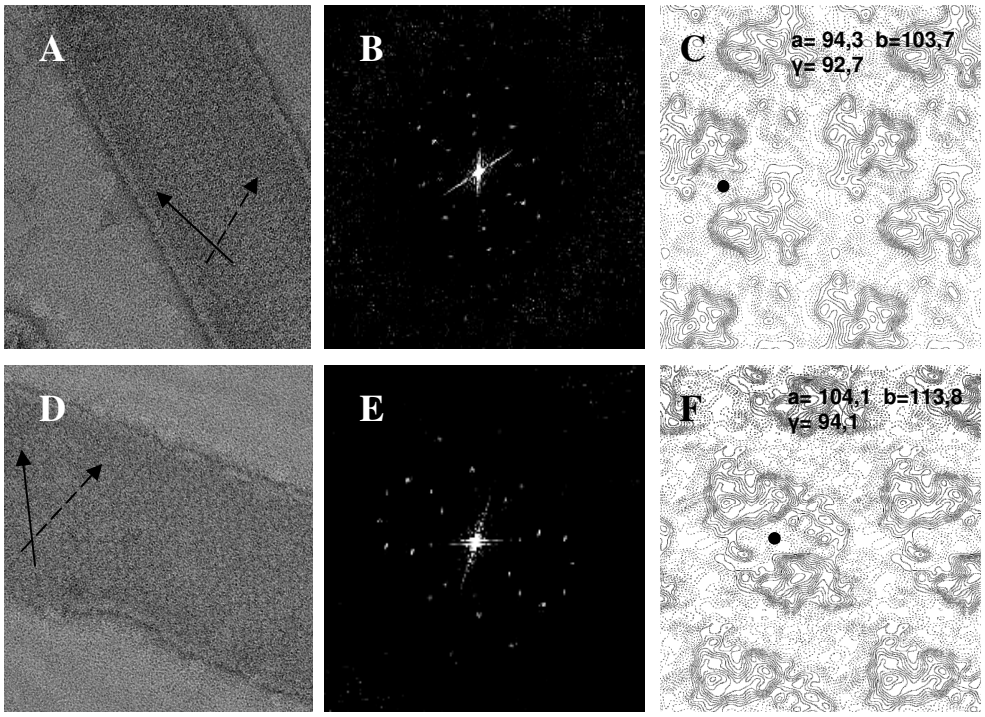

Figure 16. Electron micrographs, diffraction pattern and electron densities of PSII tubular crystals.

A and D are negatively stained tubular crystals at 53kX from two different kind of tubes. The arrows show the orientation of PSII particles on the tubular faces. The different angles between the arrows in A and D identify two different kind of crystals. B and E are the Fast Fourier Transformation from A and D, respectively. C and F are the equivalent electron densities with space group $P22_12_1$. The spots indicate the internal (pseudo)symmetry axes, numbers on top define the unit cell parameters.

III. Discussion

Current protocols used for PSII purification are based on the work of Bertold A. D. et al. 1981 and its modifications. PSII is purified by differential centrifugation to obtain a fraction of thylakoid membranes enriched in PSII (BBY). This purification includes a solubilisation with Triton followed by a centrifugation to separate the thylakoid membranes in stroma membranes and grana membranes. After centrifugation the fraction of grana membranes is used for a second solubilisation with a mild detergent such as DDM, OG or HTG in order to extract functional PSII dimers. The advantage of these methods is the possibility to purify high amounts of intact and functional PSII dimers; nevertheless the disadvantage is the residual amount of detergent especially triton that can interfere in the following studies. Furthermore, the inconstant level of impurities and the possibility to compromise the stability of the complex as an affect of the step of purification by triton is also a possible inconvenience. These reasons make the samples not suitable to sensitive techniques such as crystallography and electron microscopy in structural studies or spectroscopy in functional studies. In these cases only homogeneous samples with high levels of purity are employable for analysis.

In order to prevent the inconveniences related with the impurities and the residual detergent in the samples purified by differential centrifugation, a purification protocol through the Ni-NTA affinity chromatography has been created. Nevertheless, on one hand it is possible to get a final sample more pure and homogeneous by Ni-NTA affinity chromatography but on the other hand this system is not able to separate between the different forms of PSII such as PSII under repair, functional PSII and PSII under assembly. In fact in this technique PSII is purified directly from the thylakoids avoiding the use of triton as detergent for obtaining the grana membranes were mainly functional PSII is concentrated. Through the use of the Ni-NTA, PSII can be purified by using only one mild detergent as DDM. This raises the stability of the sample preventing the use of strong detergents as triton that stays as residue in the final sample.

In the present study, PSII was purified in a single-step by Ni-NTA affinity chromatography from two modified *N. tabacum* strains having 6x or 10x His-tag extensions at the N-terminus of the PsbE subunit (H. Fey PhD thesis). For the first time a protocol is presented to isolate His-tagged oxygen-evolving PSII of higher plants

which exhibits high rates of oxygen-evolving activity (tab.10). The purified PSII, devoid of LHCs and PSI apoproteins, was characterized for functionality and subunit composition (fig.12). Several advantages were associated with the His-tag methodology to isolate PSII. Isolations by using other methodologies such as protocols of differential centrifugation required less amount of time but resulted in a final sample with low purity. Alternatively PSII purification by centrifugations with sucrose gradients required less purification time but resulted in a sample of high purity but very low amount (Hankamer *et al.* 1997, Boekema *et al.* 1995). In our protocol the entire procedure was completed in less than 14 hours getting a sample of high purity and high amount. Besides, it should be also noted that this PSII preparation was made by using a low column pressure so that even less time would be required if medium or high pressure columns were used. Furthermore in other purification protocols a pre-solubilisation with a first detergent as Triton followed by a second solubilisation with a mild detergent is frequently required (Hankamer *et al.* 1997), whereas by NTA a single step solubilisation by using only a mild detergent such as DDM is possible. This fact becomes more relevant considering that Triton is kept during further procedures as shown here by TLC (fig.9). This can interfere during the following studies on the protein structure and functionality.

In this work it was also demonstrated that the addition of 6 or 10 histidine residues at the N- terminus of the PsbE subunit did not give rise to serious losses in stability of the manganese cluster as corroborated by the thylakoid proteins pattern (fig.17) and the high oxygen evolving activity of PSII (tab.10). The isolated PSII core complex exhibited an averaged rate of oxygen evolution exceeding 1350 μmol/mg·chls·h among other preparations for higher plants PSII complexes that were between 1000 and 1500 μmol/mg·chls·h (Haag *et al.* 1990, van Leeuwen *et al. 1992* and Hankamer *et al.* 1997). Besides, the oxygen evolution was strongly dependent on the presence of specific chemicals and the pH either during purification or during oxygen evolution tests. Even though PsbP and PsbQ subunits where always found in minor and variable amounts, the oxygen evolution of the PSII particles was not directly affected. Hence, PsbO that was present in constant levels can be considered as the main stabilizing protein in the group of the extrinsic subunits of PSII as already described by De Las Rivas (2005).

The yield of the His-tagged PSII complex from detergent-solubilized thylakoids was depending on the solubilisation conditions (see tables 1 and 2). The averaged yield was found to be ~2% with the highest values at 3.8% on chlorophyll basis. However, assuming that the ratio of chlorophylls for PSII in the thylakoid membrane is around 590:1 (Wild *et al.* 1986) and considering that only 35 chlorophylls are bound to the PSII reaction centre core proteins (Loll *et al.* 2005) the maximum theoretical yield for pure PSII core isolated from thylakoid membranes is around $^{35}/_{590}$ = 5.9 % of chlorophylls. Taking this as a maximum, the actual yield of the purification reaches an averaged value of ~34% with the highest values at ~64.5%. This amount could be even higher considering that a part of the chlorophylls of the unsolubilized thylakoids were removed during the centrifugation after solubilisation. Nevertheless, it should be reminded that for the calculations the PSII / chlorophyll stoichiometry from *S. elongatus* and the same ratios in thylakoids from pea were used. Furthermore the mutants might have some difference in the PSII / chlorophyll ratio as well as the PSI/PSII stoichiometry.

The complete removal of LHCs and PSI was essential for obtaining a highly pure PSII complex. In this respect PSII preparations from higher plants are not always a suitable material because of their high contents of LHCs and PSI. In the thylakoid membrane the LHCIIs (LHCII trimer, CP24, CP26, CP29) stay in close proximity to PSII (fig.4). For this reason LHCII polypeptides are the main impurities that can be found in PSII preparations. The use of the His-tag strategy allowed a isolation of the PSII core complex without contaminations of LHCs as judged from the extreme elimination of the chl b band in the absorption spectrum (Fig.13), the absence of the characteristic LHC apoprotein bands on the SDS-PAGEs profile (Fig. 12) and finally the very high chl a/b ratio (between 40-100) in the isolated PSII core complex. Furthermore the sample was confirmed to be free of PSI contaminations as shown in the SDS-PAGEs and the immunoblots (fig.12).

Molecular size analysis performed by gel filtration and BN-PAGEs revealed that most of the PSII core complex particles isolated from *N. tabacum* were in the dimeric form (Fig.6) with a molecular mass of about 500 kDa. A similar molecular weight was obtained indirectly by calculation considering the subunit composition of PSII and using the work of Barber *et al* as reference (1997). Nevertheless, the use of concentrators with a high cut-off (300kDa) doesn't exclude the possibility that in tobacco PSII stays mainly

in dimer form. In fact it is possible that a part of the monomers could be lost during the concentration step as partly confirmed by the presence of a band in the BN-PAGEs and a slight peak in the gel filtration (fig.6) of samples analysed after concentration. On the other hand the low amount of monomers could also be related with the normal degradation of the PSII dimer.

Molecular characterisation indicated that the PSII particles were constituted from the main core subunits (fig.5). Nevertheless, two unexpected subunits PsbS and the predicted luminal protein Psb27 were also found as component in the core. Presence and amount of Psb27 were not constant and its behaviour was therefore very similar to the extrinsic subunits PsbP and PsbQ that were also not constantly present. This similarity between PsbP, PsbQ and Psb27 can be related to their similar chemical-physical properties indicating the same behaviour during the steps of purification and confirming the probable extrinsic position of Psb27 as in the case of PsbP and PsbQ. Nevertheless, considering that Psb27 is reported to be involved in the PSII assembly (Roose *et al.* 2004) and in the PSII repair (Chen *et al.* 2006; Nowaczyk *et al.* 2006) its low concentration in the sample could be equivalent to its physiological concentration. Psb27 should be associated transiently during PSII assembly or PSII regeneration and its level depends on the quantity of the intermediate PSII complexes in the sample. In general the concentration of functional PSII where Psb27 is not bound is higher with respect to the amount of PSII under assembly or regeneration where also Psb27 is present. According to Rögner *et al.* (2006), the low amount of Psb27 in the sample can also be an indication for a low amount of the monomeric PSII population as confirmed by the BN-PAGEs, the analytical gel filtration, the high levels of PsbO and the high oxygen evolution (fig.5, 6 and tab.10). Regarding the oxygen evolution and the PsbO levels it should also be reminded that the D1 cycle and hence the photodamage of PSII are the main reasons for PSII regeneration and that in PSII regeneration and PSII assembly a new positioning of PsbO and the manganese cluster are requested (Chen *et al.* 2006; Nowaczyk *et al.* 2006). In this process where the oxygen evolution is blocked Psb27 should play a primary role in the mechanism of assembly and regeneration of PSII. In conclusion the low concentration of Psb27 and the high oxygen evolution observed in the sample are a good indication for a predominant amount of intact PSII.

Interesting was also the unexpected presence of PsbS with constant amount in the sample. Initially the presence of PsbS tightly bound to PSII was interpreted as an effect of the His-tag that maybe induced a stress in the plant, responsible for increasing both the amount of PsbS and the interaction with PSII. Furthermore several comparison between wild type and mutants in terms of leaf chlorophyll content, thylakoid oxygen evolution and leaf pulse amplitude modulated fluorometry have shown significant difference (Personal communication). Moreover PAGEs of purified thylakoids from wild type and mutants revealed different levels of PsbS in wild type tobacco with respect to tobacco mutants (Personal communication).

PsbS was also considered to be a copurified component but after several tests the subunit was considered to be stably bound to the PSII core. Several evidences led to this idea, in first place PsbS is always stoichiometrically related with the main core subunits behaving differently with respect to the other impurities which were always found in irregular amounts. Second, considering the homology of PsbS to the LHCIIs a co-purification of these apoproteins should be expected but not any band related to them was found. As third point experiments on BN-Pages have shown that PsbS can be immunodetected in bands related to PSII dimer and monomer (fig.7). The fourth point is that PsbS with a molecular weight of 22 kDa was not removed during the step of concentration that was performed with a cut-off of 300kDa.

Even if evidences in this sense were not found, the extensive hydrophobicity of PsbS could be responsible for a firm binding in some unspecific region of PSII. However, psbS in tobacco has no stronger hydrophobicity than its counterparts in other species like e.g. Arabidopis or spinach. Nevertheless, in previous work on pea and spinach no evidence was found indicating that PsbS is stablely bounded to PSII.

The constant levels of PsbS in the sample should only partially be related with the purification protocol. A stronger binding affinity of PsbS to PSII in tobacco with respect to the same proteins from spinach (*Spinacea oleracea*) or arabidopsis (*Arabidopsis thaliana*) also used as model for this kind of experiments could be possible. This hypothesis is corroborated by the fact that the origins of tobacco are in the equatorial areas were the light intensity, the photoperiod and the temperatures are stronger with respect to plants that come from higher latitudes as spinach, arabidopsis or pea. As shown by several authors PsbS is involved in the non photochemical quenching process

(Szabo *et al.* 2005). Therefore it is possible that this process and the related interactions of PsbS with PSII could be more sensitive and efficient in tobacco respect to the other plants used as model for PSII studies. This fact together with the very mild purification protocol could lead to the stable binding of PsbS to the core.

Immunodecoration experiments with PsbS antibodies made on native complexes have shown that this subunit was a component of the PSII core, PSII monomer and incomplete PSII forms like the Reaction Centre-CP47 (RC-CP47) as shown by BN-PAGEs (fig.7). These results allow some hypothesis about the possible location of PsbS in PSII. Assuming that in every complex and subcomplex the subunit PsbS is located in the same position and considering that the α-PsbS signal in the immunoblot was in the main bands of the BN-PAGE, it could be concluded that the subunit PsbS can be located in the CP47 region if the incomplete monomer is the RC-CP47. In this region two possible zones where PsbS could be located were found. The first one between the subunits PsbE and PsbH and the second between PsbH and CP47 (Section I fig.2). Besides it cannot be excluded that other PsbS subunits are bound in other regions of the PSII dimer, in particular in the region of CP43. Single particle analysis of PSII from tobacco showed little extra areas around the CP47 region with respect to the PSII references from *Arabidopsis thaliana* without PsbS. Nevertheless, the extension of these areas is not big enough for fitting the predicted shape and dimension of this subunit (fig.8). Furthermore the presence of violaxanthin in the sample can also be related with the PsbS subunit. As discussed in the paragraph 2.3.3. several evidences indicated that violaxanthin was not related to the LHCIIs proteins but could be stablely bound to PsbS since the other subunits of PSII are not known for having a violaxanthin binding site. This fact might locate the main steps of the xanthophyll cycle in the PsbS subunit.

The observations that PsbS could be located in an area with a high density of chlorophylls like the CP47 region and the indications that PsbS could be able to bind zeaxanthin (Szabo *et al.* 2005) and maybe also violaxanthin lead to the hypothesis that a direct and fast quenching of the excitation energy excess is possible in PSII. According to this hypothesis, a place for the non photochemical quenching in the PSII from higher plant can be found through a xanthophyll cycle probably completely located in the PsbS subunit. Nevertheless should be mentioned that other works indicated PsbS as overall

distributed in the chloroplast and interacting with several other components like PSI, ATPase and minor subunits of LHCII (Teardo *et al.* 2007)

In conclusion, the present study demonstrated that application of the His-tag methodology to the higher plant *N. tabacum* was successful for producing PSII in large scale, in high purity and capable of oxygen evolution in a high rate. The obtained core complex is advantageous not only for its crystallisation but also for a variety of studies on the structure and the function of this fascinating protein.

Simultaneously to the experiments of PSII purification from tobacco also 2D crystallisation experiments on spinach PSII were done. The experiments were carried out to study the effects of several salts and detergents in crystallisation trials. In these experiments it was found that the salt $BiNO_3$ in presence of OG is able to induce PSII tubular crystals with a new crystalline lattice having new cell constants. The results obtained with these groups of experiments were important because on one hand a new kind of crystal from spinach was obtained and on the other hand an improved protocol to crystallise tobacco PSII is now available. Although spinach PSII used for 2D-crystallisation experiments was capable of crystallisation, the method of differential centrifugation used for its purification had some limitation related to the LHCII and PSI impurities. The amount of impurities is responsible for disturbance in the crystal formation, growth and homogeneity (Kühlbrandt 1992). By using the spinach crystallisation protocol on tobacco His-PSII it could be possible to get crystals from a sample almost free of LHCII and other typical impurities. Crystallisation trials using this kind of samples could lead to obtain bigger and higher ordered crystals leading to a higher resolution structure with respect to spinach PSII crystals. However, experiments performed with tobacco His-PSII showed problems for inducing crystallisation. These problems were related with the low amount of lipids in the pure protein (fig.9) and the use of DDM instead of OG or HTG during the purification of PSII. In conclusion, it should only be possible to get crystals from tobacco His-PSII by the addition of lipids in order to obtain the ideal lipid-protein ratio necessary for crystallisation. Moreover, for the same reason it will be necessary to find new volumes and times of dialysis considering that the critical micelle concentration (CMC) for OG or HTG is much higher with respect the one of DDM.

V. References

Abigail C., Malcom R., Balz S., Craig P. and Ian W. (2006): Nature 440: 714-718

Mark Aspinall-O'Dea, Mark Wentworth, Andy Pascal, Bruno Robert, Alexander Ruban, and Peter Horton (2002): In vitro reconstitution of the activated zeaxanthin state associated with energy dissipation in plants. PNAS 25:16331-16335

Barber J, Nield JJ, Morris EP, Hankamer B. (1999): Subunit positioning in Photosystem II revisited. Trends Bioch. Sc. 24: 43-45

Barber J., Nield J., Morris E. P., Zheleva D. and Hankamer B. (1997): The structure, function and dynamics of photosystem two. Physiologia plantarum 100:817-827

Beddard G.S., Porter G. (1976): Concentration quenching in chlorophyll. Nature 260: 366-367

Bergantino E., Brunetta A., Touloupakis E., Segalla A., Szabos I. and Giacometti G. M. (2003): Role of the PSII-H subunit in photoprotection. JBC 278: 41820-41829

Bertold A. D., Babcock G. T. and Yocum C. (1981): A highly resolved, oxygen evolving photosystem II preparation from spinach thylakoid membranes. FEBS letters 134: 231-234

Billsten, H. H., Sundstrom, V., Polivka, T. (2005): Self-Assembled Aggregates of the Carotenoid Zeaxanthin: Time-Resolved Study of Excited States. J. Phys. Chem. 109, 1521-29

Blankenship R. and Hartmen H. (1998): The origin and evolution of oxygenic photosynthesis. Trend bioch. Sc. 23: 94-97

Blankenship RE. (1992): Origin and early evolution of photosynthesis. Photosynth Res 33: 91–111

Boekema E. J., Hankame B., Bald D., Kruip J., Nield J., Boonstra A., Barber J., Rogner M. (1995): Supramolecular structure of the Photosystem II complex from green plants and cyanobacteria. PNAS 92(1): 175-179

Bricker T., Frankel L. (2002): The structure and function of CP47 and CP43 in photosystem II. Phot. Res. 72: 131-146

Büchel C. & Kühlbrandt (2005): Structural differences in the inner part od Photosystem II between higher plants and cyanobacteria. Phot. Research 85: 3-13

Büttner M, Xie D-L, Nelson H, Pinther W, Hauska G, et al. (1992): Photosynthetic reaction center genes in green sulphur bacteria and in Photosystem 1 are related. Proc. Natl. Acad. Sci. USA 89: 8135–8139

Hua Chen, Dongyuan Zhang, Jinkui Guo, Hao Wu, Meifang Jin, Qingtao Lu, Congming Lu and Lixin Zhang (2006): A Psb27 homologue in Arabidopsis thaliana is required for efficient repair of photodamaged Photosystem II. Plant Mol Biol 61: 567-575

Coughlan S.J., Heber U. (1982): The role of glycinebetaine in the protection of spinach thylakoids against freezing stress. Planta 156: 62-69

Crowther R., Henderson R. (1996): MRC image processing programs. J. Struct. Biol. 116: 9-16

De Las Rivas J. and Roman A. (2005): Structure and evolution of the extrinsic proteins that stabilize the oxygen-evolving engine. Photochem. Photobiol. Sci. 4: 1003-1010

Dekker Jan P., Boekema Egbert J. (2005): Supramolecular organization of thylakoid membrane proteins in green plants. BBA 1706:19-39

Demmig-Adams and Adams W. W. (1996): The role of xanthophyll cycle carotenoids in the protection of photosynthesis. Trends Plant Sci. 1: 21-26

Deutscher M. P. (1990): Methods in enzimology Vol. 182 (guide to protein purification). Academic Press New York

Paola Dominici, Stefano Caffarri, Franca Armenante, Stefania Ceoldo, Massimo Crimi, and Roberto Bassi (2002): Biochemical properties of the PsbS subunit of photosystem II either purified from chloroplast or recombinant. JBC 277:22750-22758

Drew A., Fleming G., Heard-Gordon M (2003): Charge-transfer state as a possible signature of a zeaxanthin-chlorophyll dimer in the non-photochemical quenching process in green plants . J. Phys. Chem. B 107: 6500-6503

Ferreira, Iverson, Maghlaoui, Barber, Iwata (2004): Architecture of the Photosynthetic Oxygen-Evolving Center. Science 303: 1831-1838

Fey Holger (2006): Biochemical and Biotechnological Approaches As Basis For Structure Determination Of Pigment-Protein Complexes Of Oxygenic Photosynthesis. Fey Holger PhD Thesis 2006 University of Frankfurt

Funk C. (2000): Functional analysis of the PsbX protein by deletion of the corresponding gene in Synechocystis sp. PCC 6803. Plant Mol. Biol. 44: 815-827

Christiane Funk, Wolfgang P. Schroeder, Artur Napiwotzki, Staffan E. Tjus, Gernot Renger, Bertil Andersson (1995): The PSII-S protein of higher plants: a new type of pigment binding protein. Biochemistry 34: 11133-11141

Gorham J (1995): Betaines in higher plants-biosynthesis and role in stress metabolism. In: Wallsgrove RM (ed) Amino acids and their derivatives in higher plants. Cambridge University Press, Cambridge pp 171-203

Haag E., Irrgang K. D., Boekema E. J. and Renger G. (1990): Functional and structural analysis of photosystem II core complex from spinach with high oxygen evolution capacity. Europ. Journ. Biochem. 189: 47-57

Hankamer B., Nield J., Zheleva D., Boekema E., Jansson S. and Barber J. (1997): Isolation and biochemical characterisation of monomeric and dimeric photosystem II complexes from spinach and their relevance to the organisation of photosystem II in vivo. Eur. J. Biochem. 243: 422-429

Heathcote P, Jones MR, Fyfe PK. (2003): Type I photosynthetic reaction centres: Form and Function. Phil Trans Roy Soc 358: 231–243

Nancy E. Holt, Donatas Zigmantas, Leonas Valkunas, Xiao-Ping Li, Krishna K. Niyogi, and Graham R. Fleming (2005): Carotenoids cation formation and the regulation of photosynthetic light harvesting. Science 307: 433-436

Holt N. E., Fleming G. R., Niyogi K. K. (2004): Toward an understanding of the mechanism of non-photochemical quenching in green plants. Biochemistry 43: 8281-8289

Horton P. and Ruban A. (2005): Molecular design of the photosystem II light-harvesting antenna: photosynthesis and photoprotection. Journ. Exp. Bot. 56: 365-373

Hua Chen, Dongyuan Zhang, Jinkui Guo, Hao Wu, Meifang Jin, Qingtao Lu, Congming Lu, Lixin Zhang (2006): A Psb27 homologue in Arabidopsis thaliana is required for efficient repair of photodamaged photosystem II. Plant. Mol. Biol. 61: 567-575

Ifuku K., Yamamoto Y., Ono T., Ishihara S. and Sato F. (2005): PsbP protein, but not PsbQ protein, is essential for the regulation and stabilisation of photosystem II. Plant Phys. 139: 1175-1184

Ikeuchi M., Inoue Y. and Vermaas W. (1995): Characterization of photosystem II subunits from the cyanobacterium Synechocystis sp. PCC 6803. In Mathis P (ed.) photosynthesis: from light to biosphere, pp 297-300. Kluwer academic publishers, Dordrecht

Ishikita H. et al. (2007): Function of two β-carotenes near the D1 and D2 proteins in photosystem II. BBA 1767: 79-87

Jeffrey, Mantoura and Wright (1997): Phytoplankton pigments in oceanography: Guidelines to modern methods, UNESCO, Paris

Katoh H. and Ikeuchi M.(2001): Targeted disruption of psbX and biochemical characterisation f photosystem II complex in the thermophilic cyanobacterium Synechococcus elongatus. Plant cell Physiol. 42(2): 179-188

Kern J., Loll B., Lüneberg C., DiFiore D., Biesiadka J., Irrgang K., Zouni A. (2005): Purification, characterisation and crystallisation of photosystem II from thermosynechococcus elongatus cultivated in a new type of photobioreactor. BBA 1706: 147-157

Kitajima Y. and Noguchi T. (2006): Photooxidation pathway of chlorophyll Z in photosystem II as studied by fourier transfrom infrared spectroscopy. Biochemistry 45: 1938-1945

Komenda J., Lupinkova L. and Kopecky J. (2002): Absence of the psbH gene product destabilizes photosystem II complex and bicarbonate binding on its acceptor side in Synechocistis PCC 6803. 269: 610-619

Komenda J., Tichy M. and Eichecker A. (2005): The PsbH protein is associated with the inner antenna CP47 and facilitates D1 processing and incorporation into PSII in the cyanobacterium Synechocystis PCC 6803. Plant Cell Phys. 46(9): 1477-1483

Kügler M., Jänsch L.; Fruft V.; Schmitz U. K. and Braun H. P. (1997): Analysis of the chloroplast protein complexes by blue native polyacrilamide gel electrophoresis. Photosyth. Res. 53: 35-44

Kühlbrandt W. (1992): Two-dimensional crystallisation of membrane protein. Quarterly Reviews of Biophysics. 25: 1-49

Lichtenthaler H. (1987): Chlorophylls and carotenoids: pigments of photosynthetic biomembranes. Meth. in enzymology, 148: 359-382

Xiao-Ping Li, Olle Björkman, Connie Shih, Arthur R. Grossman, Magnus Rosenquist, Stefan Jansson, Krishna K. Niyogi (2000): A pigment binding protein essential for regulation of photosynthetic light harvesting . Nature 403: 391-395

Liebl U, Mockensturm-Wilson M, Trost JT, Brune DC, Blankenship RE, et al. 1993. Single core polypeptide in the reaction center of the photosynthetic bacterium Heliobacillus mobilis: structural implications and relations to other photosystems. Proc Natl Acad Sci USA 90: 7124–7128

Zhenfeng Liu, Hanchi Yan, Kebin Wang, Tingyun Kuang, Jiping Zhang, Lulu Gui, Xiaomin An, Wenrui Chang (2004): Crystal structure of spinach major light-harvesting complex at 2.72Å resolution. Nature 428: 287-292

Loll, Kern, Seager, Zouni & Biesiadka (2005): Towards complete cofactor arrangement in the 3.0Å resolution structure of photosystem II. Nature 438:1040-1044

Meyer T.E. (1994): Evolution of photosynthetic reactionn centers and light harvesting chlorophyll proteins, Biosystems 33: 67-175

Morris, Hankamer, Zheleva, Friso and Barber (1997): The three-dimensional structure of a photosystem II core complex determined by electron crystallography. Structure 6: 837-849

Moya, I.; Silvestri, M.; Vallon, O.; Cinque, G.; Bassi, R. (2001): Time-Resolved Fluorescence Analysis of the Photosystem II Antenna Proteins in Detergent micelle and liposomes. Biochemistry 40: 12552-12561

Mulkidjanian AY, Junge W. (1997): On the origin of photosynthesis as inferred from sequence analysis. Photosynth Res 51: 27–42

Nakazato, Toyoshima, Eami and Inoue (1996): Two-dimensional crystallisation and Cryo-electron Microscopy of Photosystem II. J. Mol. Biol. 257: 225-232

Nancy A. Eckardt (2001): The role of PsbZ in the core complex of photosystem II. The plant cell 13: 1245-1248

Nelson and Adam (2005): The structure of Photosystem I and evolution of phosythensis. BioAssay 27: 914-922

Nield J., Funk C. and Barber J. (2000): Supramolecular structur of photosystem II and location of the PsbS protein. Phil. Trans. R. Soc. Lond. B 355: 1337-1344

Nitschke W, Rutherford AW. (1991): Photosynthetic reaction centers: variation on a common structural theme? Trends Biochem Sci 16:241–245

Krishna K. Niyogi, Xiao-Ping Li, Vanessa Rosenberg, and Hou-Sung Jung (2005): Is PsbS the site of non-photochemical quenching in photosynthesis? J. Exp. Bot. Vol. 56: 375-382

Norikazu Ohnishi and Yuichiro Takahashi (2001): PsbT Polypeptide is required for efficient repair of photodamaged photosystem II reaction center. J. Mol. Biol. 276: 33798-33804

Marc M. Nowaczyk, Romano Hebeler, Eberhard Schlodder, Helmut E. Meyer, Bettina Warscheid, and Matthias Rögner (2006): Psb27, a cyanobacterial lipoprotein, is involved in the repair cycle of Photosystem II. Plant Cell 18: 3121-3131

Ohira S., Morita N., Suh H., Jung J. and Yamamoto Y. (2005): Quality control of photosystem II under light stress-turnover of aggregates of the D1 protein in vivo. Phot. Res. 84: 29-33

Ohnishi N. and Murata N. (2006): Glycinebataine counteracts the inhibitory effects of salt stress on the degradation and synthesis of D1 protein during photoinhibition in synechococcus sp. PCC 7942. Plant phys. 141: 758-765

Jean-Benoît Peltier, Olof Emanuelsson, Dário E. Kalume, Jimmy Ytterberg, Giulia Friso, Andrea Rudella, David A. Liberles, Linda Söderberg, Peter Roepstorff, Gunnar von Heijne, and Klaas J. van Wijk (2002): Central function of the lumenal and peripheral thylakoids proteome of Arabidopsis determined by experimentation and genome-wide prediction. Plant Cell 14: 211-236

Pawel Penczek, Michael Radermacher and Joachim Frank (1992): Three dimensional reconstruction of single particles embedded in ice. Ultramicroscopy 40: 33-53

Peterson R.B. and Havir E. A. (2000): A non-photochemical-quenching-deficient mutant of Arabidopsis thaliana possessing normal pigment composition and xanthophyll-cycle activity. Planta 210: 205-214

Tomas Polivka, Jennifer L. Herek, Donatas Zigmantas, Hans-Erik Åkerlund, and Villy Sundström (1999): Direct observation of the (forbidden) S1 state in carotenoids. PNAS 96: 4914-4917

Porra R.J., Thompson W. A., P. E. Kriedmann (1989): Determination of accurate extinction coefficients and simultaneous equations for assaying chlorophylls a and b

with four different solvents: verifications of the concentration of chlorophyll standard by atomic absorption spectroscopy. BBA 975: 384-394

Prafulla K. (2006): Three-dimensional model of zeaxanthin binding PsbS protein associated with nonphotochemical quenching of excess quanta of light energy absorbed by the photosynthetic apparatus. J. Mol. Model. 12: 847-853

Remy R, Tremolieres, A, Duval JC, Ambardbretteville F, Dubacq JP. (1982): Study of the supramolecular organization of light-harvesting chlorophyll protein (LHCP): conversion of the oligomeric form into the monomeric one by phospholipase-a2 and reconstitution with liposomes. FEBS letters 137: 271-275

Rhee, Morris, Zheleva, Hankamer, Kühlbrandt and Barber (1997): Two-dimensional structure of plant photosystem II at 8-Å resolution. Nature 389: 522-526

Rokka A., Suorsa M., Saleem A., Battchikova N. and Aro E. (2005): Synthesis and assembly of thylakoids protein complexes: multiple assembly steps of photosystem II. Biochem. J. 388: 159-168

Roose J. L. and Pakrasi H. B. (2004): Evidence that D1 processing is required for manganese binding and extrinsic protein assembly into Photosystem II. JBC 279: 45417-45422

Rouhier N., Villarejo A., Srivastava M., Gelhaye E., Keech O., Droux M., Finkemeier I., Samuelsson G., Dietz K.J., Jacquot J.P., Wingsle G. (2005): Identification of plant glutaredoxin targets. Antioxid Redox Signal 7: 919-929

Sakamoto A., Murata N. (2000): Genetic engineering of glycinebetaine synthesis in plants: current status and implications for enhancement of stress tolerance. J. Exp. Bot. 51: 81-88

Caterina Santini, Valentino Tidu, Giuseppe Tognon, Anna Ghiretti Magaldi and Roberto Bassi (1994): Three dimensional structure of the higher plant photosystem II

reaction centre and evidence for its dimeric organisation in vivo. Eur. J. Biochem. 221: 307-315

Schägger H., V. Jagow G. (1987): Tricine sodium dodecyl-sulfate polyacrylamide-gel electrophoresis for the separation of proteins in the range from 1kDa to 100kda. Anal. Bioch. 166 (2): 368-379

Schägger H., V. Jagow G. (1991): Blue native electrophoresis for isolation of membrane protein complexes in enzymatically active form. Anal. Bioch. 199: 223-231

Schopf J. W. (1993): Microfossils of the early archean Apex Chert: new evidence of the antiquity of the life. Science 260: 640-646

Schubert W-D, Klukas O, Saenger W, Witt H-T, Fromme P, et al. (1998): A common ancestor for oxygenic and anoxygenic photosynthetic systems: a comparison based on the structural model of photosystem I. J. Mol. Biol. 280: 297–314

Schwenkert S., Umate P., Dal Bosco C., Volz S., Mlcochova L., Zoryan M., Eichacker L. (2006): PsbI affect the stability, function and phosphorylation patterns of photosystem II assemblies in tobacco. JBC doi.M604888200

Shi L., Lorkovic Z., Oelmüller R. and Schröder P. (2000): The low molecular biology mass PsbW protein is involved in the stabilisation of the dimeric photosystem II complex in Arabidopsis thaliana. JBC 275: 37945-37950

Jörg Standfuss[1], Anke C Terwisscha van Scheltinga[1], Matteo Lamborghini and Werner Kühlbrandt (2005): Mechanisms of photoprotection and nonphotochemical quencing in pea light-harvesting complex at 2.5Å resolution. EMBO 24: 919-92

Sugimoto I. and Takahashi Y. (2003): Evidence that the PsbK polypeptide is associated with the photosystem II core antenna complex CP43. JBC 278: 45004-45010

Suleyman I. Allakhverdiev, Hidenori Hayashi, Yoshitaka Nishiyama, Alexander G. Ivanov, Jalal A. Aliev, Vyacheslav V. Klimov, Norio Murata and Robert Carpentier (2003): Glycinebetaine protects the D1/D2/Cytb559 complex of photosystem II against photo-induced and heat-induced inactivation. J. Pl. Phys. 160: 41-49

Marjaana Suorsa, Sari Sirpiö, Yagut Allahverdiyeva, Virpi Paakkarinen, Fikret Mamedov, Stenbjörn Styring, and Eva-Mari Aro (2006): PsbR, a missing link in the assembly of the oxygen-evolving complex of plant photosystem II. JBC 281: 145-150

Suorsa M., Regel. R., Paakkarinen V., Battchikova N., Herrman R. and Aro E. (2004): Protein assembly of photosystem II and accumulation of subcomplex in the presence of low molecular mass subunits PsbL and PsbJ. Eur. J. Biochem. 271: 96-107

Szabo I., Bergantino E. and Giacometti M. G. (2005): Light and oxygenic photosynthesis: energy dissipation as a protection mechanism against photo-oxidation. EMBO 6: 629-634

Enrico Teardo, Patrizia Polverino de Laureto, Elisabetta Bergantino, Francesca Dalla Vecchia, Fernanda Rigoni, Ildikò Szabò and Giorgio Mario Giacometti (2007): Evidences for interaction of PsbS with photosynthetic complexes in maize thylakoids. BBA 1767:703-711

Thornton E., Ohkawa H., Roose J., Kashino Y., Keren Nir and Pakrasi B. (2004): Homologs of plant PsbP and PsbQ proteins are necessary for regulation of photosystem II activity in the cyanobacterium Synechocystis 6803. The Plant Cell 16: 2164:2175

Van Hell M. (1987): Similarity measures between images. Ultramicroscopy 21: 95-100

Peter J. Leeuwen, Maaike C. Nieveen, Erik Jan Meent, Jan P. Dekker and Hans J. Gorkom (1991): Rapid and simple isolation of pure photosystem II core and reaction center particles from spinach. Phot. Res. 28: 149-153

Vermaas WF. (1994): Evolution of heliobacteria: Implications for photo synthetic reaction center complexes. Photosynth Res 41:285–294

Wild A. (1986): Changes in the stoichiometry of photosystem II components as an adaptive response to high-light and low-light conditions during growth. Zeitschrift für Naturforschung C 41(5-6): 597-603

Xiao-Ping Li, Olle Björkman, Connie Shih, Arthur R. Grossman, Magnus Rosenquist, Stefan Jansson and Krishna K. Niyogi. (2000): A pigment-binding protein essential for regulation of photosynthetic light harvesting . Nature 403: 391-395

Xiong J. and Bauer C.E. (2002): Complex evolution of photosynthesis. Annual Review of Plant Biology 53: 503-521

Xiong J., Fisher W., Inoue K., Nakahara M., Bauer C. (2000): Molecular evidence for the early evolution of photosynthesis. Science 289: 1724-1730

Yao D., Kieselbach T., Komenda J., Promnares K., Hernández Prieto M.A., Tichy M., Vermaas, W, and Funk, C. (2007): Localization of the small cab-like proteins in photosystem II. J Biol Chem 282: 267-276

Acknowledgments

In this page I would like to thank all the people for making the accomplishment of my Ph.D. possible:

Prof. Dr. Claudia Büchel for giving me the opportunity to join her group and for her constant help during these three years of work.

All the members of my group for being always ready to help me and for their kindness. Particular thanks to Kerstin Pieper, Matthias Schmidt and Christel van Oijen for their precious technical assistance.

A very special thanks to Regina Ennemann for helping me in everything related with the administration and the bureaucracy.

Holger, for his help during these three years in and out of the lab and for the crucial advice in writing this thesis.

A special thanks to Thomas, Anja, Gudrun, Marion and Kathy for the very good time that we spent together and for the very interesting discussions.

All the students and especially Simone and Nadine for taking me around all over in the city looking for good food and music and again Simone for helping me in the thesis.

All the people involved in the Interdisciplinary Network for Training and Research on Photosystem II and for the extremely high level of science in the activities related with this network. Especially I would like to thank Jan Dekker for the perfect coordination of the network, William A. Rutherford and Egbert J. Boekema for the work and the nice time in Paris and Groningen.

And last but not least, I would like to express my deepest gratitude to the Max Planck Institute for Biophysics in Frankfurt and the International Max Planck Research School. In particular, huge thanks to Claudia Büchel and Werner Kühlbrandt for giving me the opportunity of this PhD; Deryck Mills and Vinoth Kumar for the precious advice and the technical help in the Max Planck Institute.